Study of the metabolism during microspore embryogenesis in wheat DH lines using –omics approaches

Dissertation

zur Erlangung des

Doktorgrades der Naturwissenschaften (Dr. rer. nat.)

der

Naturwissenschaftlichen Fakultät I

– Biowissenschaften –

der Martin-Luther-Universität

Halle-Wittenberg

vorgelegt

von Frau Teresa Pérez-Piñar López

geb. am 04.11.1986 in Madrid, Spanien

Gutachter

1. Prof. Dr. Klaus Humbeck
2. PD. Dr. Hans-Peter Mock
3. Prof. Dr. Iwona Żur

Verteidigung: Halle (Saale), den 09.01.2019

Parts of this thesis will be published in:

Perez-Pinar T, Hartmann A, Bössow S, Gnad H, Mock HP. Metabolic changes during wheat microspore embryogenesis induction using the highly responsive cultivar Svilena. BMC Plant Biology Submitted.

Perez-Pinar T, Meister A, Bössow S, Gnad H, Mock HP. Metabolic changes during androgenic induction in a segregating population of bread wheat and prediction of green plant regeneration**.** Under preparation.

Table of contents

1.   Summary

Microspore embryogenesis is a process defined by a switch in the microspore development, from the gametophytic to the sporophytic pathway. The process is triggered by the application of a stress pretreatment. The final result, after chromosome doubling, is a doubled haploid (DH) plant. Although the morphological events in microspore embryogenesis are well known, the molecular basis is still poorly understood in bread wheat. Practically, microspore embryogenesis allows the study of cellular reprogramming, phase change and totipotency, however, the applicability is limited by the genotype. This also applies for bread wheat, the most important crop species in a worldwide scale.

Hence, the major aim of this thesis was to determine the metabolic pathways that define the microspore embryogenesis in bread wheat. Microspores from doubled haploid genotypes were used as studied material, and low temperature was applied as stress pretreatment. The metabolome of 'Svilena', a genotype with high plant regeneration efficiency through microspore embryogenesis, was explored in the first stages of the process. The metabolic dataset, obtained from targeted and untargeted analysis, was interpreted together with a transcriptomic dataset (kindly given by Dr. Scholten) obtained from microspores of the same plants. Both datasets were integrated within the functional context of metabolic pathways using VANTED software (Visualization and Analysis of Networks containing Experimental Data). As a second part, a metabolic comparison was made between microspores of DH lines differing in their green plant regeneration (GPR) efficiency after microspore embryogenesis. These lines were obtained from the cross of 'Svilena' and 'Berengar', a genotype with poor plant regeneration rate. Later, a proteome analysis of the two parent cultivars complemented the results. The comparison allowed the identification of the molecular basis from which successful green plant regeneration after microspore embryogenesis can be achieved. Practically, the prediction of the regeneration rate was possible by building a mathematical model from few detected metabolites.

The results revealed starch metabolism and tricarboxylic acid (TCA) cycle as key pathways during the cold stress pretreatment, and then, the amino acid metabolism after the next

stage (the first nuclear division). Additionally, cytosolic glutamine synthetase 1 (GS1) was found predominant and more abundant in the last studied stage.

Furthermore, the metabolic analysis of microspores of DH lines with different GPR rate revealed similar profiles, but different concentrations in every stage. From the concentrations of few selected metabolites analyzed in the vacuolated stage a robust prediction model for the GPR rate was built.

 The analysis of the proteome showed the biological processes that were relevant to the GPR rate: amino acid, carbohydrate and lipid metabolism, cytoskeleton organization, nucleic acid metabolism, protein biosynthesis, protein modifications and stress response. These showed a different profile between 'Svilena' and 'Berengar' even before the process started.

The results presented in this thesis indicate that energy was produced during the de-differentiation process and highly active amino acid metabolism was essential in the first nuclear division stage. Practically, the prediction of the GPR rate in the vacuolated stage using few metabolites might reduce the time of selection of responsive genotypes. This study shows for first time the key metabolic pathways that determine the microspore embryogenesis in early stages in bread wheat. Additionally, the molecular basis that leads the microspore to a successful green plant regeneration after microspore embryogenesis is given. Also for first time, a reliable and useful GPR rate predictive model is built.

Key words: *Triticum aestivum*, microspore embryogenesis, regeneration efficiency, cold stress, totipotency, metabolome, proteome, prediction.

2.   Introduction

2.1.   Triticum aestivum

Bread wheat (*Triticum aestivum* L.), a monocot belonging to the Poaceae family, is one of the main food sources for the human population. The first utilization of wheat occurred 19000 years ago, at the start of human agriculture (Nevo et al., 2002), and its domestication was achieved 10000 years ago (Lev-Yadun et al. 2000). Originally coming from the south-eastern part of Turkey (Shewry, 2009), bread wheat contains an allohexaploid genome that has 7 sets of 2 homologous chromosomes in each subgenome A, B, D (2n=6x=42). This genome arose through two polyploidization events (figure 1) between species of the *Triticum* and *Aegilops* genera. In the first one, the genomes of *Triticum urartu* (2n=2x=14; AA) and another species related to *Aegilops speltoides* (2n=2x=14; SS) formed the *Triticum turgidum* species (2n=4x=AABB). This allotetraploid hybridized with *Aegilops tauschii* (DD) resulting, finally, the *Triticum aestivum* species (AABBDD) (Petersen et al., 2006).
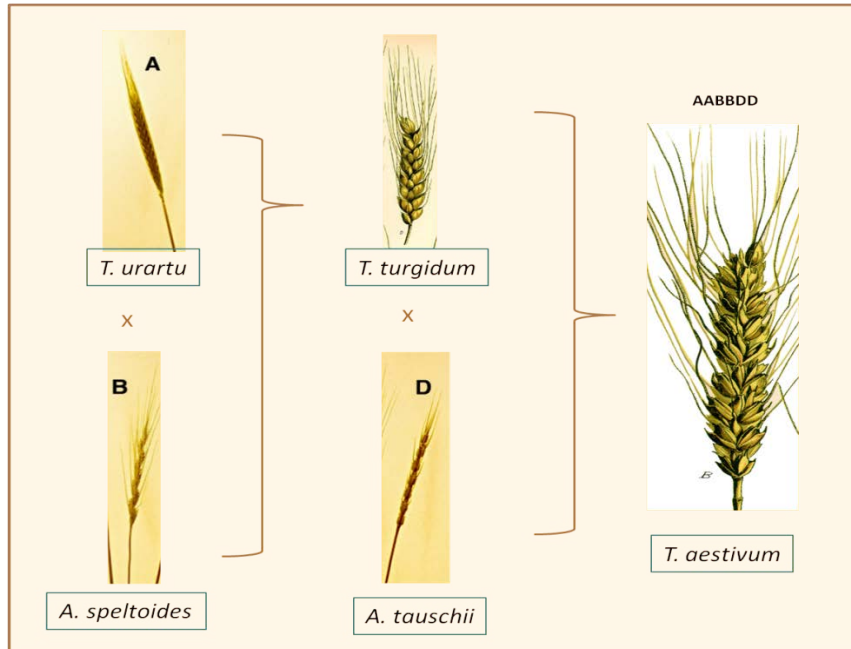
Figure 1: **Origin of *Triticum aestivum*.** *Triticum urartu* and *Aegilops speltoides* brought genomes A and B, respectively, and formed the *Triticum turgidum* species. *Triticum aestivum* arose, finally, after hybridization between *T. turgidum* and *Aegilops tauschii*. Pictures of the scheme are taken from Kasarda, 2013 and Thomé, 1886.

Nowadays, it is one of the most cultivated cereals in the world, with more than 700 million tons produced in 2014 (FAOSTAT, http://faostat.fao.org/) in a wide range of environments in the five continents. Therefore, developing varieties with desired agronomic traits is of high importance for animal and human nutrition. Desirable traits include resistance to diseases, such as the mosaic virus (Talbert et al., 1996); stress tolerance, such as drought (Quarrie et al., 1994); quality traits, such as the color of the flour (Parker et al., 1998); or morphological traits, like dwarfing (Korzun et al., 1998).

2.2. Doubled haploids

Breeders aim to select and propagate the best individual of a line in order to produce new cultivars (Baenziger and DePauw, 2009). For this purpose, homozygosity is an important goal. Conventional breeding programs require up to six cycles of self-pollination to achieve homozygosity. In those programs, sexual plant crossing is used to combine favorable traits in a new improved variety. This time-consuming process can be short-circuited through the use of the doubled haploid approach, in which homozygosity is achieved within a single generation (Shariatpanahi et al., 2006). In this method, the haploid chromosome complements are doubled, either spontaneously or by the addition of colchicine (Guzy-Wróbelska and Szarejko, 2003). Haploid plants, which have one set of gametic chromosomes, are generally derived from either ovaries or unfertilized ovules (gynogenesis and wide crossing) or microspores (androgenesis) in a process called gametophytic embryogenesis (Baenziger and DePauw, 2009). After the chromosome doubling step, the haploid plant becomes diploid and fertile again (Soriano et al., 2013).

In gynogenesis, ovaries and unfertilized ovules are incubated in both inducing and regenerating medium, to produce a haploid plant that will be subjected to chromosome doubling treatments. Besides the reduced number of cells that can be obtained from a plant, the efficiency of regeneration is low (Niroula and Bimb, 2009). Therefore, it is mainly used in species were the other methods failed, such as onion (*Allium cepa*) or sugarbeet (*Beta vulgaris*) (Forster et al., 2007).

The wide or distant crossing method consists of a double fertilization of individuals from different species or genera. Thereafter, the paternal chromosomes are eliminated, presumably as a result of different interaction of the centromeres of the parents with the mitotic spindle (Liu et al., 2014), and thus, a haploid is obtained from one of the parents. This method has been widely used, particularly for commercial production, as it shortens the plant breeding by the production of doubled haploids. It also presents low rates of genotype dependence and no formation of albino plants. However, the reduced number of female gametes, the necessity of matching the flowering time of both plants and the rescue of the haploid embryos are some of the disadvantages. Maize (*Zea mays*) is frequently used as pollen donor with wheat plants (Campbell et al., 2000).

Nowadays, doubled haploids have been achieved in a large number of plant species (Forster et al., 2007). This approach does not only reduce the time to obtain new varieties and genotypes, but also has applications in research, such as for mapping, genetic analysis, mutations, transformation or biochemical analysis, among others (Niemirowicz-Szczytt, 1997).

2.3. Microspore embryogenesis

In microspore embryogenesis, also called androgenesis or pollen embryogenesis, the haploid plant originates from a microspore of a plant. These microspores present in the microsporogenesis (or gametophytic) pathway deviate their path to the sporophytic development (Seguí-Simarro and Nuez, 2008), after a stress pretreatment application (Zheng, 2003) since it is unfrequent in nature (Silva, 2012).

2.3.1. Pollen development

Successful pollen development in microgametogenesis is necessary for the achievement of pollen germination and fertilization. During the pathway (figure 2), the microspore mother cell, surrounded by a callose wall, undergoes meiosis. As a result, a tetrad is formed, with 4 haploid microspores. The callose wall decomposes and the microspores are released to the

anther locule. In this stage the microspores are surrounded by the tapetum cells and the pollen wall starts forming. Then, 2 mitotic divisions take place. In the first one, 2 asymmetric cells are formed, called the generative and the vegetative cells. The former undergoes a second mitotic division. Hence, the pollen grains are formed by 3 cells at the time of anthesis (Hesse et al., 2009). The pollen wall includes an intine and an exine layer. The former is composed of cellulose, hemicelluloses and pectin (Jiang et al., 2012), and the later is formed by sporopollenin (Quilichini et al., 2014).

Regulation of the pollen development and provision of compounds for the pollen wall formation are some roles attributed to the tapetum. In particular, some cereals like wheat or rice present secretory tapetum, in which spheroid structures appear, which are called Ubisch bodies. Although, no evidence is yet reported for the role of these structures, sporopollenin transport is suggested (Wang et al., 2003). Additionally, regulatory genes have been identified, such as BAM (Barely Any Meristem) or SERK (Somatic Embryogenesis Receptor-Like Kinase), both implied in tapetum development.

Best results in microspore embryogenesis have been obtained when the microspores are in the mid- to late uninuclear stage of microsporogenesis. At this step, microspores have a big central vacuole and the nucleus is located close to the sporoderm at the opposite pole of the microspore operculum (Bárány et al., 2010). The developmental stage of the microspore along with other factors affects the effectiveness of the embryogenesis. In fact, at the point of starch accumulation in the binucleate pollen microspore embryogenesis is not possible (Touraev et al., 1997).

2.3.2. The switch towards the sporophytic development

Other factors affecting the effectiveness include, for example, the harvesting stage or the stress pretreatment used for induction (Żur et al., 2009). Furthermore, the co-culture of microspores with longitudinally bisected pistils can improve the success of the embryogenesis (Lippmann et al., 2015).

The stress pretreatment can be either abiotic or biotic, including heat, cold, starvation and osmotic stress treatments. The stress applied depends on the species. For example, a combination of starvation and osmotic stress, achieved by the use of mannitol, is used in barley microspores (Hoekstra et al., 1992), whereas cold stress is used in wheat genotypes (Poersch-Bortolon et al. 2016).

In contrast to the pollen development in microgametogenesis, the nucleus in induced microspores is displaced to the centre of the cell, due to rearrangements of the cytoskeleton, and a symmetrical division of the nuclei occurs after the stress pretreatment. Cold pretreatment benefits the anther culture response, promoting a higher callus yield and a higher frequency of spontaneous chromosome doubling (Zheng, 2003). Additionally, cold stress has been reported to provide a high percentage of enlarged microspores that may develop into green plants (Ayed et al., 2009). After the pretreatment, microspores are devoid of a large central vacuole and show small vacuoles, a clear and alkaline cytoplasm and a star-like morphology (figure 2), since the vacuole has divided in several small vacuoles acquiring the appearance of a star (Maraschin et al., 2005a). This morphology is found also in non-embryogenic microspores, but with a different time of occurrence. For example, only the barley microspores that exhibit this morphology later than the others success in the embryo formation (Maraschin et al., 2005b).

Enlarged microspores during the first stages of androgenesis were considered to be a sign of change in the developmental pathway (Dubas et al., 2010). However, not all species show enlarged microspores after the stress treatment, such as *Dactylis glomerata* (Somleva et al., 2000). Therefore, other markers are also studied.

2.3.3. First nuclear division

With the first nuclear division two nuclei of equal size are formed and chromatin is condensed (Silva, 2012). Thereafter, more nuclear divisions happen while the pro-embryo and androgenic structures are formed (figure 2). However, not all the microspores undergo the sporophytic development (Rodríguez-Serrano et al., 2011). Some of them do not

continue with the embryo development after few divisions, others form callus structures and only a few of them will form embryos. Periclinal divisions of the cells surrounding the embryo-like structures precede the heart and torpedo embryo stages in *B. napus* (Telmer et al., 1995; Hause et al., 1994). Epidermis, cotyledon and parenchyma are already seen in the torpedo stage (Bárány et al., 2005). Finally, after chromosome doubling, a doubled haploid plant appears. Chemical agents are often used to improve chromosome doubling, such as colchicine, which disrupts mitotic division. Colchicine can be applied at different points of the microspore embryogenesis process (Chen et al., 1994; Möllers et al., 1994; Mathias and Röbbelen, 1991).
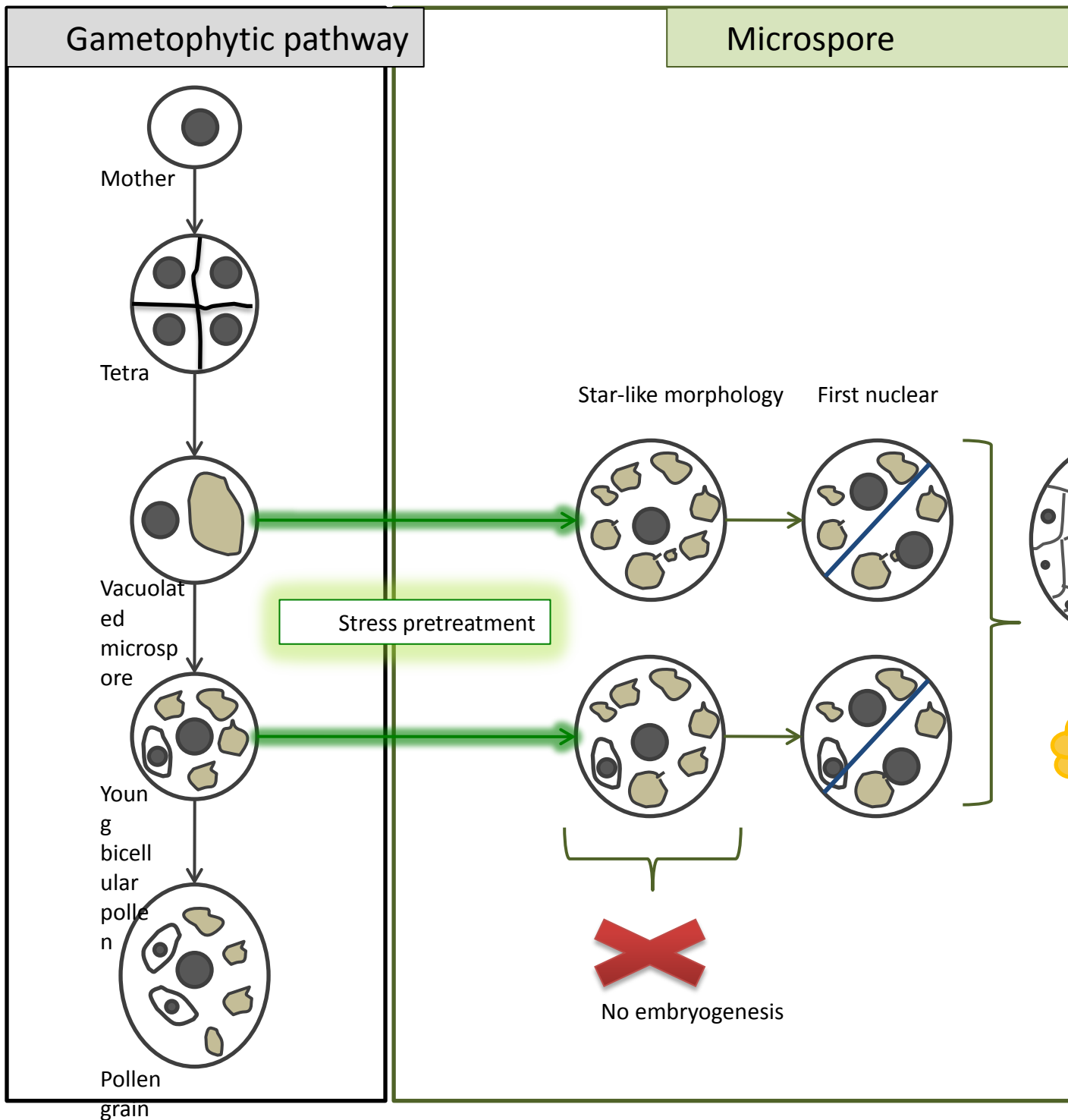
Figure 2: **Switch of the microspore from the gametophytic to the sporophytic pathway.** Main stages and events of both pathways are shown. In the gametophytic pathway, the vacuolated microspore and the young bicellular pollen can be subjected to a stress pretreatment and the microspore embryogenesis can take place. When successful, after the star-like morphology stage, divisions of the cell will happen and a green plant arises.

The doubled haploid plant can be achieved either by culturing isolated anthers or isolated microspores (Forster et al., 2007). Isolated microspores culture consists in the extraction of the microspores from the anthers and later culture in a liquid medium that provides all the necessary compounds for their growth and development, such as carbon, vitamins and minerals. Anther culture uses an agar medium in a Petri dish that provides the necessary components. Additionally, the medium has to be refreshed periodically. This can be regarded as a disadvantage compared to the isolated microspores culture, in which the liquid medium does not have to be renewed. However, its simplicity makes the anther culture applicable to a wide range of crops (Maluszynski et al., 2003). Still, anther culture is a more reliable method to produce doubled haploids in winter wheat (Lantos et al., 2013) than isolated microspore culture, which produces more albinos (Lantos et al., 2006).

Anther culture was used first time for haploid production in *Datura innoxia* (Guha and Maheshwari, 1964). Later, isolated microspore culture was developed in *Brassica napus* (Lichter, 1982). Nowadays, microspore embryogenesis has been applied in more than 100 species (Maluszynski et al., 2003), either using isolated microspores or anther culture.

The described process provides interest both for breeders and scientific researchers. It allows the study of cellular reprogramming, phase change and totipotency in higher plants. It is also used for molecular and biochemical analysis in order to study different cell processes. In addition, genetic engeneering by transformation can use microspores as targets, to produce homozygous genotypes with the gene of interest. For these reasons, this method is more commonly applied. However, there are still some recalcitrant species, such as tomato or *Arabidopsis* (Soriano et al., 2013), and some other disadvantages, like genotype dependence or albino plant formation.

2.4. Identified molecular events and markers of the microspore embryogenesis

2.4.1. Genetic markers of microspore embryogenesis

The already mentioned morphological markers, such as a star-like morphology or the first nuclear division, are not considered sufficient to identify microspores that will develop into embryos. Therefore, other markers have been examined. The molecular basis of the totipotency occuring in this process has been the focus of some studies. In such studies model systems have been used, including barley, wheat or tobacco, due to their high regeneration efficiency (Touraev et al., 1997). The comparison between the sporophytic and gametophytic development is important, as most microspores in the same culture do not switch to the sporophytic pathway, but continue under the gametophytic one. Thus, whilst microspore transcripts have been found to encode for proteins with structural and metabolic roles, the transcripts found in gametophytic development encode for pollen-specific proteins, such as pollen germination or tube growth proteins (Soriano et al., 2013). The transcriptome of the microspore before the stress pretreatment is more similar to the ones in the sporophytic development than to the mature pollen (Joosen et al., 2007). Additionally, differential gene expression occurs after the microspore induction. Genetic studies have focused more in the early embryo than in the stages prior to the divisions. Malik et al. (2007) identified several genes specific for embryo development, which were absent in pollen development (table 1). Some examples of these markers are FUSCA3 (FUS3), BABY BOOM (BBM), LEAFY COTYLEDON1 and 2 (LEC), among others, that are related to embryo maturation or seed devolpment. In particular, LEC1 and LEC2 participate in the specification of cotyledon identity and embryo maturation; FUS3 participates also in late embryogenesis; and BBM, expressed in embryo and roots, can induce somatic embryogenesis when applied to seedlings of several species as *Arabidopsis* or *B. napus* (Bäumlein et al., 1994; Malik et al., 2007). BBM is also reported as a genetic marker in wheat (Seifert et al., 2016). Furthermore, since the expression of glutathione-S-transferase gene is increased during wheat, barley and rapeseed microspore embryogenesis, reactive oxygen species might be formed that can produce oxidative damage (Sánchez-Díaz et al., 2013; Maraschin et al., 2006; Joosen et al., 2007).

Joosen et al. (2007) identified a number of genes and proteins expressed in embryogenic rapseed microspore cultures. In that study, the proteomic analysis revealed differences between pollen and microspores after stress pretreatment. Since the transcriptome analysis did not show differences between these two analyzed stages, there must be pollen-specific non-translated mRNA in the microspore in the early stage of the sporophytic development (Soriano et al., 2013).

Genetic markers of microspore embryogenesis	Rapseed	Barley	Wheat
Arabinogalactan protein	+	-	+
BabyBoom	+	-	+
FAD-dependent oxidoreductase family protein	+	+	-
Glutathione s transferase	+	+	+
Lipid transfer protein	+	+	-

Table 1: **Genetic markers of microspore embryogenesis in rapseed, barley and wheat**. Genes and transcripts are detected in at least two species. Detection was carried out by cDNA microarray and RNA-seq in microspores, embryogenic microspores or microspore derived embryos, obtained with different stress treatments, such as heat or cold. Data taken from Malik et al. (2007), Joosen et al. (2007), Maraschin et al. (2006), Sánchez-Díaz et al. (2013) and Seifert et al. (2016).

In addition, gene expression is induced by several hormones, such as abscisic acid, during the stress treatment in microspore embryogenesis (Maraschin et al., 2006). A crosstalk and balance between hormones is essential for androgenesis effectiveness (Żur et al., 2015).

Taking together the genetic data obtained from these model species, the number of genetic markers found for microspore embryogenesis in at least two of the species is rather low (table 1). Hence, there is still lack of knowledge that allows generalizing the molecular events relevant to the microspore embryogenesis process.

2.4.2.   Metabolic dynamics in microspore embryogenesis

Concerning primary metabolism, changes have been associated with microspore embryogenesis in tobacco (Hosp et al., 2007). For example, starch synthesis was associated with differentiation processes. The same assumption was reported in other species, such as pepper (Bárány et al., 2010). Additionally, altered transcript levels can be connected with altered metabolic levels. An example is found in the up-regulation of ATP-synthase transcript levels that correlates with an increased citrate concentration in tobacco microspore embryogenesis, reported by Hosp et al. (2007). In the same work, sugar and nitrogen changes were suggested to define the differentiation process. On the other hand, this study did not find increased levels of both some common stress-induced genes and some amino acids.

2.4.3.   Protein markers of microspore embryogenesis

Furthermore, several proteins and enzymes have been reported to increase in rapeseed embryogenic cultures compared to pollen (Joosen et al., 2007). Signaling, redox processes, DNA replication or amino acid metabolism represent the main processes induced in the microspore embryogenesis. 14-3-3 proteins, monodehydroascorbate reductase, GST or heat shock protein 90 (HSP90) are some of the key proteins participating in this induced process (table 2). 14-3-3 proteins mediate protein-protein interaction (Yaffe et al., 1997). 14-3-3A and 14-3-3C isoforms have a role during microspore embryogenesis. When the former isoform is absent the cells die during the process (Maraschin et al., 2003). Monodehydroascorbate reductase, which reduces monodehydroascorbate to ascorbate, and GST, are both involved in redox processes. Finally, some heat shock proteins have been reported to induce after heat stress in *Zea mays* microspores (Magnard et al., 1996), but also during cold treatments in poplar leaves (Renaut et al., 2004). In particular HSP90, a cold-induced protein in *Brassica napus*, is suggested to have a role in plant growth and development (Krishna et al., 1995). Antifreeze activity has also been given to glucanases of winter rye leaves (Yaish et al., 2006), by breaking down glucan molecules. Freezing tolerance in Arabidopsis and strawberry transgenic plants was increased by the wheat dehydrins

WCS19 and WCOR410 (Miura and Furumoto, 2013). Dehydrins have different reported roles such as chaperones or as antioxidants (Hanin et al., 2011). The antioxidant enzymes act during cold treatment as scavengers of reactive oxygen species (Nejadsadeghi et al., 2014; Sugie et al., 2006), which have been shown to play a dual role during cold stress, as toxic species but also as signaling molecules (Heidarvand and Maali Amiri, 2010). In the de-differentiation stage, where the cold stress pretreatment is applied, mechanisms that lead to a clear cytoplasm, such as the proteasome activity or autophagy, have been reported as markers of that stage (Corral-Martínez et al., 2013). Therefore, proteases may have an important role during acquisition of microspore embryogenic potential.

Rapeseed
14-3-3 protein
Ascorbate peroxidase
Chaperonin
Dehydroascorbate reductase
Disulfide isomerase
Glutathione-S-transferase
Glyceraldehido-3-P-dehydrogenase
Heat shock protein
Monodehydroascorbate reductase

Table 2: **List with some examples of proteins induced in *Brassica napus* embyogenic cultures**. Proteins were detected by 2-D gel electrophoresis, followed by MS identification. Data are taken from Joosen et al., 2007.

Moreover, cold stress treatment has been shown to influence the production of secondary metabolites, such as phenolics, anthocyanins, or polyamines (Ramakrishna and Ravishankar, 2011).

2.4.4.   Epigenetic modifications of microspore embryogenesis

Additionally, epigenetic changes have also been suggested to regulate the cold stress response (Boyko et al., 2010; Tang et al., 2012). Besides the cellular rearrangements during microspore embryogenesis, the plant cell reprogramming changes the genome organization (Solís et al., 2012). Epigenetic events modulate gene expression and thus participate in the genome organization. Genome modifications include DNA and histones methylation and acetylation, or the presence of microRNA (miRNA), among others. Briefly, DNA methylation is carried out by DNA methyltransferases, which catalyze either the de novo or the maintenance of the cytosine methylation pattern (Pikaard and Scheid, 2014), leading to gene silencing (Köhler et al., 2012). In addition, methylation can be lost, either passively or actively, via a failure in methylation maintenance or via enzymatic acitivity, respectively. Histones can be covalently modified at different positions. Acetylation is associated with active chromatin, and it is achieved by histone acetyltransferases. In histone methylation, depending on the residue and the level of methylation, we find transcriptionally active and inactive chromatin. Cytosine methyltransferases bind to methylated histones, maintaining their methylation modifications (Pikaard and Scheid, 2014). Phosphorylation or ubiquitination of histones are other types of modification. Histone phosphorylation has been associated with DNA repair, control of chromosome segregation and cell division (Pikaard and Scheid, 2014). In addition, these epigenetic modifications can be heritable or even reversible (Ay et al., 2014; Stelpflug et al., 2014), which was suggested to be essential during development (Pikaard and Scheid, 2014).

Transcriptional and posttranscriptional modifications are also involved in gene silencing, such as miRNAs or small interfering RNAs (siRNAs). These bind to specific mRNAs regulating their expression (Pikaard ans Scheid, 2014). Epigenetic changes have been found in many stages of plant development, such as leaf senescence (Ay et al., 2009). Studying microspore embryogenesis in barley, El-Tantawy et al. (2014) found low DNA methylation in the early multicellular embryo and increasing in later stages. In addition, histone modifications have been studied in pollen and microspore embryogenesis of barley (Pandey et al., 2013, 2017), revealing early cytoplasmic accumulation of modified histones. Other studies have shown an

association between cold stress and histone modifications (Yaish et al., 2011). Studies in *Brassica napus* microspores, pollen and microspores-derived embryos revealed also a hypermethylation during pollen gametophytic development that was absent in microspore derived pro-embryos (figure 3) (Solís et al., 2012). However, there is a lack of knowledge in microspores of wheat undergoing microspore embryogenesis.

5-mdC%
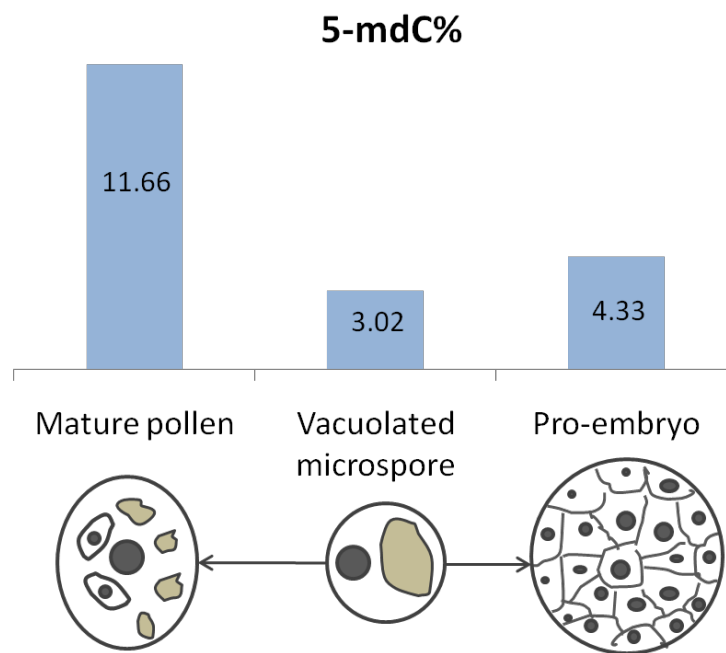
Figure 3: **5-methyldeoxycytidine percentage detected in mature pollen, vacuolated microspore and pro-embryo derived from microspore embryogenesis in *Brassica napus*.** Data are taken from Solís et al., 2012.

Finally, as a genetically controlled mechanism, programmed cell death (PCD) has been associated with embryogenesis (Suarez et al., 2004).

Microspore embryogenesis has been examined at transcriptional and metabolomic level in a number of species including *Brassica napus*, *Hordeum vulgare*, and tobacco microspores (Malik et al., 2007; Maraschin et al., 2006; Hosp et al., 2007). However, little is still known about the metabolic processes taking place during the early steps of microspore embryogenesis in bread wheat. In particular, cultivar 'Svilena', a Bulgarian winter wheat, has

established itself as an ideal model-genotype due to its high regeneration efficiency (Lantos et al., 2013).

2.5. Genotype dependence and albino formation

Practically, microspore embryogenesis has two disadvantages: the genotype dependence and the albino formation.

Genotype dependence in microspore embryogenesis has been reported in many species, such as pepper (Mitykó et al., 1995), *Raphanus sativus* (Takahata et al., 1996) or *Triticum aestivum* (Bitsch et al., 1998). Malik et al. (2007) compared the expression of several genetic markers in *Brassica napus* genotypes with different regeneration efficiency and found a high correlation with the embryogenic potential (figure 4). In *Hordeum vulgare*, three DH lines with different response to microspore embryogenesis were subjected to a transcriptome analysis revealing a number of genes related to the efficiency of the process, such as PR genes. Particularly, beta-1,3-glucanase is suggested as a marker of high green plant production (Muñoz-Amatriaín et al., 2009). Moreover, PCD events were suggested to appear differentially in genotypes with different regeneration efficiency in barley (Jacquard et al., 2009).
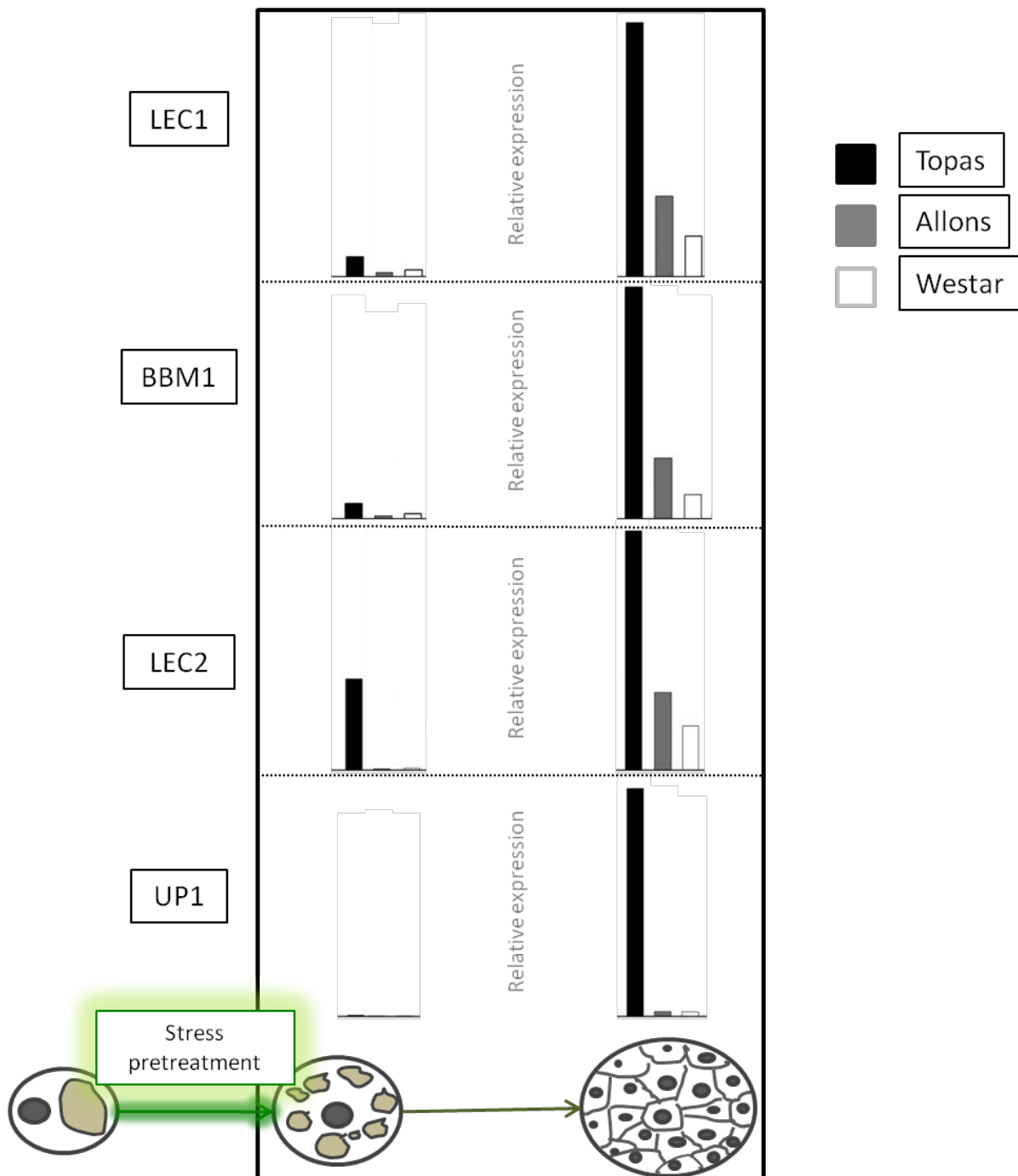
Figure 4: **Relative expression of 4 microspore embryogenesis markers in 3 differentially regenerating lines of *Brassica napus* at 3 and 7 days after the heat stress pretreatment.** The high regeneration efficiency line 'Topas' shows a higher increase 7 days after treatment in the expression of the selected genes than the low efficiency lines 'Allons' and 'Westar'. LEC1, BBM1, LEC2 and UP1 stand for Leafy cotyledon 1, BabyBoom 1, Leafy cotyledon2 and Unknown protein 1. Graphs are modified from Malik et al., 2007.

The regeneration efficiency dependent on the genotype has been shown to be a stable trait in the first generations of several species, such as pepper (Cheng et al., 2013) or coffee (Molina et al., 2002). This suggests that it could be a predictable parameter. In addition, detection of useful genotypes has been the aim of studies, such as rice varieties used for in vitro hybridization or transformation (Khalequzzaman et al., 2005) and durum wheat genotypes tolerant to salt stress (Arzani and Mirodjagh, 1999). The selection of favorable alleles for regeneration of wheat would be a desirable approach to obtain the best genotype.

Albino plants are devoid of chloroplasts and unable to perform photosynthesis. Albinism occurs in several species such as wheat, rye or barley, and it is also a genotype dependent trait (Makowska and Oleszczuk, 2014). In microspore embryogenesis, albinism is produced when the proplastids are not able to become chloroplasts (Makowska and Oleszczuk, 2014). Differences in plastids of different genotypes are evident in early stages in barley. After a first decrease in the plastid number during the cold stress, their number increases and they transform into chloroplasts after a certain time in induction medium. At this point, the plastids of albino plants are characterized by higher starch content and by loss of thylakoids and differentiation into amyloplasts (Caredda et al, 1999; 2000). The source of genotype dependence and albinism events in the microspore embryogenesis is still unclear and requires further investigation.

2.6. Aims of the study

The main aims of this thesis are:

- To elucidate the major metabolic pathways that define the microspore embryogenesis process in a time-dependent manner in *Triticum aestivum*.
- To identify the initial molecular events that allow a successful plant regeneration after microspore embryogenesis in bread wheat.

The novelty of the study and the expected outcome will be the metabolic events that carachterize the first stages of the process visualized in the context of the metabolic

pathways in bread wheat. The metabolic and proteomic comparison of DH lines with different green plant regeneration rates will additionally show the source of the successful plant regeneration that has not been elucidated in bread wheat until now. Practically, one can wonder whether some metabolites will arise as markers of the process and whether they could be used for GPR rate prediction. Using them as GPR rate prediction markers would allow shorting the time to develop new varieties and genotypes through microspore embryogenesis induction.

3. Material and methods

3.1. Plant material for microspore embryogenesis and genotype dependence studies

Donor plants (*Triticum aestivum* 'Svilena' and 'Berengar') were grown by the Saaten Union Biotech GmbH, as described by Rubtsova et al. (2013). Cultivar 'Svilena' is highly responsive to stress-induced microspore embryogenesis (Schlegel et al., 2000) and hence it was used to study the first stages of microspore embryogenesis. Cultivars 'Svilena' and 'Berengar', which present high and low regeneration capacity, respectively, were used to study the regeneration efficiency related to the genotype.

These cultivars were crossed by Saaten Union Biotech GmbH to generate a mapping population of DH lines for the study of the regeneration rate. The parents were generated using interspecific crosses of F1-plants with maize, to avoid any bias for further analysis of the doubled haploid lines using the microspore-based anther culture. The GPR rate of the 137 generated DH lines and the parents during microspore embryogenesis was calculated as the green regenerants per spike. The GPR and albinos rates were measured in triplicate, and the average was taken for further analysis. In this study, microspores were collected from the 7 DH lines with highest and the 7 with lowest GPR rate and their parents.

3.2. Androgenesis induction and microspore isolation

Anthers were harvested by Saaten Union Biotech GmbH when the microspores reached the mid-late uninuclear stage (referred to as T1) of the pollen developmental pathway. The second harvesting point followed a 10 days exposure to 4°C (T2), when slightly enlarged microspores with a star-like structure were seen. The final point of harvest of microspores (T3) was taken 4 to 8 days after in vitro cultivation of the anthers in induction media (Rubtsova et al., 2013). At that stage the first nuclear division had occurred. The developmental stage of the microspores was checked daily using a light microscope (20x magnification). When 5-10% of microspores showed visible karyokineses, all anthers of a petri dish were used for isolation. The responsiveness of the used spikes and thus the quality of isolated microspores were checked also by regenerating plants from incubated anthers.

Therefore, anther culture was done using up to 12 spikes that were left for regeneration and were not used for extracting microspores. The resulting somatic embryos were transferred to the regeneration media and finally the number of green and albino plants was counted as described in Lantos et al. (2006). Since the amount of responding microspores was reduced with each stage, the number of spikes had to be adapted to obtain a similar number of responding microspores in each isolation replicate.

After collecting the anthers, the microspores were isolated also by Saaten Union Biotech GmbH with gradient centrifugation in a Heraeus Biofuge Primo R with a swing bucket rotor (ThermoFisher Scientific, Darmstadt, Germany) that allowed the enrichment of microspores at the selected developmental stage and the exclusion of dead or arrested microspores. Collected anthers were homogenized in 0.4 M mannitol and then centrifuged at 100 g for 5 min. The pellet was rinsed twice in 0.4 M mannitol, centrifuged at 100 g for 5 min, then, laid over 20% maltose and centrifuged at 100 g for 4 min. The non-viable microspores were discarded. The interphase was rinsed with 0.4 M mannitol, centrifuged (100 g, 10 min) and suspended in a small volume of 0.1 M ammonium bicarbonate. The concentration and purity of microspores in suspension was determined by direct counting using light microscopy (20x magnification) from three suspensions of 1 µL. The microspores were pelleted by centrifugation (100 g, 10 min), immediately frozen in liquid nitrogen and kept at -80°C. For the following analyses, everything was done on ice. I resuspended and vortexed the samples in 1 mL 0.1 M ammonium bicarbonate pH 7.5. Finally, the suspension with lysed microspores was mixed and centrifuged (18000 g, 10 min, 4°C). For each of T1 through to T3, at least four biological replicates were analyzed, with each replicate represented by three technical replicates.

3.3. Untargeted analysis of metabolites

From the supernatant of the lysate of the microspores, different volumes that corresponded to a range of 600 to 60000 'Svilena' microspores were used to identify the maximum number of detected peaks with gas chromatography coupled to mass spectrometry (GC-MS). For untargeted metabolite analysis, the volume of 6000 microspores (the optimal number of microspores obtained) firstly of 'Svilena' and then of the DH lines and the parents was

vacuum-dried. Metabolite extraction was done in 1 vol. methanol, containing [13]C Glucose (Cortecnet, Voisins-Le-Bretonneux, France) as internal standard, 1 vol. pure water (18.2 MΩ cm; Merck Millipore, Darmstadt, Germany) and 0.5 vol. $CHCl_3$. The detection of the metabolites from the polar and apolar phases was performed following Lippmann et al. (2009), with minor modifications. Both the upper methanol-water phase and the lower apolar phase (100 µL and 30 µL, respectively) were vacuum-dried. The polar phase was derivatized by adding 25 µL 20 mg mL^{-1} methoxyamine hydrochloride (MAH) for oximation in pyridine and holding at 37°C for 120 min with shaking, then, by adding 25 µL MSTFA (N-methyl-[N-trimethylsilyl]trifluoroacteamide) for silylation of the molecules, and holding at 37°C for 30 min with shaking. The apolar phase was derivatized only with MSTFA. Both derivatizations were done using a multipurpose sampler (Gerstel, Mülheim an der Ruhr, Germany). Retention time shifts were controlled with a C7-C30 n-alkane mixture (Sigma-Aldrich, St. Louis, MO, USA) in MSTFA at a concentration of 1 µg mL^{-1}. For normalization purposes, additional vials of reference samples were prepared by taking the proportional part of each sample to a final amount of 6000 microspores. The metabolites from these vials were extracted with the same procedure as the samples. One microliter aliquot of every sample was then injected into an Agilent A7890 device (Agilent Technologies, Waldbronn, Germany) in split-less mode at 240°C. Separation was achieved by passing through a 30 m GC fused silica capillary column of thickness 0.25 µm and internal diameter 0.25 mm (Restek, Bad Homburg, Germany). Helium was used as the carrier gas supplied at a flow rate of 1 mL min^{-1}. The chromatography program started with a column isothermal temperature of 80°C for 3 min, then the temperature was increased at 5°C min^{-1} until reaching 300°C. After a 5 min hold, the column was cooled down to 80°C over 7 min. Primary metabolites were identified with a Tof mass spectrometer GCT Premier (Waters, Eschborn, Germany), set to measure compounds over the *m/z* range 50-700 in centroid mode, taking advantage of the dynamic range enhancement mode. Identification and annotation of compounds was facilitated by reference to the NIST 05 library (Waters), while quantification was obtained using MassLynx software (Waters). Validation of the annotated compounds was further performed by the calculation of the retention index of each compound. These indices were compared to those documented in the Golm Metabolome Database (http://gmd.mpimp-

golm.mpg.de/). Normalization was achieved using the deviation-from-the-mean factor, calculated by dividing the mixed sample value by the average value of all the mixed samples.

3.4. Targeted analysis of amino acids

From the supernatant of the lysate, different volumes corresponding to the range of 30 - 30000 'Svilena' microspores were first taken to identify the detection limit of the method. Although the detection limit was set in 600 microspores, a higher number of microspores was used in order to obtain high-intensity peaks, which allow for an easier analysis of chromatograms. The volume corresponding to 2000 microspores firstly of 'Svilena' and then of the DH lines and the parents was used for quantification. After vacuum drying, the samples were incubated for 30 min in 80 µL methanol at 70°C with shaking. Then, 0.5 and 1 volume of $CHCl_3$ and pure water (18.2 MΩ cm; Merck Millipore) were added, respectively. In order to separate the polar and apolar phases the samples were centrifuged (18000 g, 15 min, 4°C), and an 80 µL aliquot of the upper methanol-water phase was vacuum-dried and re-dissolved in 10 µL water. The AccQ Fluor kit (Waters) was used for derivatization of amino acids, following the manufacturer's instructions. A serially diluted standard mixture of amino acids was derivatized similarly for quantification purposes. A 1 µL aliquot was injected into an AccQ-Tag Ultra 1.7 µm, 2.1x100 mm UPLC column (Waters), as recommended by the manufacturer. Derivatized amino acids were excited at 266 nm and detected by fluorescence with an emission wavelength of 473 nm. The identification and absolute quantification of amino acids was achieved by comparing the peaks with the corresponding standards using Empower software (Waters).

3.5. Integrative 'omics approach

The metabolomic data were integrated with existing transcriptomic data obtained by Seifert et al. (2016) who conducted an RNA-seq analysis of 'Svilena' microspores at T1 through T3 stages. The analysis was performed within a functional context of metabolic pathways, using the software VANTED (Rohn et al., 2012), in combination with MetaCrop (Schreiber et al., 2012). The wheat-specific metabolic pathways obtained from MetaCrop were manually

extended for the γ-aminobutyric acid (GABA) shunt and selected reactions within lipid and starch metabolism.

3.6. Analysis of the abundance of glutamine synthetase

3.6.1. Sample preparation

The pellet of the lysate was suspended in 1 mL 0.1 M ammonium bicarbonate pH 7.5. The volume equivalent to 10000 microspores, from each of the T1, T2 and T3 stage preparations, was vacuum-dried, and then, extracted in loading buffer containing 56 mM Na_2CO_3, 56 mM dithioerythritol (DTT), 0.1% (w/v) SDS, 12% (w/v) sucrose and 0.04% bromophenol blue. As a positive control, homogenized leaf material from 'Bob White' was extracted in 100 mM HEPES-KOH (pH 7.5), 5 mM magnesium acetate, 1 mM EDTA, 1 mM EGTA, 0.1% (v/v) Triton X-100, complete EDTA-free protease inhibitor cocktail tablets (Sigma-Aldrich), 1% (w/v) PVP and 2mM DTT. After incubation for 10 min at 4°C, the extract was centrifuged (16000 g, 5 min) and the supernatant was desalted through a Sephadex G25 spin column (GE Healthcare Life Sciences; Freiburg, Germany), following the manufacturer's protocol. After protein determination by Bradford method (Bradford, 1976), 5 µg aliquot of protein was re-suspended in loading buffer prior to loading it into the SDS-PAGE gel.

3.6.2. Western blotting procedure

Electrophoresis through a 12% SDS polyacrylamide gel was used to separate the proteins in the samples. Semi-wet transference to PDVF membrane (Bio-Rad Laboratories GmbH, München, Germany) was followed by blocking with 5% (w/v) milk powder in Tris buffered saline with Tween-20 (TBST). The membrane was probed with anti GS antibody at 1:10000 dilution (anti- GS1 and GS2; AgriSera, Vännäs, Sweden). After rinsing in TBST, the membrane was incubated in a 1:15000 dilution of IRDye 800 anti-rabbit antibody (LiCor-Biotechnology GmbH, Bad Homburg, Germany), and the signal was visualized using a LiCor Odyssey® scanner.

3.6.3.   Sequence-based GS isoform differentiation

The sequence of the GS transcript (given by Prof. Dr. Scholten) was subjected to a BlastN search against the genome of *Triticum aestivum* of the Ensembl Plant database (plants.ensembl.org/index.htmL). The top hit gene encoded an uncharacterized protein, which was then used as a search string to identify the protein via a BlastP search. The top hit result was the sequence of GS1 from rye.

3.7.   Correlation analysis

A correlation analysis (Spearman correlation) was performed between the concentration of each metabolite and the GPR rate of the plants, or with the albino plant rates, using SigmaPlot v13.0 (Systat software Inc.). In the case of amino acids two values were obtained, one from the untargeted and one from the targeted analysis. Here, correlation analysis was performed only with data from the targeted analysis, because it has a higher dynamic range and therefore leads to more pronounced differences between amino acid profiles than GC-MS (Böttcher et al., 2008).

3.8.   Predictive model development

In order to develop a predictive model (performed by Dr. Armin Meister) for the GPR rate, firstly, a forward stepwise regression was performed between the variables (metabolites) used for the correlation analysis. In this model, only the identified compounds were considered, whereas those annotated as unknown were excluded. This type of regression fits the general equation:

$y = b_0 + b_1 x_1 + b_2 x_2 + b_3 x_3 + ... b_k x_k,$

where y is the GPR rate, x_1, x_2, x_3, ..., x_k are the metabolite concentrations, and b_0, b_1, b_2, b_3, ..., b_k are the regression coefficients.

The number of variables present in the model was set in 7 after using the following criteria: passing normality (Shapiro-Wilk test), constant variance tests, high adjusted-R^2 (above 0.8) and low standard error of estimate (below 5.6). The regression coefficients were calculated for each variable. Together with the prediction success the practicality of the model was also considered. Therefore, 3 sets of input variables were used to build the model: metabolites detected in GC-MS only, metabolites detected in UPLC only and metabolites detected in both measurements.

The model was validated by using the metabolic data of 2 DH lines (one of each group) that were left out of the model development. These lines (DH line 38 and 86) were randomly selected from the high and low regeneration efficiency groups. In order to validate the findings, the metabolite concentrations of the two lines were applied into the model.

The model was developed using Sigmaplot v.13.0 (Systat Software Inc.), while the validation test was performed using Microsoft Excel 2010 (Microsoft).

3.9. Proteome analysis by nano LC-ESI-Q-TOF

3.9.1. Protein precipitation

The pellet of the lysate from cultivars 'Svilena' and 'Berengar' was used for this analysis. Protein extraction was performed following Witzel et al. (2009), with some modifications. Different volumes were first extracted and tested, to determine the necessary number of microspores to obtain sufficient signal intensities. Based on the initial test, the volume corresponding to 10000 microspores was used for protein precipitation. Ten volumes of 10% trichloroacetic acid and 0.5% DTT in acetone were added. After mixing and keeping the samples for 45 min at -20°C (mixing every 15 min), they were centrifuged at 20000 g 15 min and 4°C. The pellet was then resolved in 100% acetone with 0.1% DTT and kept 1 h at -20°C. Finally, after drying in vacuum, samples were resolved in 50 µL TE buffer containing 10 mM Tris and 1 mM EDTA. Protein content was measured by Bradford method (Bradford, 1976). However, it was not detectable in the 10000 microspores samples. Thus, it was calculated

from a 20000 microspores sample of 'Svilena', meaning that all the samples were less abundant. Three biological replicates and two technical replicates were prepared for the analysis of each cultivar in each stage of the microspore embryogenesis. However, due to the low availability of samples, some of the replicates analyzed from cultivar 'Berengar' had been isolated in mannitol without the last wash in ammonium bicarbonate. Since there were no differences between the replicates with and without the wash in ammonium bicarbonate, these replicates were included in the analysis.

3.9.2. In-filter peptide digestion with trypsin

The precipitated protein was dissolved in denaturation buffer (8 M Urea, 0.1 M Tris, 5 mM EDTA, pH 8) to 100 µL of final volume, and it was applied into a Microcon YM-10 filter (Merck Millipore). The filter unit was centrifuged for 60 min at 14000 g and room temperature. After washing three times with 100 µL denaturation buffer, 150 µL of 20 mM DTT in denaturation buffer was added and the filter unit incubated for 1 h at 60°C. Then, 50 µL of 0.08 mM of iodoacetamide in denaturation buffer were added and mixed. The filter unit was then incubated 30 min at 37°C in darkness. These solutions were removed by centrifugation at 14000 g 30 min at room temperature, and by washing three times with 100 µL of 50 mM ammonium bicarbonate. After centrifuging until dryness, protein digestion was carried out by the addition of 10 ng µL^{-1} of trypsin in 5 mM ammonium bicarbonate and 5% AcN (Promega, Madison, USA) in a trypsin:protein ratio of at least 1:50 at 37°C overnight. Resulting peptides were passed through the filter by centrifugation at 14000 g for 30 min and dried in vacuum. Finally, they were resolved in 0.1% formic acid in pure water (18.2 MΩ cm; Merck Millipore).

3.9.3. Untargeted detection of peptides by liquid chromatography mass spectrometry

The digested samples were subjected to nano-liquid chromatography (nanoLC) analysis on an UltiMate 3000 RS system (ThermoFisher Scientific), controlled with Chromeleon Xpress software (ThermoFischer Scientific). Peptide separation was achieved by injecting 10 µL of

the digestion into a Nano Trap Column (Acclaim PepMap100 C18, 5 μm, 100 Å) and 50 cm x 75 μm analytical column (Acclaim PepMap RSLC C18, Thermo Fisher Scientific), at 8 and 60 °C, for the samples and column temperatures, respectively. The nanoLC program was set using HyStar version 3.2 software (Bruker Daltonics, Bremen, Germany). The flow rate of the two solvents A (0.1% formic acid in water) and B (0.1% formic acid in AcN) was 0.300 μL sec^{-1}. For the first 5 min, solvent B was provided at a constant concentration of 2%. Then, the concentration of solvent B increased gradually to 40% within 125 min, and to 95% within 5 min, where it was held in this concentration for 20 min. Finally, solvent B concentration dropped down to 2% in 1 min and was held at this level for 9 min. The effluent was directed to the CaptiveSpray ion source coupled to an impact II mass spectrometer (Bruker Daltonics), operating in a positive ion mode with a source temperature of 150°C, a gas flow of 3 L min^{-1} and 1600 V. The instrument was calibrated by using selected fragment ions of 10 mM sodium formate. Spectra were acquired and integrated in centroid mode using auto MS and MS/MS mode from the predefined InstantExpertise method (Bruker Daltonics) with a fixed cycle time of 3 s, implemented in the OtofControl version 4.0 software (Bruker Daltonics), in the *m/z* range of 150 to 2200.

3.9.4. Peptide and protein identification and quantification

Resulting data files were imported in Progenesis QI for Proteomics software (Nonlinear Dynamics, Newcastle upon Tyne, UK) for data processing, with a filter strength of x15 in order to reduce signal noise. Automatic processing of the samples included automatic selection of a reference run and automatic alignment of the runs and peak picking (set between 30 and 136 min, excluding signals from eluents and contaminants). Peptide identification was performed using the MASCOT v. 2.5.1 search engine (Matrix Science, London, UK; www.matrixscience.com) with a database file downloaded from UniProt (www.uniprot.org) that contained protein sequences from *Triticum aestivum*, human keratin and trypsin (downloaded on November 16, 2016, containing 114216 entries). The following search parameters were used: 10 ppm peptide and 0.1 Da fragment mass tolerance, one missed cleavage, variable modifactions: methionine oxidation, cysteine propionamide, and the fixed modification cysteine carbamidomethylation.

Peptide and protein relative quantification were done with Progenesis QI for Proteomics software (Nonlinear Dynamics). Only unique peptides were used for the protein normalized relative concentration, which was taken for protein abundance comparisons. Other filters applied were p value < 0.05 in peptide identification (peptide ion score cut-off 13), at least 2 unique peptides and fold change > 1.5 in characterized proteins from *Triticum aestivum*.

3.10. Statistical analysis

Metabolome data normalization and quantification were generated in Microsoft Excel 2010 (Microsoft, CA, USA). Significant differences between the stages T1, T2 and T3 in 'Svilena' microspores were tested by a Kruskal-Wallis One Way Analysis of Variance on Ranks test, since the data did not follow a normal distribution. Significant differences between means of the microspores of the DH lines and the parents were tested by Mann-Whitney U test.

Proteome statistics included a Mann-Whitney U test when comparing data of 'Svilena' and 'Berengar'. Additionally, ANOVA on ranks test was performed between the stages in the lines in order to validate and to add information to the subsection 3.3., in the characterization of the three studied stages of the process.

Statistical analysis was performed using SigmaPlot v.13.0 software (Systat Software Inc., San Jose, CA, USA).

4. Results

In this section, the results of the metabolic analysis in 'Svilena' are first shown, and interpreted together with transcriptomic data (given by Dr. Scholten) in the context of metabolic pathways. Later, the metabolism is presented in DH lines with different regeneration efficiency coming from the cross of 'Svilena' and 'Berengar', with high and low regeneration rate, respectively. Practically, potential metabolic markers for the green plant regeneration rate identified are exposed. Finally, the results from the proteome analysis of 'Svilena' and 'Berengar' are displayed.

4.1. Metabolome characterization during microspore embryogenesis in 'Svilena' microspores

4.1.1. Untargeted analysis of metabolites

Gas chromatography-mass spectrometry analysis revealed more than 100 primary metabolites in 'Svilena' samples. Although a number of compounds could be detected in a sample containing 600 microspores, the highest number of compounds in the polar phase was detected in a sample with 6000 microspores (figure 5). Relative quantification was possible for more than 60 compounds from the polar and apolar phases (figures 6 to 10), including amino acids, organic acids and fatty acids, sugars and a set of unknown compounds.
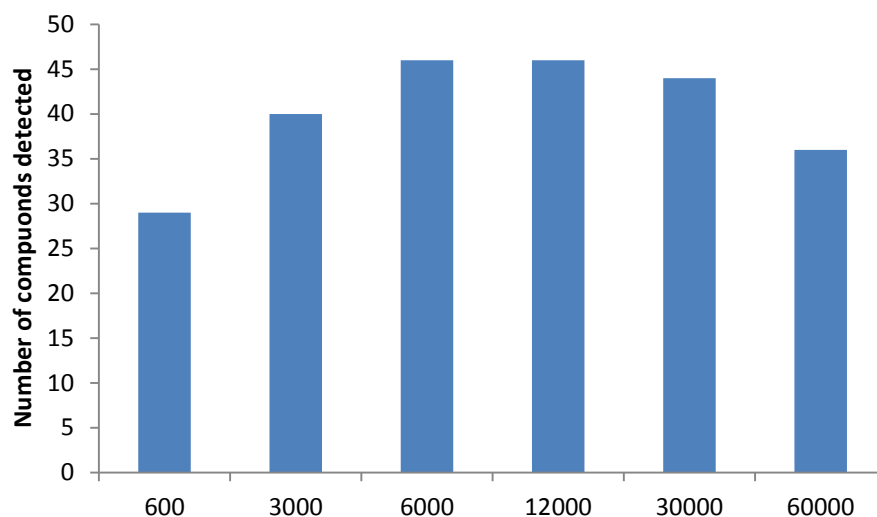
Figure 5: **Limit of detection of the untargeted analysis of metabolites using gas chromatography mass spectrometry**. The number of compounds of the polar phase that are quantificable and identified (saturated and unknown compounds excluded) were detected in 'Svilena' samples in T1 stage with different amount of microspores, ranging from 600 to 60000. The highest number of compounds is detected first in the 6000 microspore sample, and also in the 12000 one, after which the number decreased due to the saturation of compounds.

Amino acid levels differed through the T1-T3 period (figure 6). Most of the content of amino acids detected between T1 and T2 was stable, while some of them increased in T3 stage, particularly asparagine, aspartate and ornithine-1,5-lactam (might be ornithine, being the lactam an artifact). Different profile was found for alanine and glycine, which showed a tendency to increase in T2, and to decrease in T3. Such a profile was also similar for organic acids, in particular for the TCA cycle intermediates malic, fumaric and citric acids (figure 7). Among them, malic acid had the highest concentration.

Figure 6: **Amino acids detected in the polar phase of cultivar 'Svilena' microspores during the first steps of microspore embryogenesis**. T1 represents the stage when the microspore is in its uninucleate stage; T2, the stage after a cold stress treatment; and T3, the stage after the early first nuclear division. Statistical analysis: Kruskal-Wallis ANOVA on ranks, * when p value < 0.05.
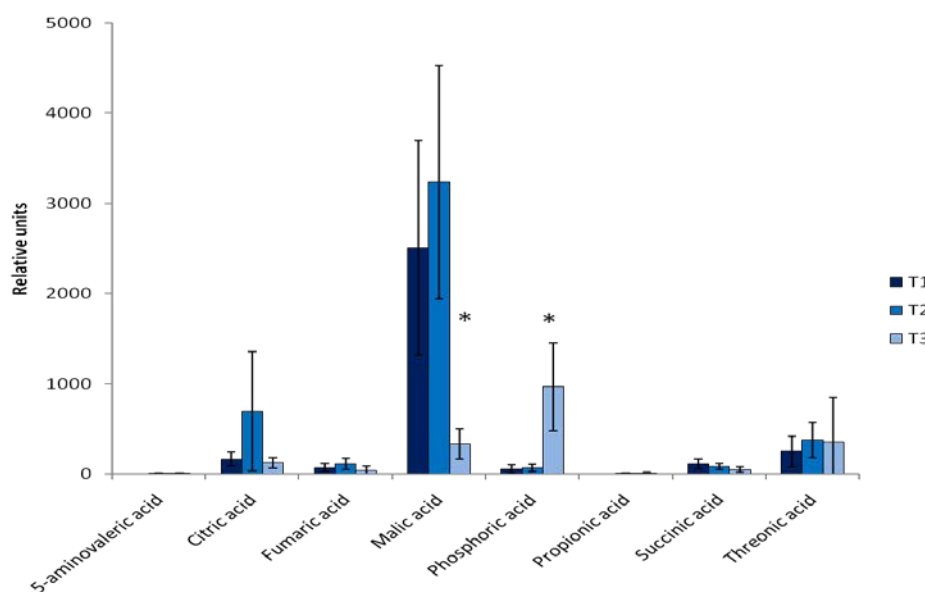
Figure 7: **Organic acids detected in the polar phase of cultivar 'Svilena' microspores during the first steps of microspore embryogenesis**. T1 represents the stage when the microspore is in its uninucleate stage; T2, the stage after a cold stress treatment; and T3, the stage after the early first nuclear division. Statistical analysis: Kruskal-Wallis ANOVA on ranks, * when p value < 0.05.

An increase, although without statistical significance, in T2 stage was also experimented by the average levels of the sugars trehalose, myo-inositol, sucrose and maltose (figure 8). While sucrose continued to increase in T3 stage, the concentration of glucose, trehalose and maltose tended to decrease in that stage. Among all sugars, glucose and maltose had the highest concentration.
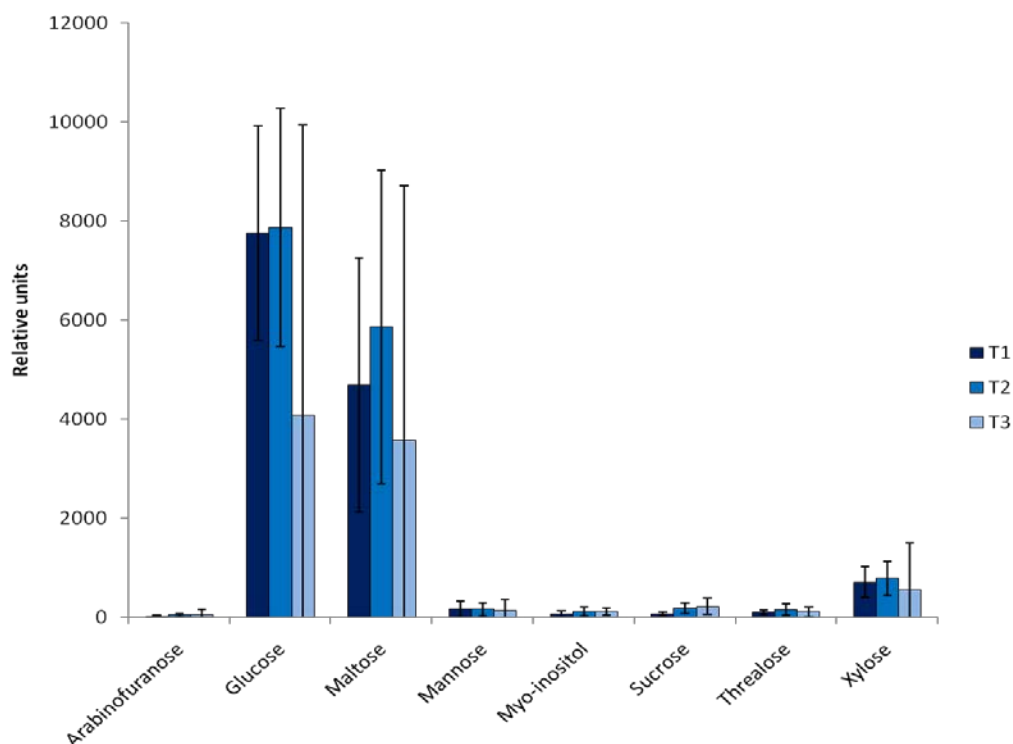
Figure 8: **Sugars detected in the polar phase of cultivar 'Svilena' microspores during the first steps of microspore embryogenesis**. T1 represents the stage when the microspore is in its uninucleate stage; T2, the stage after a cold stress treatment; and T3, the stage after the early first nuclear division. Statistical analysis: Kruskal-Wallis ANOVA on ranks, * when p value < 0.05.

Concerning fatty acids, slight differences between the concentrations were found, although without statistical significance (figure 10). Dicarboxylic acids azelaic and suberic acids both tended to accumulate between T1 and T2. Finally, two of the unknown compounds from the polar phase showed either a decrease or an increase in T3 stage. These were unknown #4 and #9, respectively (figure 9).The abundance of the compounds detected by the GC-MS analysis varied markedly between biological replicates.
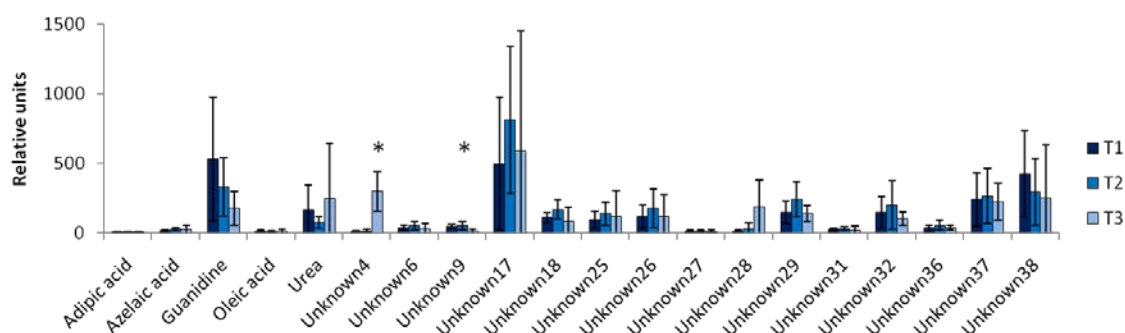
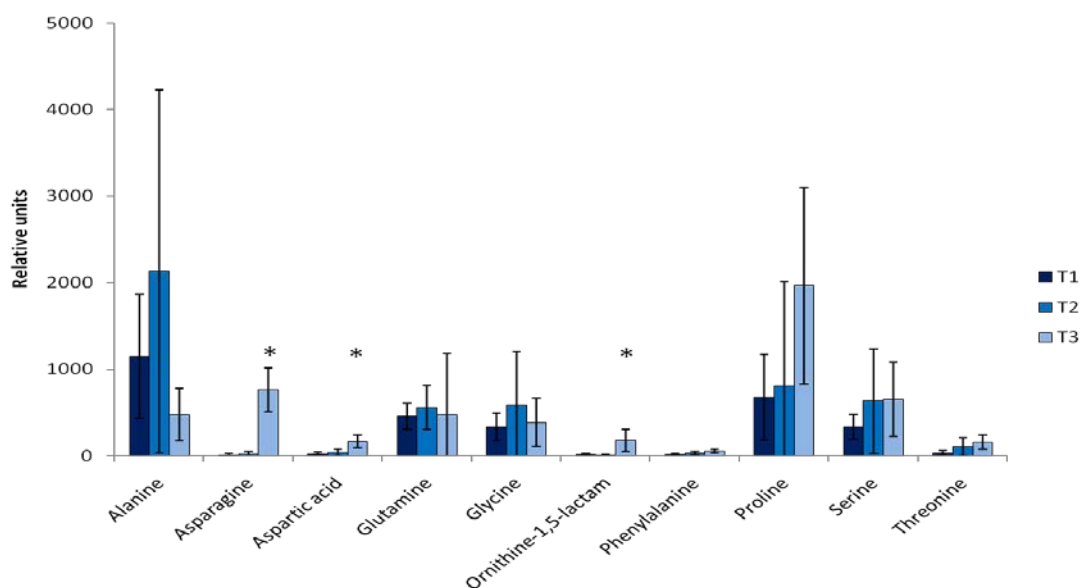Figure 9: **Other metabolites detected in the polar phase of cultivar 'Svilena' microspores during the first steps of microspore embryogenesis**. T1 represents the stage when the microspore is in its uninucleate stage; T2, the stage after a cold stress treatment; and T3, the stage after the early first nuclear division. Statistical analysis: Kruskal-Wallis ANOVA on ranks, * when p value < 0.05.
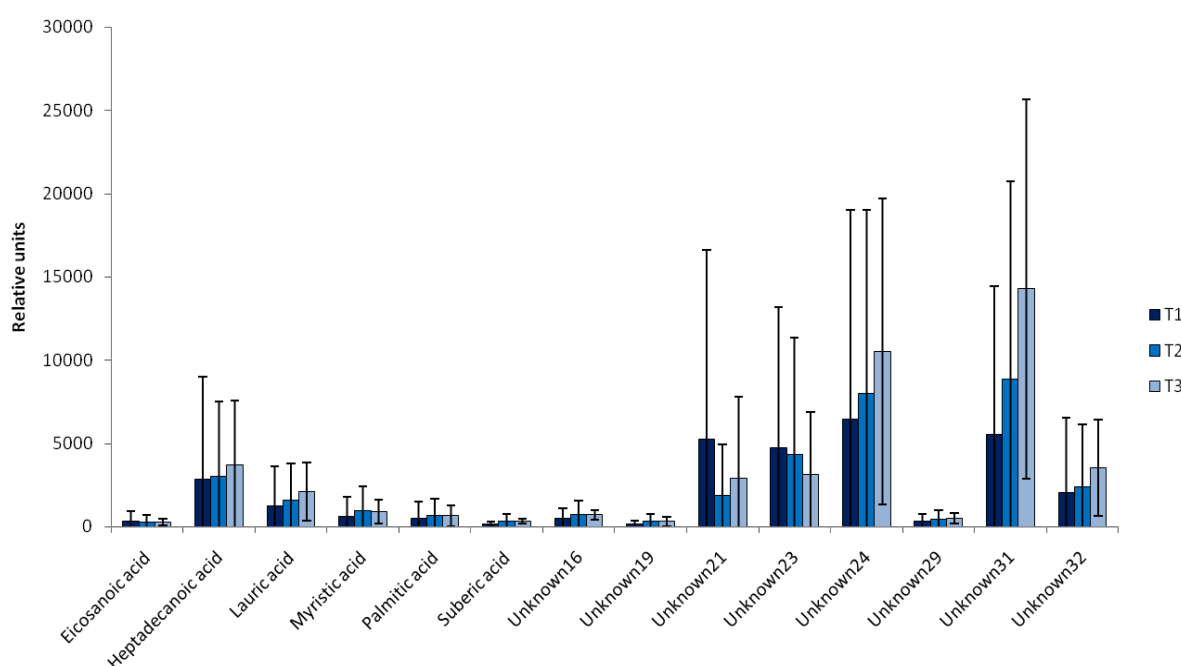

Figure 10: **Metabolites detected in the apolar phase of 'Svilena' microspores during the first steps of microspore embryogenesis**. The relative concentrations are shown for the fatty acids, dicarboxylic acids and unknown compounds. The three studied stages are shown, T1, when the microspore is in its uninucleate stage, T2 after a cold stress treatment and T3 after the early first nuclear division. Statistical analysis: Kruskal-Wallis ANOVA on ranks, * when p value < 0.05.

4.1.2. Targeted analysis of amino acids

Targeted analysis of amino acids using UPLC has previously been shown to give more pronounced differences between amino acid profiles due to a higher dynamic range than GC-MS (Böttcher et al., 2008). Therefore, the results from the untargeted analysis were complemented and validated with the UPLC analysis. Repeatability of results could be obtained even with 600 microspores, however, the standard deviation was lower for the samples containing 1200 microspores (figure 11).

In this targeted analysis, 22 amino acids were detected in the samples through fluorescence detection. The total amino acid amount, seen as the sum of all individual amino acid peaks detected, showed a significant increase only in the T3 stage (figure 12). The concentrations recovered from the UPLC analysis, using serial dilutions of amino acid standards, were 116 pmol per 100 microspores (T1), 110 pmol per 100 microspores (T2) and almost a four-fold increase, 406 pmol per 100 microspores (T3).

When the level of individual amino acids was examined, the highest concentrations were found for alanine and tyrosine, both in T1 (respectively 31 and 22 pmol per 100 microspores) and T2 (34 and 28 pmol per 100 microspores), while in T3, asparagine (121 pmol per 100 microspores) and glutamine (141 pmol per 100 microspores) showed extremely high concentrations (figure 13). The latter explained mostly the four-fold increase in T3 of the total amino acid content shown in figure 12. Significant differences between T2 and T3 were also observed for arginine, asparagine, GABA, glutamine, histidine, isoleucine, leucine, lysine, phenylalanine, proline, threonine and valine.
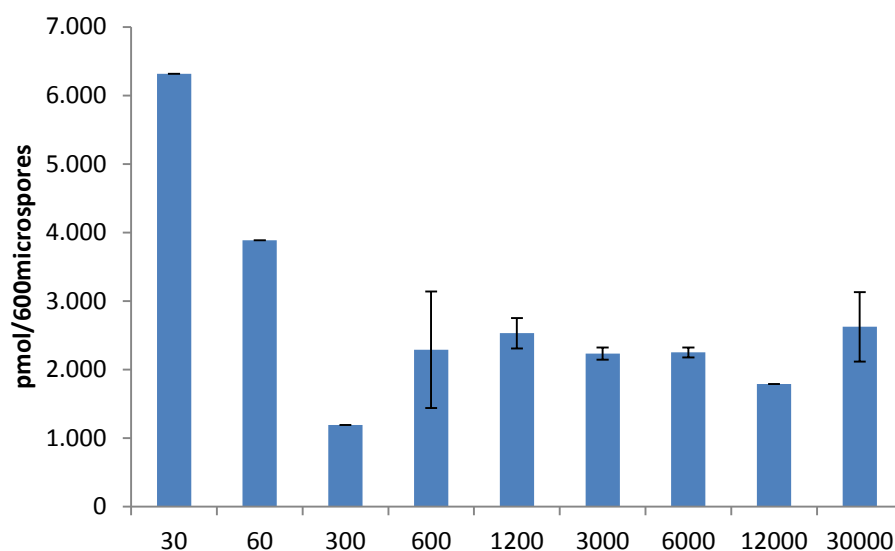
Figure 11: **Limit of detection of the targeted analysis of amino acids**. Total amino acid concentration detected in 'Svilena' samples in T1 with different amount of microspores, ranging from 30 to 30000. Concentrations in pmol 600 microspores^{-1}. Although, two technical replicates were measured for each sample, the result of one was omitted in the first three samples (30-300 microspores) since it gave no consistent results. Repeatability is shown rom the sample with 600 microspores on.
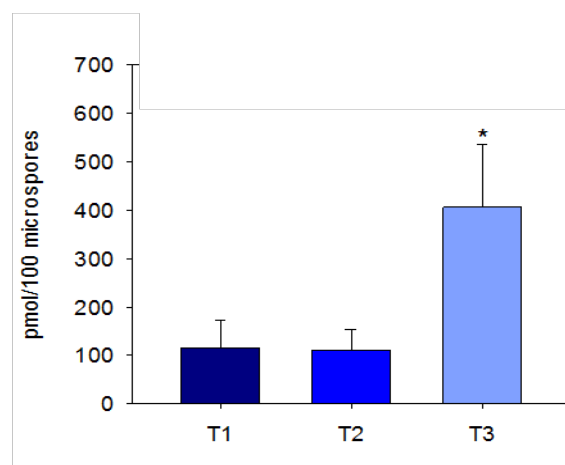
Figure 12: **Total amino acid content detected by UPLC in microspores of wheat cultivar 'Svilena'**. The concentrations were calculated from the sum of all individual amino acid peaks detected. The three studied stages are shown, T1, when the microspore is in its uninucleate stage, T2 after a cold stress treatment and T3 after the early first nuclear division. The data were subjected to a Kruskal-Wallis analysis of variance on ranks, * $p < 0.05$.
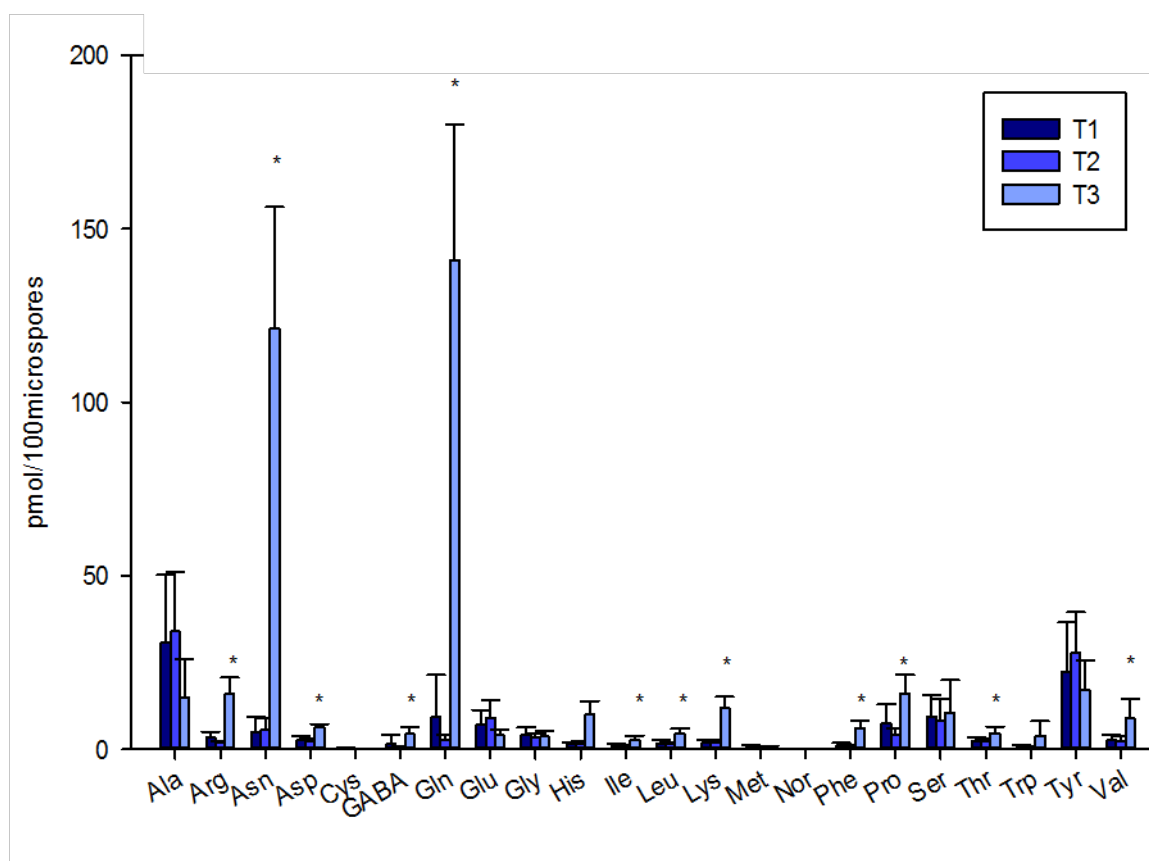
Figure 13: **Abundance of individual amino acids detected by UPLC in the microspores of wheat cultivar 'Svilena'**. The three studied stages are shown, T1, when the microspore is in its uninucleate stage, T2 after a cold stress treatment and T3 after the early first nuclear division. The data were subjected to a Kruskal-Wallis analysis of variance on ranks, * $p < 0.05$.

4.1.3. Integrative –omics view of the metabolome during microspore embryogenesis

Metabolite and transcript profiles were co-analyzed within the context of metabolic pathways. Figure 14 presents a schematic representation of the cell compartments showing the metabolic pathways in which both metabolite and transcript profiles were examined together during the microspore embryogenesis. A prompt recognition of the biosynthesis and degradation processes arises from this map. Details of this map are shown in following figures.

Metabolic reactions are found inside the cell compartments: cytosol (beige), mitochondrion (blue), plastid (green), peroxysome (light blue), glyoxysome (orange), vacuole (lila), and unknown compounds in the external yellow compartment. Reversible (double headed arrows) and irreversible (single headed arrows) reactions are catalyzed by the corresponding enzymes (squares). For each enzyme, a bar chart showing the dynamics of transcription of the encoding gene is given. The bar charts relating to metabolites (circles) represent metabolite profiles over the T1-T3 period. Metabolites or enzymes occurring multiple times in the metabolic network are marked with a clone marker, represented in the map as a black mark inside the glyph. A red border indicates a p value < 0.05 in at least one comparison (based on a Kruskal-Wallis analysis of variance on ranks).

4.1.3.1. Starch and sugars metabolism

In starch metabolism, the degradation and accumulation of starch (referred to as "glucan" in figure 15) between T1 and T2 and between T2 and T3, respectively, was consistent with the expression of β-amylase and starch synthase genes. The transcription of β-amylase (EC 3.2.1.2), which converts starch into maltose, decreased in T3 stage. Starch synthase (EC 2.4.1.21) uses glucose as substrate to synthesize starch, and its transcript expression decreased slightly in T2, but then increased highly in T3. These results are consistent with the profiles of both maltose and glucose, where the concentrations showed a tendency to decrease in T3 stage. Finally, the transcript levels of two genes coding for UDP-glucuronate decarboxylase and xylan 1,4-beta-xylosidase (EC 4.1.1.35 and 3.2.1.37, respectively) decreased in T3 stage. These enzymes are involved in the xylan and xylose biosynthetic pathway. UDP-glucose wouldn´t be catalyzed into UPD-xylose, but might pursue the glucan synthesis. Overall, these findings suggest that starch is formed in T3 stage. Therefore, this compound should be measured in the samples in additional studies.

Regarding sugar metabolism (figure 16), both metabolic and transcriptomic datasets showed high diversity of profiles. For instance, in the trehalose synthesis pathway, a tendency to decrease in trehalose was noted between T2 and T3, while the transcript abundance of the gene encoding trehalose phosphate synthase (EC 2.4.1.15)

increased. Similarly, the concentration of sucrose tended to increase gradually throughout the T1-T3 period, while the abundance of sucrose synthase (EC 2.4.1.13) transcript decreased. Many transcripts mostly decreasing in the T3 stage, were annotated in invertase (EC 3.2.1.26), an enzyme which splits sucrose into fructose and glucose.

Figure 15: **The metabolism of starch in wheat 'Svilena'**.

(Figure legend continues in next page)

The systems biology graphical notation (SBGN) style metabolic network depicts reversible (double headed arrows) and irreversible (single headed arrows) reactions catalyzed by the corresponding enzymes (squares). For each enzyme, a bar chart showing the dynamics of transcription of the encoding gene is given. The EC codes 2.4.1.11 and 2.4.1.21, 2.4.1.1, 3.2.1.2, 3.2.1.20, 2.7.7.27, 1.1.1.22, 4.1.1.35, and 3.2.1.37 correspond to starch synthase, glycogen phosphorylase, beta-amylase, alpha glucosidase, glucose-1-phosphate adenylyltransferase, UDP-glucose 6-dehydrogenase, UDP-glucuronate decarboxylase and xylan 1,4-beta-xylosidase, respectively. The bar charts relating to metabolites (circles) represent time-resolved metabolite profiles in relative units, based on the GC-MS output. Glc, glu, xyl and G1P stand for glucose, glucuronic acid, xylose and glucose-1-phosphate, respectively. Metabolites or enzymes occurring multiple times in the metabolic network are marked with a clone marker, represented in the map as a black mark inside the glyph (e.g., EC 2.4.1.1). Each bar represents the mean and standard deviation of replicates taken at one of the three stages sampled (T1, uninucleate microspores prior to low temperature treatment; T2, uninucleate microspores following a 10 days-exposure to low temperature stress; and T3, microspores showing first nuclear divisions after 4-8 days in culture). A red border indicates a p value < 0.05 in at least one comparison (based on an analysis of variance on ranks). The results pointed to starch synthesis in T2 and degradation in T3. The diagram was extracted and modified from the VANTED map shown in figure 14.
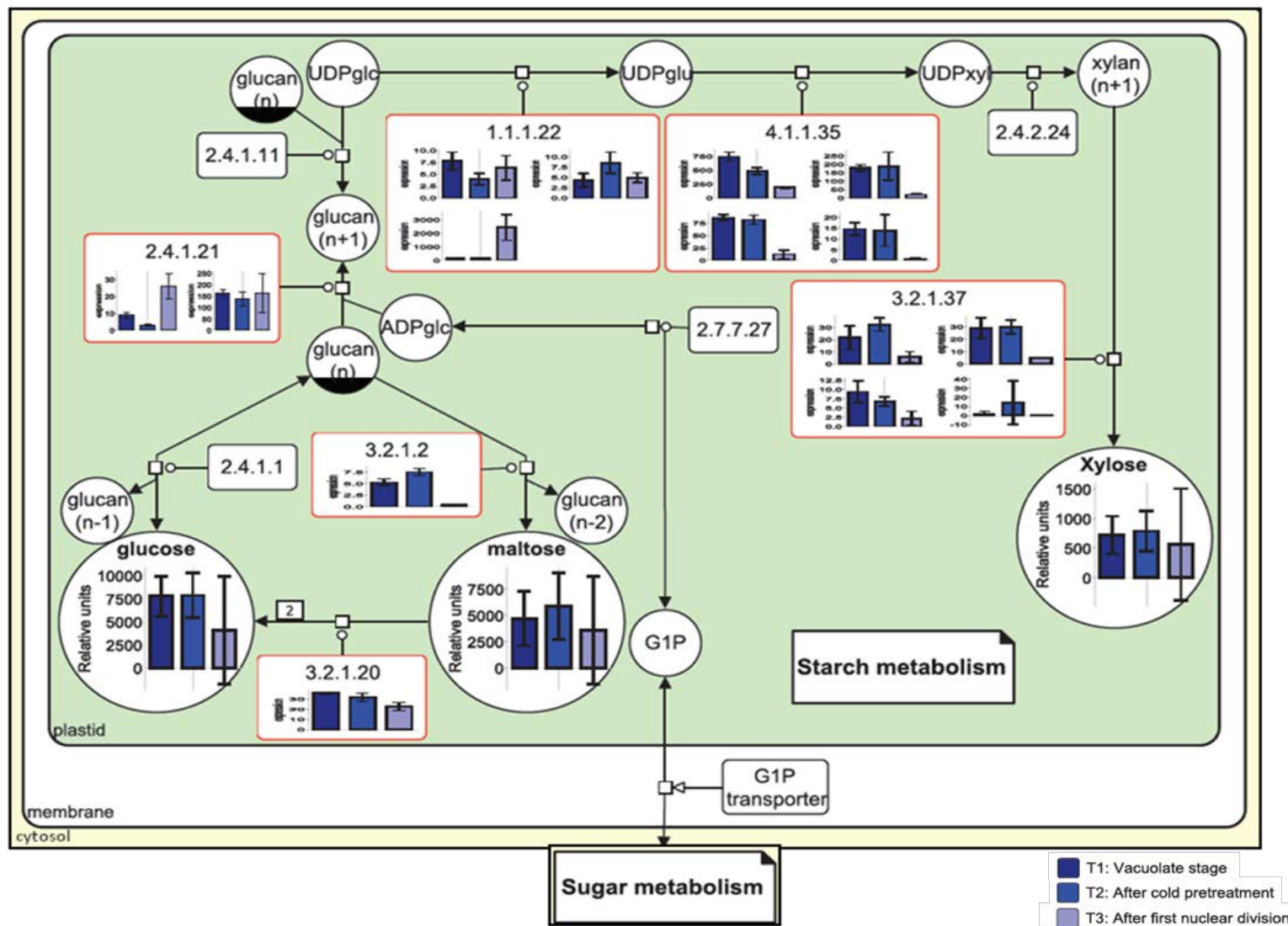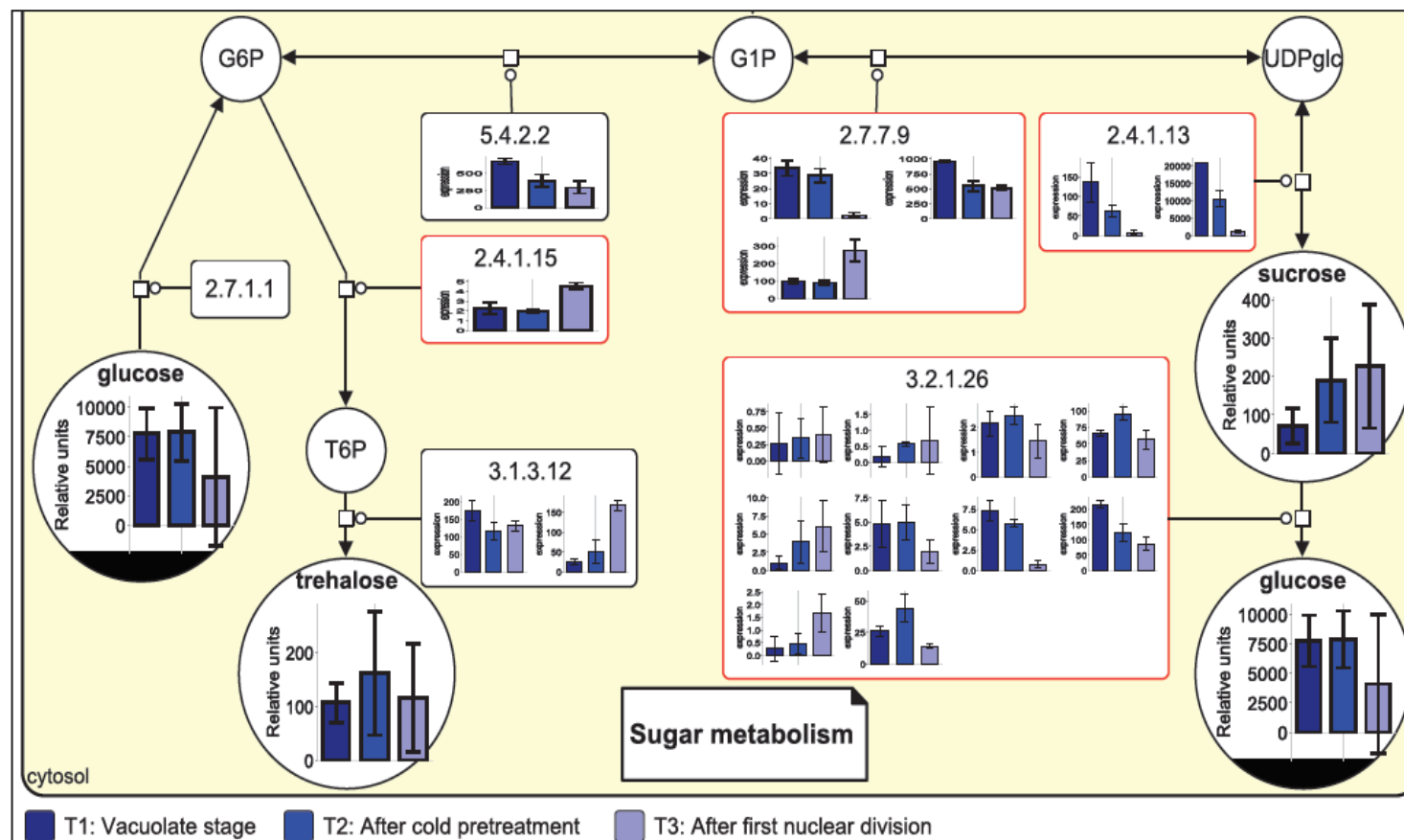
Figure 16: **The metabolism of sugars in wheat 'Svilena'**.

(Figure legend continues in next page)

The systems biology graphical notation (SBGN) style metabolic network depicts reversible (double headed arrows) and irreversible (single headed arrows) reactions catalyzed by the corresponding enzymes (squares). For each enzyme, a bar chart showing the dynamics of transcription of the encoding gene is given. The EC codes 2.7.1.1, 5.4.2.2, 2.4.1.15, 3.1.3.12, 2.7.7.9, 2.4.1.13, and 3.2.1.26 correspond to hexokinase, phosphoglucomutase, alpha,alpha-trehalose-phosphate synthase, trehalose phosphatase, UTP-glucose-1-phosphate uridylyltransferase, sucrose synthase, and beta-fructofuranosidase, respectively. The bar charts relating to metabolites (circles) represent time-resolved metabolite profiles in relative units, based on the GC-MS output. G1P, G6P, T6P and glc stand for glucose-1-phosphate, glucose-6-phosphate, trehalose-6-phosphate, and glucose, respectively. Metabolites or enzymes occurring multiple times in the metabolic network are marked with a clone marker, represented in the map as a black mark inside the glyph (e.g., glucose). Each bar represents the mean and standard deviation of replicates taken at one of the three stages sampled (T1, uninucleate microspores prior to low temperature treatment; T2, uninucleate microspores following a 10 days-exposure to low temperature stress; and T3, microspores showing first nuclear divisions after 4-8 days in culture). A red border indicates a p value < 0.05 in at least one comparison (based on an analysis of variance on ranks). The results showed different profiles of the sugars. The diagram was extracted and modified from the VANTED map shown in figure 14.

4.1.3.2.   Tricarboxylic acid cycle

Tricarboxylic acid cycle exhibited enzymes with more than one transcript associated, with the exception of fumarate hydratase (EC 4.2.1.2) and aconitate hydratase (EC 4.2.1.3) (figure 17). Fumarate hydratase interconverts malate and fumarate. The abundance of the transcript did not change significantly over the period, even though the contents of both malate and fumarate increased between T1 and T2, and fell between T2 and T3. The expression of genes coding for isocitrate dehydrogenase and succinate CoA ligase (EC 1.1.1.41/42 and EC 6.2.1.5, respectively) reduced in T3 stage. This coincided with the increase in the transcript abundance of the gene encoding for glutamate dehydrogenase (EC 1.4.1.2), involved in the GABA shunt and correlating also with the observed increase in GABA content between T2 and T3.
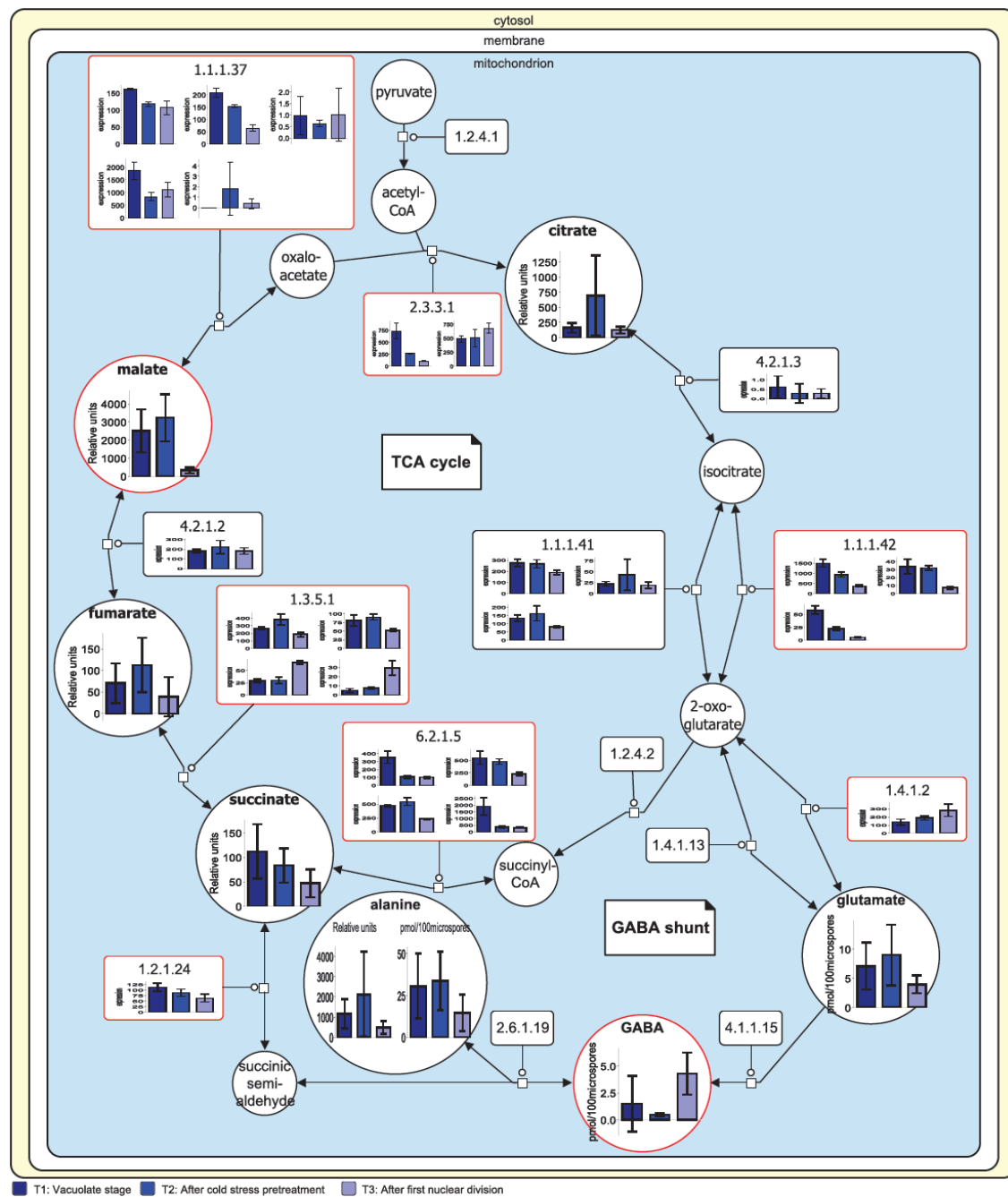
Figure 17: **The TCA cycle and GABA shunt pathways in wheat 'Svilena'**. The systems biology graphical notation (SBGN) style metabolic network depicts reversible (double headed arrows) and irreversible (single headed arrows) reactions catalyzed by the corresponding enzymes (squares). For each enzyme, a bar chart showing the dynamics of transcription of the encoding gene is given. The EC codes 1.2.4.1, 2.3.3.1, 4.2.1.3, 1.1.1.41 and 1.1.1.42, 1.2.4.2, 6.2.1.5, 1.3.5.1, 4.2.1.2, 1.1.1.37, 1.4.1.13, 1.4.1.2, 4.1.1.15, 2.6.1.19, and 1.2.1.24 correspond to pyruvate dehydrogenase, citrate synthase, aconitate hydratase, isocitrate dehydrogenase, oxoglutarate dehydrogenase,

succinate CoA-ligase, succinate dehydrogenase, fumarate hydratase, malate dehydrogenase, glutamate synthase, glutamate dehydrogenase, glutamate decarboxylase, 4-aminobutyrate-2-oxoglutarate transaminase, and succinate-semialdehyde dehydrogenase, respectively. The bar charts relating to metabolites (circles) represent time-resolved metabolite profiles in relative units, based on the GC-MS (relative units) and UPLC (pmol per 100 microspores) outputs. Each bar represents the mean and standard deviation of replicates taken at one of the three stages sampled (T1, uninucleate microspores prior to low temperature treatment; T2, uninucleate microspores following a 10 days-exposure to low temperature stress; and T3, microspores showing first nuclear divisions after 4-8 days in culture). A red border indicates a p value < 0.05 in at least one comparison (based on an analysis of variance on ranks). The levels of some intermediates increased in T2 and decreased in T3, which coincided with the abundance of transcripts of some enzymes such as succinate CoA ligase (EC 6.2.1.5). The diagram was extracted and modified from the VANTED map shown in figure 14.

4.1.3.3. Amino acid metabolism

Amino acid synthesis was characterized by a reduction in the gene expression of most of the synthesis enzymes between T2 and T3, such as genes encoding threonine synthase (EC 4.2.3.1) and argininosuccinate lyase (EC 4.3.2.1), in contrast to the increase in the amino acids abundance in that stage. The gene encoding histidinol dehydrogenase (EC 1.1.1.23) represents an exception, for which transcript abundance was stable throughout the T1-T3 period.

4.1.3.4. Fatty acid metabolism

Finally, fatty acid metabolism showed genes encoding enzymes with a tendency to be down-regulated in T3, when no signicant differences were seen in the metabolites (figure 18).
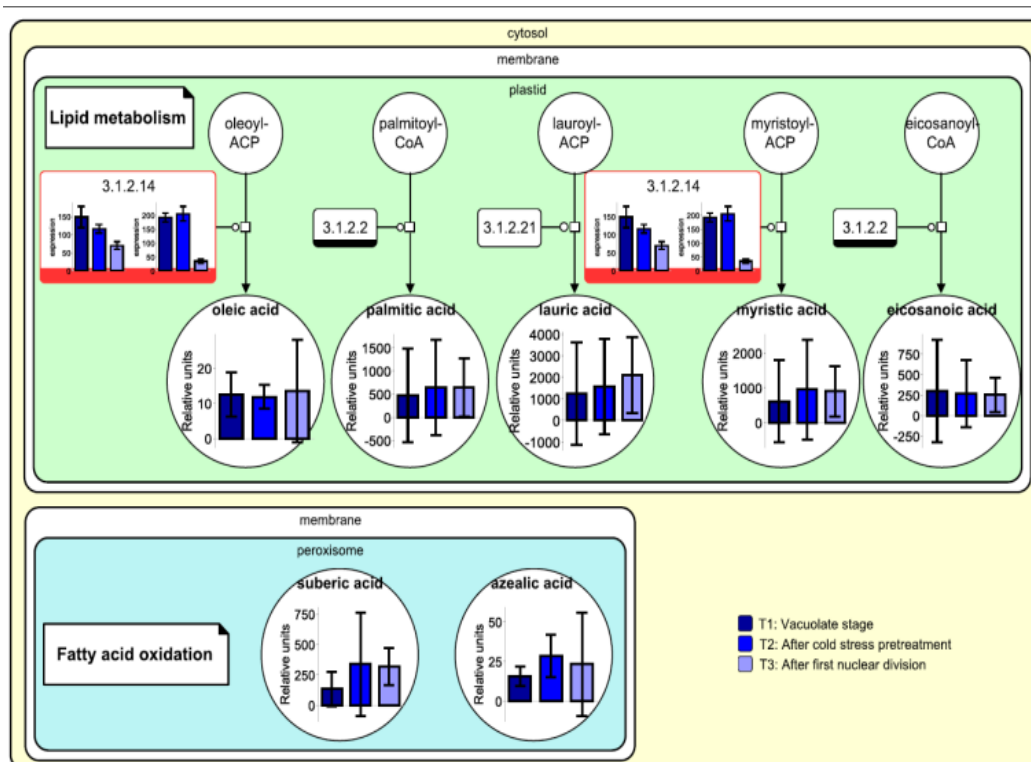
Figure 18: **Fatty acid synthesis and fatty acid oxidation pathways of wheat 'Svilena'**. The systems biology graphical notation (SBGN) style metabolic network depicts the irreversible (single headed arrows) reactions catalyzed by the corresponding enzymes (squares). For each enzyme, a bar chart showing the dynamics of transcription of the encoding gene is given. The EC codes 3.1.2.14, 3.1.2.2, and 3.1.2.21 correspond to oleoyl-[acyl-carrier-protein] hydrolase, palmitoyl-CoA hydrolase, and dodecanoyl-[acyl-carrier-protein] hydrolase. The bar charts relating to metabolites (circles) represent time-resolved metabolite profiles in relative units, based on the GC-MS (relative units) output. Each bar represents the mean and standard deviation of replicates taken at one of the three stages sampled (T1, uninucleate microspores prior to low temperature treatment; T2, uninucleate microspores following a 10 days-exposure to low temperature stress; and T3, microspores showing first nuclear divisions after 4-8 days in culture). A red border indicates a p value < 0.05 in at least one comparison (based on an analysis of variance on ranks). The diagram was extracted and modified from the VANTED map shown in figure 14.

4.1.3.5. Summary of integrative –omics analysis

The metabolic pathways map with the –omic datasets integrated in it gave an immediate appreciation of the metabolic changes occurring during the microspore embryogenesis in 'Svilena' microspores. Briefly, the profile of the sugars maltose and glucose were coincident with the one of the transcripts of the gene coding for the enzyme beta-amylase and were opposite to the profiles of the transcrits of the enzyme starch synthase (figure 15). In addition, intermediates of the TCA cycle tended to increase in T2 and then, to decrease in T3 that was correlating with an increase in GABA in the last stage (figure 17). No remarkable changes were seen in fatty acids (figure 18). In the amino acid metabolism, contrasting profiles were found between many of these metabolites and the transcripts of the genes coding for their synthesis enzymes. This is the first time that –omics data are integrated and co-analyzed in the context of the metabolic pathways in the study of wheat microspore embryogenesis.

4.1.4. Glutamine synthetase abundance

Since contrasting temporal patterns were observed between amino acid levels and transcript levels of genes involved in their biosynthesis, the abundance of one of these enzymes, glutamine synthetase, was examined as an example (figure 19A). According to the western blot experiment, variation in the abundance of the enzyme between T1 and T3 mirrored that of the relevant metabolite, decreasing between T1 and T2, then rising again up in T3. This pattern was, as noted previously, different from the profile of transcript abundance (Figure 19B, C). From the two transcripts associated to the EC 6.3.1.2 only one could be identified as glutamine synthetase. The transcript's sequence blasted to the *Triticum aestivum* gene TRIAE_CS42_1AL_TGACv1_000189_AA0005730, and this one to the glutamine synthetase 1 from rye. Therefore, the transcript´s sequence suggested that it represented the product of the gene encoding cytosolic GS1 (Figure 19D, E, F).
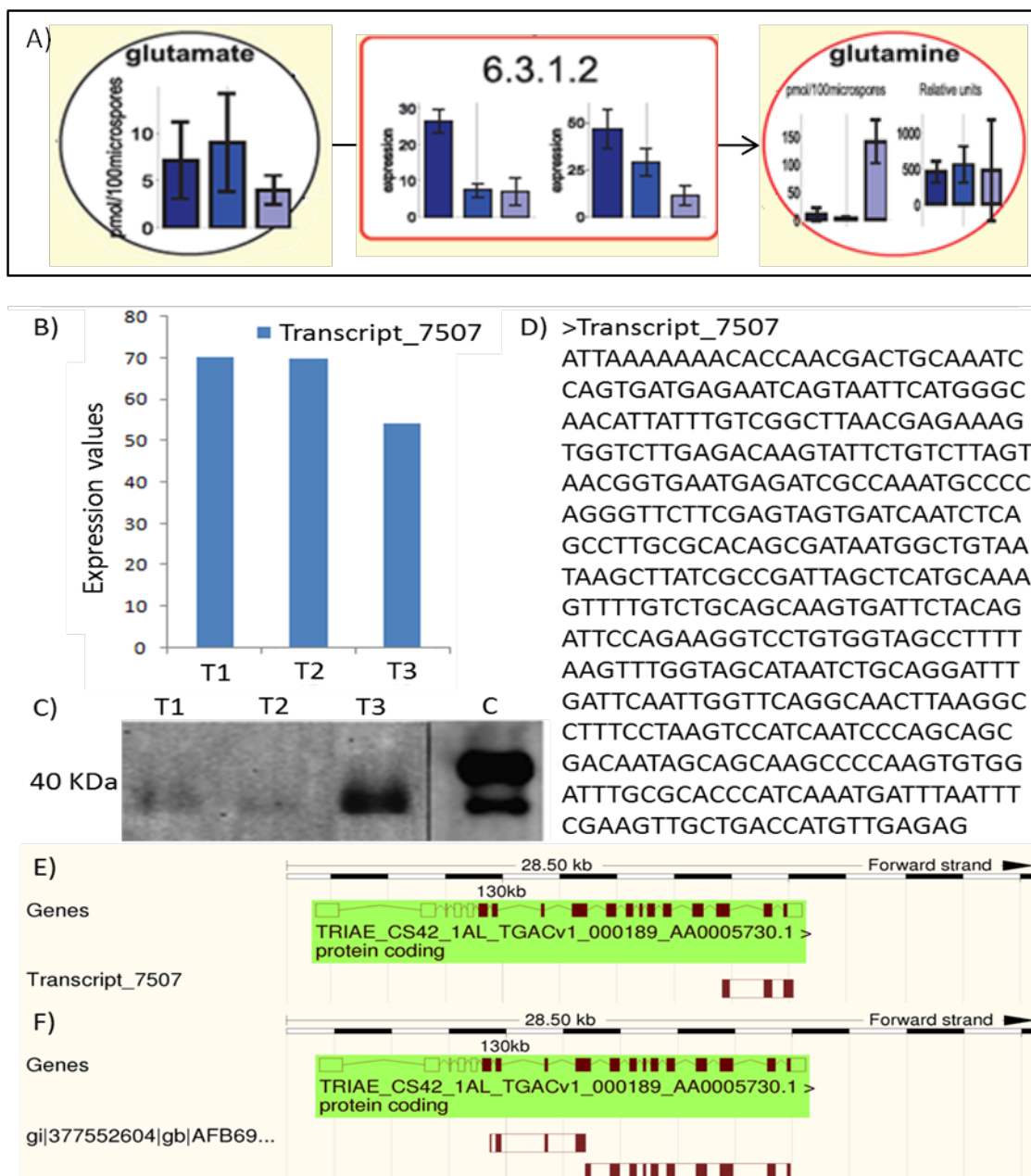
Figure 19: **The transcription and translation of GS (EC 6.3.1.2)**. (A) The cytosolic pathway (extracted and modified from the VANTED map shown in figure 14). The systems biology graphical notation (SBGN) style metabolic network depicts the irreversible (single headed arrows) reactions catalyzed by the corresponding enzymes (squares). For each enzyme, a bar chart showing the dynamics of transcription of the encoding gene is given. The EC code 6.3.1.2 corresponds to glutamine synthetase. The bar charts relating to metabolites (circles) represent time-resolved metabolite profiles in relative units, based on the GC-MS (relative units) and UPLC (pmol per 100 microspores) outputs. Each bar represents the mean and standard deviation of replicates taken at one of the three stages sampled (T1, uninucleate microspores prior

to low temperature treatment; T2, uninucleate microspores following a 10 days-exposure to low temperature stress; and T3, microspores showing first nuclear divisions after 4-8 days in culture). A red border indicates a p value < 0.05 in at least one comparison (based on an analysis of variance on ranks). (B) *GS* transcript abundance derived from the RNA-seq platform. The three stages sampled were: T1, uninucleate microspores prior to low temperature treatment; T2, uninucleate microspores following a 10 days-exposure to low temperature stress; and T3, microspores showing first nuclear divisions after 4-8 days in culture. (C) GS protein detected by Western blotting. From left to right: 'Svilena' microspores sampled at T1, T2 and T3, leaf material of 'Bob White'. (D) Nucleotide sequence of the wheat *GS* transcript (transcript_7507). (E) BlastN output using transcript_7507 as a search string against the wheat genome matches the end of TRIAE_CS42_1AL_TGACv1_000189_AA0005730. (F) BlastP output based on a search string of the polypeptide sequence of cereal rye GS1 (GenBank: JQ0746217.1) against the wheat proteome.

4.2. Metabolic study of the regeneration efficiency related to the genotype

After the study of a genotype with high regeneration rate, different genotypes were metabolically evaluated. A mapping population of DH lines with different regeneration efficiency was used for such a study. The possibility of finding potential metabolic markers for the regeneration rate was considered, and in that case, it was asked whether it was possible to predict that rate from those markers.

4.2.1. Effect of genotype on the regeneration efficiency

A population of DH lines was obtained by Saaten Union Biotech GmbH after crossing cultivars 'Svilena' and 'Berengar', with high and low GPR rates, respectively. The population consisted of 137 DH lines and the GPR rate ranged from 0 green regenerants per spike for line 001 to 37 green regenerants per spike for line 081. Results from one of the three replicates are shown in figure 20. In order to study the metabolome of lines with different regeneration efficiency, two groups were used, one with the 8 DH lines with the lowest GPR rate, and 8 lines with the highest GPR rate, including the parents (figure 21).

Additionally, the albino rates obtained were low for all the lines, ranging from 0 albinos per spike in several lines, like line 001, to 1.96 albinos per spike in average in line 069 (table 3).
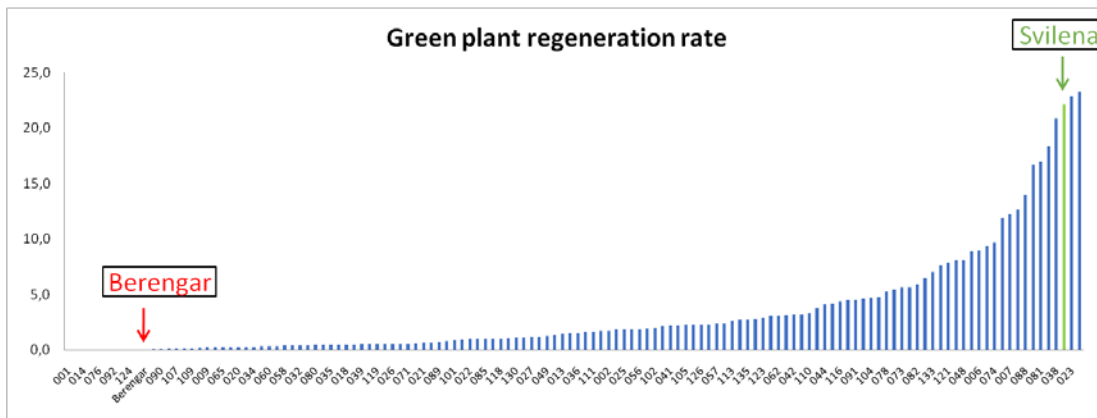
Figure 20: **Green plant regeneration rates of different DH lines coming from the cross of 'Svilena' (green bar) and 'Berengar' (under red arrow).** The figure shows the measurements of one of the three replicates measured in the study. Units shown in number of green regenerants per spike. Data given by SU BIO GmbH.
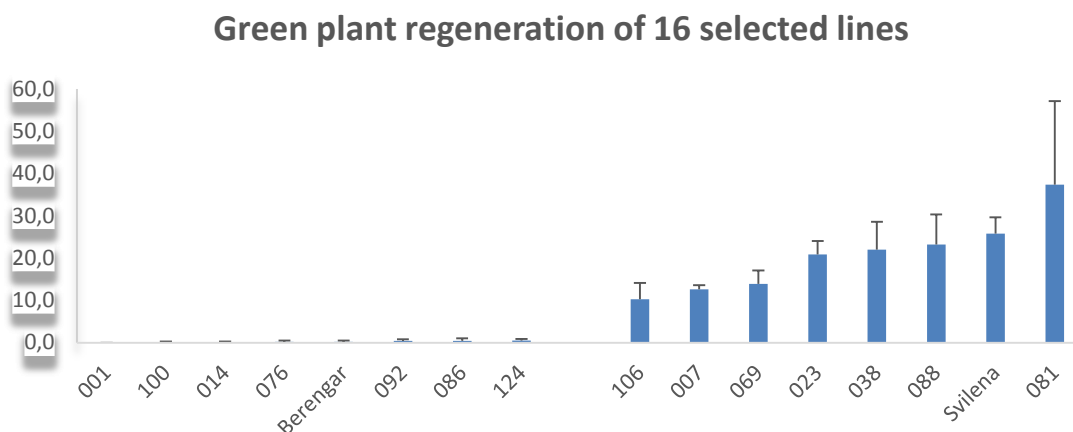
Figure 21: **Green plant regeneration rates of selected DH lines (including the parents).** Regeneration rates of the selected DH lines coming from the cross of cultivars 'Svilena' and 'Berengar' varieties. Units in number of green regenerants per spike. Results from three replicates. Data given by SU BIO GmbH.

Genotype	Albino rate
SU-BIO 001	0.00
SU-BIO 100	0.15
SU-BIO 014	0.45
SU-BIO 076	0.07
SU-BIO 092	0.07
SU-BIO 086	0.00
SU-BIO 124	0.03
SU-BIO 106	0.34
SU-BIO 007	0.61
SU-BIO 069	1.96
SU-BIO 023	1.79
SU-BIO 038	0.19
SU-BIO 088	0.36
SU-BIO 081	1.01
SU-Bio Berengar	0.00
SU-Bio Svilena	1.17

Table 3: **Albino rates of selected DH lines (including the parents) coming from the cross of cultivars 'Svilena' and 'Berengar'**. Units in number of albino plants per spike. Results from three replicates. Data were provided by SU BIO GmbH.

4.2.2. Metabolome characterization of lines differing in their regeneration efficiency

Metabolic characterization of the microspores of the DH lines revealed the relative and absolute concentrations of primary metabolites, detected by GC-MS and UPLC-fluorescence, respectively.

The untargeted analysis detected more than 80 compounds and it was possible to identify 50 out of them (figure 22). The metabolites detected were grouped into amino acids, organic acids, sugars, fatty acids and unknown compounds, for which annotation was not possible with the spectrum library used. For each compound, the relative abundance was compared between the two groups of lines (figure 22). In all lines, most amino acids increased in T3 stage, such as asparagine, ornithine or GABA. On the other hand, alanine, glutamic acid and glycine slightly increased in T2 and then decreased in T3 stage. Similar profile was also seen in most organic acids and sugars that increased in T2 and decreased later in T3, with the exception of succinic acid,

which decreased progressively during the three stages. Within the sugars, glucose and sucrose were the most abundant. Regarding fatty acids and unknown compounds, only few changes were found. Putrescine increased in T2 and later decreased in T3, whereas the unknowns, unknown #4 and an unknown here named D were increased in T3 stage.

The targeted analysis of amino acids (figure 23) presented similar profiles to those found in the untargeted analysis. Additionally, the results obtained for 'Svilena' were similar to those of the metabolome experiments shown in section 4.1. For most amino acids, the highest concentration was found in the T3 stage, except for alanine, cysteine, glycine and glutamate. In T1, alanine was the highest concentrated in both high and low GPR rate lines, with 78 pmol per 100 microspores and 34 pmol per 100 microspores on average, respectively; also alanine in T2 in high and low GPR rate lines, with 173 pmol per 100 microspores and 83 pmol per 100 microspores on average, respectively; and glutamine and asparagine in T3, reaching around 200 pmol per 100 microspores on average in both amino acids in high GPR rate lines, and 130 pmol per 100 microspores on average in both in low GPR rate lines.

The same metabolic patterns but different concentration levels characterized the two groups of lines, in both analyses (figures 22 and 23). The concentrations of amino acids and TCA cycle organic acids were significantly higher in high GPR rate lines in all the stages. Sucrose from sugars and putrescine had also significant different concentrations between the groups. Within sugars, galactose concentration was lower in the high efficiency lines than in the low efficiency lines. The remaining sugars and fatty acids showed similar concentrations between the two groups.
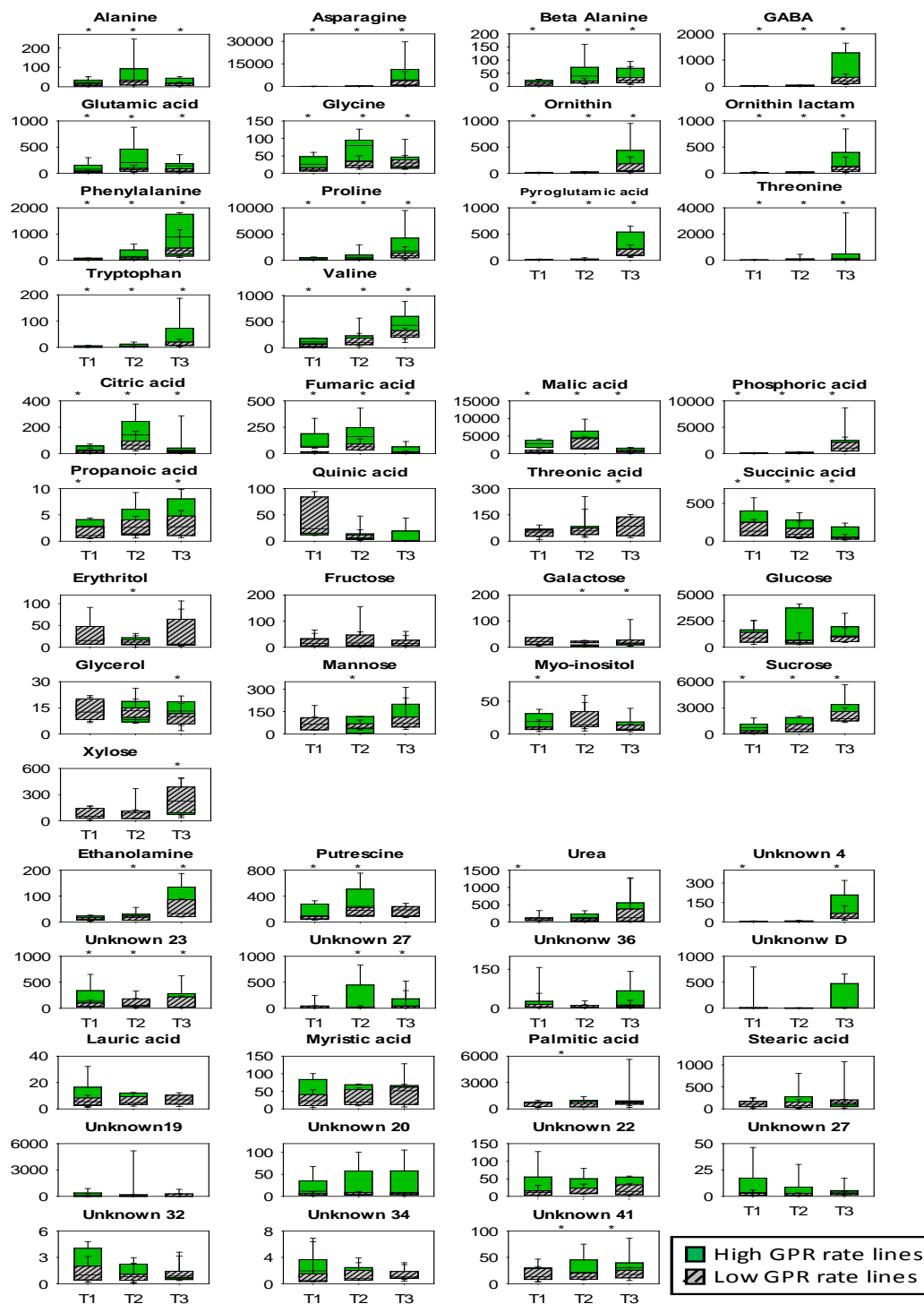
Figure 22: **Relative concentrations of metabolites of DH lines over the T1-T3 period**. The relative concentrations, obtained from the GC-MS, of the selected 8 lines with highest GPR rate (including 'Svilena') are shown in the green boxes and in gray boxes the concentrations of the lines with lowest GPR rate (including 'Berengar'). Units: relative units. When $p < 0.05$ between groups an asterisk is placed above the stage in the top of the chart.
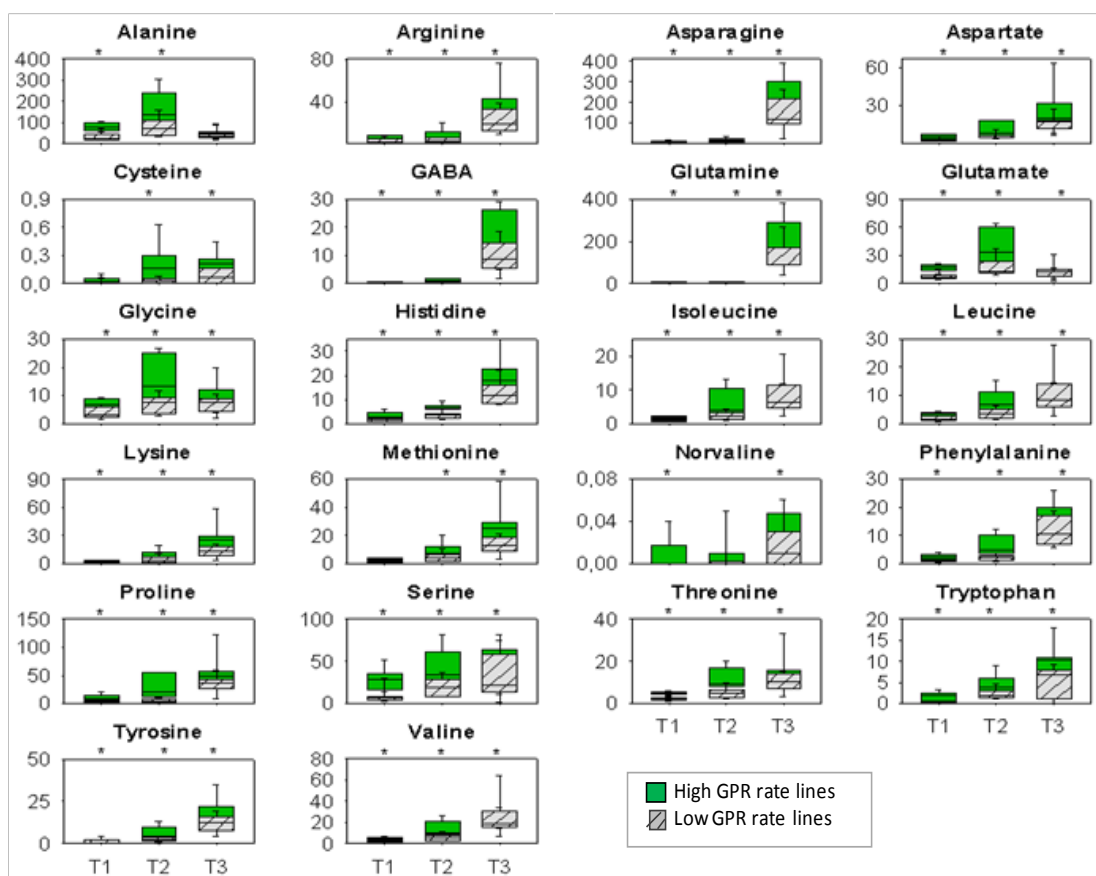
Figure 23: **Amino acid concentrations of DH lines in T1, T2 and T3 stages**. The concentrations, obtained from the UPLC, of the selected 8 lines with highest GPR rate (including 'Svilena') are shown in the green boxes and in gray boxes the concentrations of the lines with lowest GPR rate (including 'Berengar'). Units in pmol 100 microspores[-1]. When $p < 0.05$ between groups asterisk is placed above the stage in the top of the chart.

4.2.3. Metabolic markers

Correlation analysis, which examined the strength of the relationship between the detected metabolites and the GPR rate, allowed the identification of potential metabolite markers (table 4). Similar analysis was also conducted with the rates of albinos, in order to find the best marker. A high positive or negative correlation is desirable. Ideally it would have been even more desirable to obtain opposite correlation for a certain metabolite between GPR rate and the rates of albinos.

However, this was not the case, since similar correlations were found for all the metabolites between both GPR and albinos rates. Amino acids showed positive correlation in the T1-T3 period. In particular, phenylalanine had the highest correlation with the GPR rate, with r=0.79 in T1 and r=0.69 in T2, and histidine had the highest correlation in T3, with r=0.48.

Organic acids from the TCA cycle also exhibited positive correlation. The most correlated ones were fumaric and malic acids in T1 stage (r=0.70 and r=0.69, respectively); malic acid in T2 (r=0.49); and citric acid in T3 (r=0.41).

In sugars, there was either none or low negative correlation.The highest negative correlation was found for galactose, with r=-0.11 in T1 stage, r=-0.50 in T2 and r=-0.37 in T3. In addition, sucrose was found with a positive correlation of 0.5 in T1. Fatty acids and unknown compounds had low values of correlation, with a slight increase in T2 stage.

	GPR T1	GPR T2	GPR T3	Albinos T1	Albinos T2	Albinos T3
Amino acids						
Alanine	0.60	0.55	0.09	0.58	0.55	0.06
Arginine	0.50	0.48	0.47	0.17	0.23	0.43
Asparagine	0.25	0.53	0.17	0.27	0.51	0.29
Aspartic acid	0.33	0.41	0.20	0.26	0.42	0.16
Beta alanine	0.23	0.34	0.25	0.27	0.40	0.13
Cystein	0.12	0.41	0.14	0.06	0.19	0.18
GABA	0.44	0.67	-0.01	0.38	0.57	0.18
Glutamine	0.42	0.39	0.21	0.38	0.25	0.30
Glutamic acid	0.63	0.57	0.23	0.59	0.58	0.22
Glycine	0.61	0.63	0.34	0.51	0.56	0.24
Histidine	0.43	0.68	0.48	0.54	0.62	0.44
Isoleucine	0.72	0.61	0.27	0.58	0.48	0.29
Leucine	0.70	0.60	0.41	0.60	0.51	0.40
Lysine	0.61	0.49	0.46	0.50	0.45	0.42
Metionine	0.62	0.51	0.06	0.69	0.47	0.07
Ornithin	0.45	0.45	0.28	0.32	0.43	0.13
Ornithin lactam	0.52	0.47	0.42	0.33	0.36	0.39
Phenylalanine	0.79	0.69	0.43	0.71	0.57	0.39
Proline	0.72	0.60	0.33	0.60	0.62	0.37
Serine	0.65	0.66	0.41	0.48	0.50	0.22
Threonine	0.46	0.61	0.31	0.47	0.59	0.26

Tryptophan	0.49	0.07	0.27	0.36	0.20	0.25
Tyrosine	0.44	0.66	0.42	0.41	0.55	0.42
Valine	0.60	0.34	0.21	0.50	0.36	0.25

Organic acids

Citric acid	0.51	0.28	0.41	0.64	0.51	0.49
Fumaric acid	0.70	0.37	0.27	0.65	0.50	0.17
Malic acid	0.69	0.49	0.20	0.68	0.51	0.27
Phosphoric acid	0.44	0.42	0.38	0.30	0.31	0.27
Propanoic acid	0.21	0.23	0.26	0.17	0.24	0.07
Pyroglutamic acid	0.48	0.24	0.25	0.49	0.36	0.19
Quinic acid	0.03	0.09	0.01	-0.05	-0.02	0.03
Succinic acid	0.34	0.17	0.37	0.26	0.30	0.21
Threonic acid	0.03	0.20	-0.21	0.02	0.19	-0.25

Sugars

Erythritol	0.06	-0.14	-0.14	0.14	-0.11	-0.02
Fructose	-0.11	-0.07	-0.24	-0.22	-0.05	-0.22
Galactose	-0.11	-0.50	-0.37	-0.01	-0.44	-0.34
Glucose	0.05	0.20	-0.02	0.06	0.21	0.06
Glycerol	0.07	0.09	0.22	-0.15	-0.19	-0.07
Mannose	0.06	-0.11	-0.11	0.02	-0.34	-0.05
Myo-inositol	0.39	0.04	-0.03	0.51	0.35	0.05
Sucrose	0.5	0.18	0.27	0.56	0.36	0.24
Xylose	0.28	0.04	-0.25	0.11	0.13	-0.10

Other

Ethanolamine	0.20	0.35	0.45	0.05	0.21	0.35
Putrescine	0.33	0.22	-0.05	0.48	0.36	-0.15
Urea	0.29	0.18	0.21	0.32	0.13	0.08
Unknown4	0.34	0.16	0.21	0.26	0.18	0.29
Unknown23	0.41	0.09	0.16	0.27	0.23	0.12
Unknown27	0.19	0.29	0.25	0.23	0.28	0.31
Unknown36	0.30	-0.14	-0.20	0.24	0.03	-0.10
UnknownD	0.04	0.03	-0.13	0.19	0.01	-0.02

Fatty acid and apolar unknowns

Lauric acid	-0.11	0.16	0.06	0.04	0.17	-0.10
Myristic acid	-0.08	0.15	-0.06	0.03	0.21	-0.16
Palmitic acid	-0.09	0.37	0.14	-0.01	0.24	0.05
Stearic acid	0.03	0.30	-0.03	-0.06	0.17	0.02
Unknown19	0.25	0.14	-0.13	0.23	0.20	-0.26
Unknown20	0.25	0.25	0.08	0.33	0.30	0.07
Unknown22	0.07	0.19	0.02	0.16	0.29	0.03
Unknown27	-0.08	0.06	0.10	0.12	0.33	0.10
Unknown32	-0.21	-0.03	-0.12	0.08	0.09	-0.06

	0.08	0.04	0.16	0.21	0.15	-0.09
Unknown34	0.08	0.04	0.16	0.21	0.15	-0.09
Unknown41	-0.20	0.17	0.22	-0.04	0.31	0.18
Legend	1	0	-1			

Table 4: **Correlation values between metabolite concentrations and GPR and albino rates**. Results with p value > 0.05 are shown with red characters. Heat map applied to the values, going from green in value 1 to yellow in value 0, and to red in value -1.

4.2.4. Plant regeneration rate prediction from the model development

Since high correlations with the GPR rate were found for many metabolites, the possibility of prediction was assessed. Markers were predetermined and selected by building a green plant regeneration rate predictive model. Since more than one predictor was analyzed for developing the model, a multiple linear regression analysis was performed. The model was built using the set of identified potential metabolite markers, adding or removing them in a stepwise manner. In this Forward Stepwise regression, variables were introduced into the model based on their ability to predict GPR rate. The model displayed here (table 5) shows the predictive equation, where GPR rate is the green plant regeneration rate; Phe, Ser, galactose, Asp, Ala, Ethanolamine and GABA represent the values of their concentrations as these were measured with UPLC ([a]) or GC-MS ([b]); and the numbers represent the coefficients of the model predictors. In addition, the level of contribution in the prediction is shown in the order of the variables in the equation. All of them presented a significant contribution in the prediction (p value < 0.01).

Furthermore, significant variation in GPR rate was explained by the model (R^2-adjusted = 0.84), reaching the highest value when metabolites from both measurements, UPLC and GC-MS, were taken in consideration.

The accuracy of prediction, measured by the average of the distance of the observed values to the regression, was explained by a standard error of estimate of 5.6. The model was formed by 7 variables, since adding more did not highly increase the prediction accuracy.

Validation of this model comprised the use of 2 DH lines that were previously left out during the development of the regression analysis (table 6). These lines were 86 and 38, with a GPR rate of 0.44 and 21.96 regenerants per spike, respectively. The results from the metabolic measurements of these lines were applied into the model shown here. The averaged predicted values obtained were 0.84 and 24.20 renegerants per spike, respectively.

GPR rate=1.881-(1.91*Asp[a])+(6.682*Phe[a])+(0.382*Ser[a])+(0.293*Ala[b])-(0.315*Ethanolamine[b])+(0.497*GABA[b])-(0.171*galactose[b])		
Adjusted-R^2	Standard error of estimate	P value
0.84	5.6	<0.01 in all variables
[a] **Absolute amino acid concentrations from UPLC measurement**		
[b] **Relative concentrations from GC-MS**		

Table 5: **GPR rate predictive model, developed by multiple linear regression**. In the equation, GPR rate represents the plant regeneration rate as green regenerants per spike; Phe, Ser, galactose, Asp, Ala, Ethanolamine and GABA represent phenylalanine, serine, galactose, aspartate, alanine, ethanolamine and GABA values of their concentrations measured with UPLC ([a]) or GC-MS ([b]); the adjusted-R^2 is the coefficient of determination for multiple regression adjusted for the number of variables; P, is the P value calculated for F statistic.

		Validation test with DH lines excluded	
Line	GPR rate	Predicted GPR rate	Error range for predicted GPR rate (Predicted GPR rate ± standard error of estimate)
38	21.96	24.2	18.60 … 29.80
86	0.44	0.85	-5.16 … 5.60

Table 6: **Validation test of the predictive model**. Predicted GPR rate values of two DH lines (38 and 86) with high and low GPR rate, respectively, that were not included in the model development. Real GPR rate values are highlighted in green, and the predicted ones in yellow. The standard error of estimate was applied to the predicted GPR rates.

4.3. Comparison of the proteome of the cultivars 'Svilena' and 'Berengar'

The results from the metabolic analysis carried out in this thesis left open questions, such as the protein profiles during the microspore embryogenesis process, and in particular in the key pathways showed in this study. The protein analysis on wheat microspores during the process brought answers to these questions, but also might bring answers to the different regeneration efficiency between genotypes, and even open new research perspectives and questions. Therefore, the proteome between the two parents, 'Svilena' and 'Berengar' was analyzed by a LC-based proteomic approach. Peptides were detected, quantified and normalized in the samples. After grouping them by charge and identification (with a wheat database from Uniprot), proteins were then identified by grouping peptides.

A list was obtained with 87 wheat proteins that showed a fold-change > 1.5 when the stages or the cultivars were compared. From that list, 18 were characterized proteins. In the procedure, due to the low availability of samples, some of the replicates of

cultivar 'Berengar' included in the study had been isolated in mannitol without the last wash in ammonium bicarbonate. However, no differences were seen between the replicates with and without the washing step (figure 24).
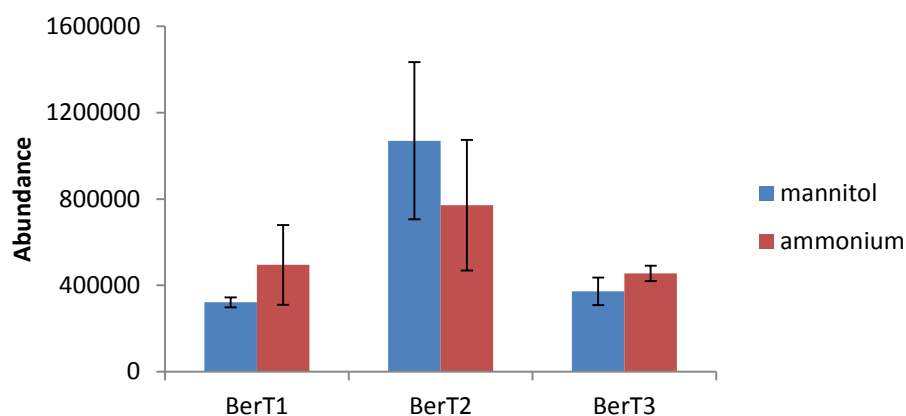
Figure 24: **Abundances of ubiquitin-like protein in 'Berengar' samples in ammonium and in mannitol, in T1, T2 and T3 stages**. No significant differences were seen between the replicates with and without the washing step in ammonium bicarbonate. The results of the abundances of the ubiquitin-like protein (C7AE89) are represented as an example.

Proteins were detected with a role in amino acid, carbohydrate and lipid metabolism (figure 25), in transcription, translation and protein metabolism (figure 26), and in cytoskeleton metabolism and stress response (figure 27).

Higher abundance was shown in most proteins in 'Svilena' T1 stage, and the same was found for 'Berengar' proteins in T2 stage. When comparing the stages, 'Svilena' showed no changes in protein abundance between T1 and T2, and different profiles in T3. Oppositely, in most proteins 'Berengar' showed an increase in protein abundance in T2, and also different profiles in T3.

Amino acid metabolism appeared represented by only one enzyme, which showed no significant differences either between the genotypes and the stages (figure 25). Same results were found between the three enzymes present in the gluconeogenesis/glycolysis pathway (figure 25). These were: enolase,

phosphoglycerate kinase and pyruvate kinase. Either a tendency to decrease or to stay unchanged in T2 was found in 'Svilena' while a tendency to increase was found in 'Berengar', which reached the protein levels of 'Svilena'. In T3 both genotypes showed a decrease in the levels of these enzymes. UDP-glucose-6-dehydrogenase and phospholipase D showed a tendency to increase in protein abundance in T3 stage.
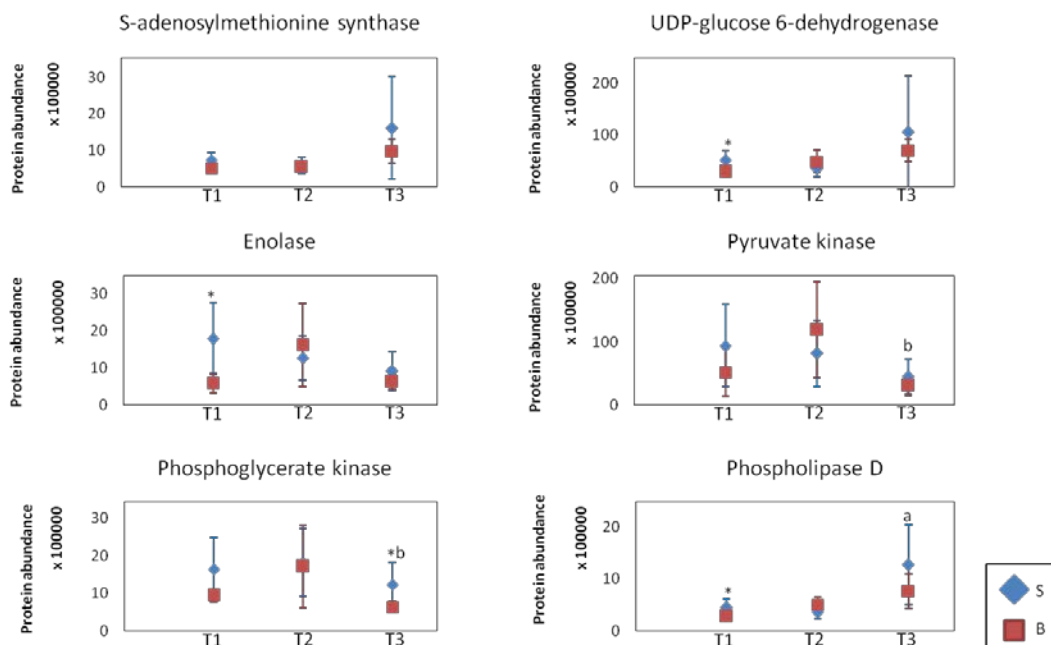
Figure 25: **Proteins with a role in amino acid, carbohydrate or lipid and fatty acid metabolism detected in 'Svilena' and 'Berengar' microspores.** The graphs show the mean and standard deviation of the protein abundance detected by nanoLC-MS. * is shown when there is a significant difference between the genotypes ($p < 0.05$). a is shown when there is a significant difference between the stages (T1, T2 and T3) in 'Svilena' (S). b is shown when there is a significant difference between the stages in 'Berengar' (B).

Proteins with roles in RNA stabilization or with protein chaperone activity were identified in the samples. These included: Cold-shock domain 2 protein, cold shock protein 1, low temperature responsive RNA binding protein, peptidyl-prolyl cis-trans isomerise, protein disulfide isomerise and small HSP23.6 (figure 26). Either a tendency to decrease or to stay unchanged in T2 was found in 'Svilena' while a tendency to increase was manifested in 'Berengar' for this group of proteins. In T3 both genotypes

showed a decrease in the levels of these enzymes, with the exceptions of peptidyl-prolyl cis-trans isomerise and protein disulfide-isomerase that tended to increase. In ubiquitin-like-protein 'Svilena' levels were stable in T2 and decreased in T3 stage (figure 26).
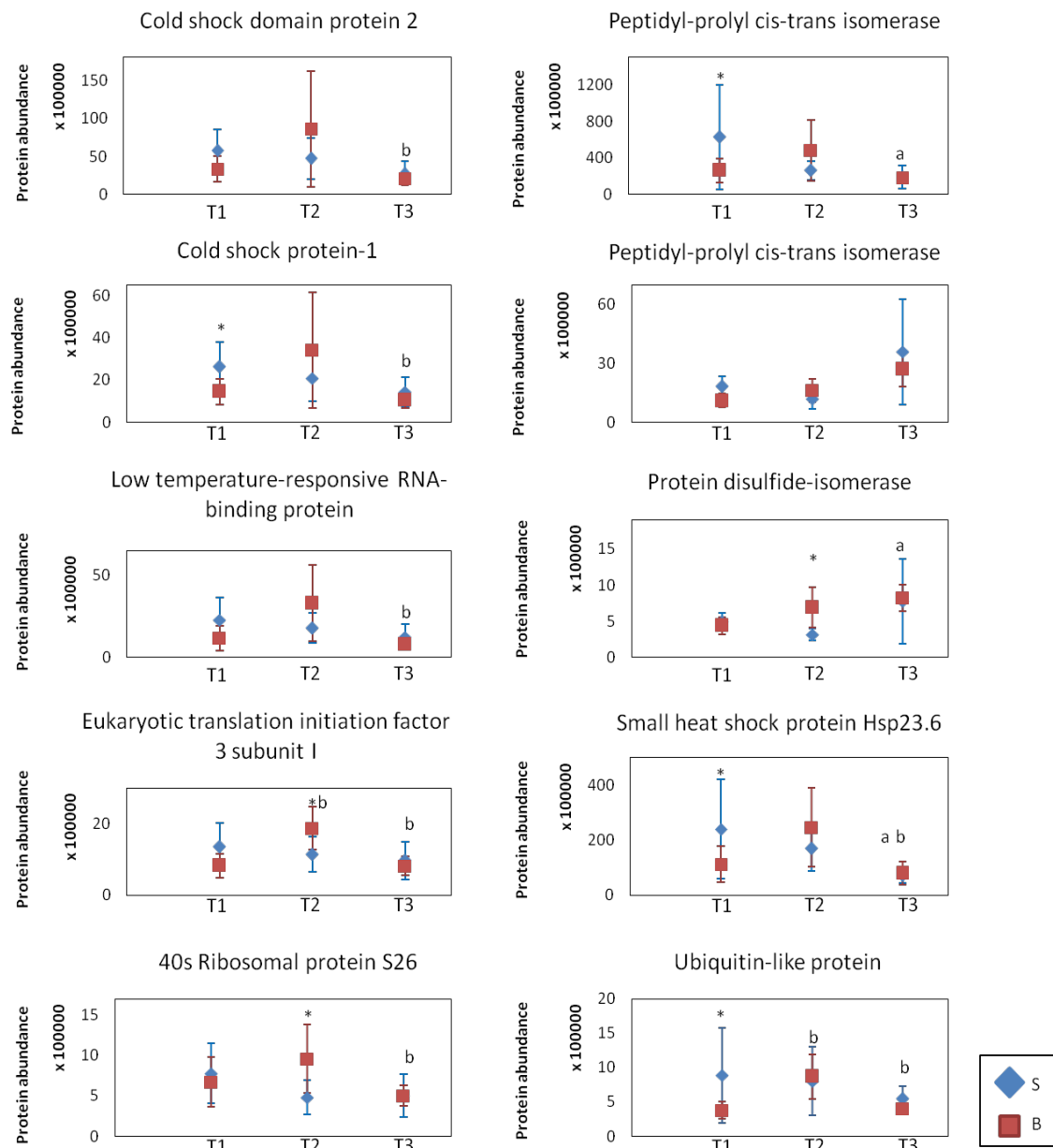
Figure 26: **Proteins with a role in transcription, translation and protein metabolism detected in 'Svilena' and 'Berengar' microspores**. The graphs show the mean and standard deviation of the protein abundance detected by nanoLC-MS. * is shown when there is a significant difference between the genotypes (p < 0.05). a is shown when

there is a significant difference between the stages (T1, T2 and T3) in 'Svilena' (S). b is shown when there is a significant difference between the stages in 'Berengar' (B).

Additionally, other proteins were detected like tubulin beta chain and ozone-responsive stress-related protein. The abundance of both proteins was found unchanged between T1 and T2, and increased in T3 stage (figure 27).
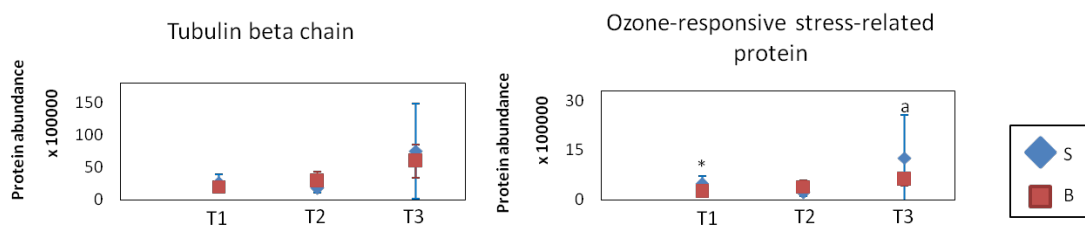
Figure 27: **Proteins with a role in cytoskeleton metabolism and stress response detected in 'Svilena' and 'Berengar' microspores**. The graphs show the mean and standard deviation of the protein abundance detected by nanoLC-MS. * is shown when there is a significant difference between the genotypes ($p < 0.05$). a is shown when there is a significant difference between the stages (T1, T2 and T3) in 'Svilena' (S). b is shown when there is a significant difference between the stages in 'Berengar' (B).

5.   Discussion

This thesis focuses on the metabolism that determines the microspore embryogenesis process and the later regeneration efficiency in bread wheat. Amino acid, organic acid and sugars represented the main metabolites establishing the first stages of the microspore embryogenesis process. After analyzing them together with the transcriptomic data, the metabolic events overrepresented during microspore embryogenesis were: starch degradation and biosynthesis, energy production, antioxidative protection and nitrogen assimilation.

With the metabolic comparison of genotypes with different regeneration rate, it was possible to identify also the factors promoting the success of the plant regeneration. Amino acids, organic acids and some sugars differed between the genotypes even before the process started, showing a correlation with the regeneration rate. Practically, the mathematical model built, using few of these metabolites, predicted with high accuracy the regeneration rate.

A preliminary proteome analysis of the microspore embryogenesis helped to complete the molecular characterization of the process. Differences in protein levels were observed between 'Svilena' and 'Berengar' already from T1 stage.

All these findings are discussed in more detail in this section.

5.1.   Metabolic changes define the microspore embryogenesis

The combination of metabolomic and transcriptomic data in this study allowed the interpretation of the changes occurring in the first stages of the process. Although the tobacco metabolome in microspores has shown changes during the first stages of the microspore embryogenesis (Hosp et al., 2007), the integrative approach used here, enabled the identification of the cellular pathways defining microspore embryogenesis in wheat. This extends the knowledge of the process in this model species and when using cold stress pretreatment, helping also to build the general view of the microspore embryogenesis. Starch and sugar metabolism, TCA cycle and amino acid pathways were identified here as essential for the microspore embryogenesis. During the cold pretreatment, the sugar content increased, while that one of starch is suggested in this

thesis to decrease due to the changes in the metabolites and the transcription of genes involved in carbohydrate metabolism.

The metabolic and transcript levels of components of starch metabolism as well as TCA cycle changed during the nuclear division. Changes in amino acid metabolism included the GABA shunt or alanine pathway, with possible protection roles, but also glutamine in nitrogen assimilation by the enzyme isoform GS1.

Two working models are proposed to happen during the cold stress pretreatment and in the first nuclear division (figures 28 and 29) that are discussed in the following sections.
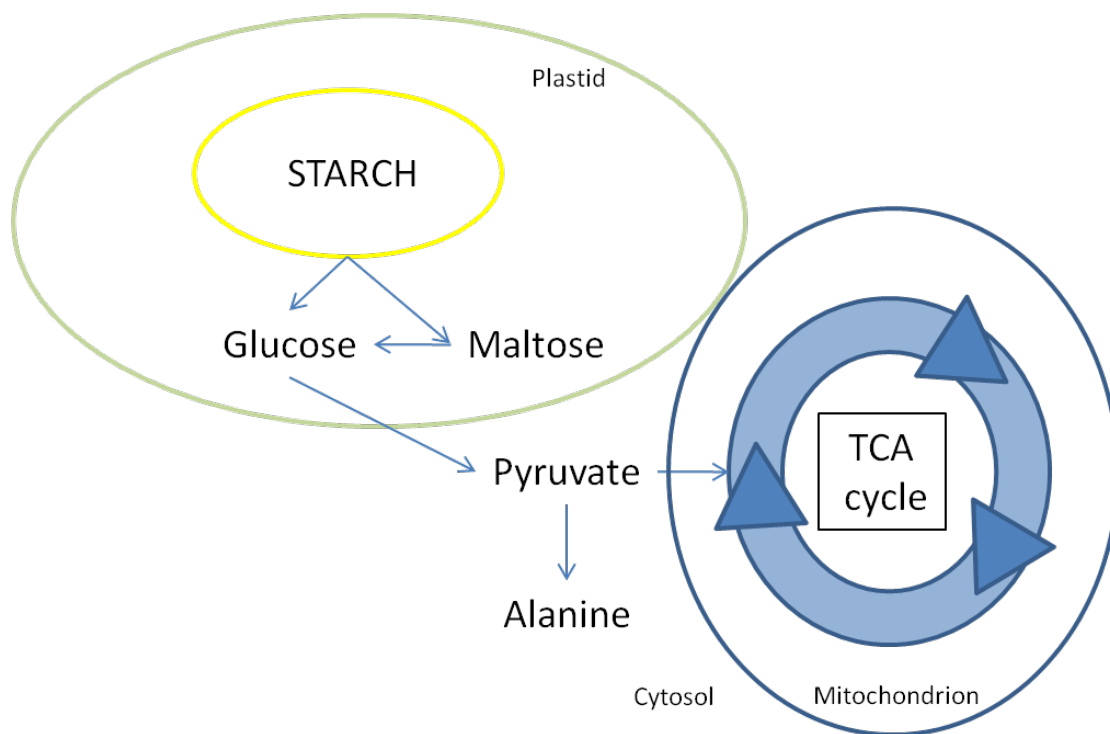
Figure 28: **Working model representing the main metabolic events during the cold stress pretreatment**. Starch is degraded into maltose and glucose, which through the glycolysis pathway might form pyruvate and enter the TCA cycle. Additionally alanine might be formed from pyruvate.
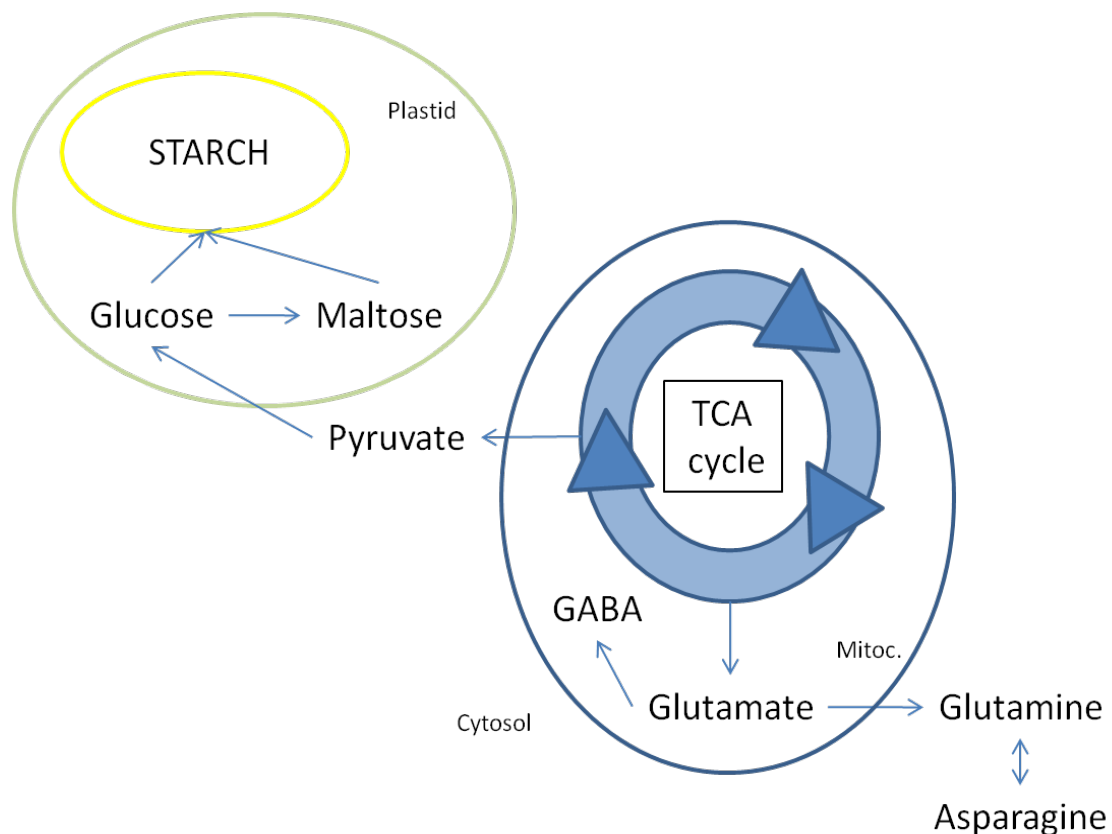
Figure 29: **Working model representing the main metabolic events after the first nuclear division**. Starch might be synthesized from maltose and glucose. Additionally the GABA shunt was more active in this stage. Finally, glutamine and asparagine were highly activated

.

5.1.1. Starch synthesis and breakdown determine the early stages of microspore embryogenesis

Starch content was suggested to decrease and later increase during the cold stress pretreatment and the nuclear division, respectively (figures 28 and 29). An increase in the content of maltose was correlated with the breakdown of starch mediated by β-amylase activity . Then maltose and also glucose may build starch in the T3 stage, since the levels of these metabolites fell. The levels of other sugars, such as xylose or trehalose, were in agreement with this assumption. Thus, the decrease of xylose after T2 would show a redirection of glucose to starch synthesis. Additionally, trehalose, a soluble non-reducing disaccharide that is considered as a stress protector, is induced by

low temperature stress (Kandror et al., 2002) and was represented among the products of starch degradation. The levels of this metabolite confirm the starch breakdown and later synthesis. Sucrose is a sugar that maintains cellular respiration and homeostasis (Winter and Huber, 2000), responds to low temperature treatment (Strand et al., 1999) and promotes the formation of androgenic somatic embryos (Tina et al., 2013). The higher abundance of this sugar in the cold treatment is associated with the loss of starch during the pretreatment period.

Furthermore, the results shown here are in line with the observed absence of starch deposits in vacuolated microspores of pepper (Bárány et al., 2010). Microspores may benefit from the degradation of starch to soluble sugars, since the latter may provide energy for the switching of the gametophytic to the sporophytic growth.

Finally, the results of the first nuclear division shown in this study agree with other studies in which starch does not accumulate until the first mitosis (Hosp et al., 2007; Bárány et al., 2010), indicating the onset of differentiation and proliferation.

5.1.2. TCA cycle is active during the cold stress pretreatment and amino acid metabolism after the first division stage

The main roles of TCA cycle include the provision of energy in the form of adenosine triphosphate (ATP), maintenance of 2-oxoglutarate levels to support nitrogen assimilation, provision of carbon skeletons and limitation of reactive oxygen species damage (Fernie et al., 2004). Intermediates of the TCA cycle, such as fumarate, malate or citrate, are produced in response to low temperature stress (Kaplan et al., 2004) and this was the case also in this study (figure 28). Energy in the form of ATP can be used to synthesize sugars to promote osmotic adjustment (López-Bucio et al., 2000). Thus, with the consumption of ATP, the abundance of these intermediates also decreased in T3 stage, which was accompanied by a decrease in sugars (figure 29). One exception was the succinic acid, which decreased in abundance in the T1-T3 period. The reduced levels of succinic acid were related to the increase in alanine between T1 and T2, and the increase in GABA between T2 and T3. This suggests a possible role of alanine under

cold stress and also a boost to the GABA shunt pathway around T3. The redirection of alanine to GABA shunt could explain the induction of carbohydrate metabolism, since the GABA shunt links nitrogen metabolism to carbon metabolism. Furthermore, following the first nuclear division of the microspore, nitrogen metabolism was induced via glutamate, probably as a result of the changed developmental pathway.

5.1.3. Different roles of amino acids during microspore embryogenesis

A very active amino acid metabolism characterized the first nuclear division stage. Besides their role during protein biosynthesis, different roles have been attributed to the amino acids, such as signaling (Haüsler et al., 2014). In the GABA shunt pathway, it was observed an increase in the alanine content in T2 and a decrease in T3. The higher content of alanine in the T2 stage could be explained with the production of this amino acid from pyruvate (figure 28). Alanine enables the reduction of oxygen and the level of reactive oxygen species (Zabalza et al., 2009), suggesting a role in controlling oxidative damage during cold stress. It may be used later for GABA production in T3 (figure 29), which has been suggested to be a transient nitrogen storage metabolite. A dual function as a signaling molecule and a metabolite has been suggested for this amino acid (Bouché and Fromm, 2004).

Nitrogen metabolism was induced mainly via glutamine and asparagine, serving the former as substrate to produce the latter. The GS/GOGAT cycle enzymes might assimilate nitrogen in T3 stage (figure 29), although the corresponding transcription data did not support this observation (discussed in the following section). Moreover, arginine might also assimilate nitrogen in T3 stage, but might additionally be serving as precursor of polyamines or nitric oxide (Winter et al., 2015).

5.1.3.1. Discordancy in amino acid metabolism between transcriptomics and metabolomics

In the study of amino acids, the metabolomic and transcriptomic data were not always in agreement. Such a discrepancy has previously been shown (Gibon et al., 2004), and could be explained by differences between the time of mRNA synthesis and the one of metabolite production. Translational regulation and protein turnover have also been suggested to explain the differences in abundance between transcript and protein levels (Fernie and Stitt, 2012). This could additionally be explained by the fact that most amino acids are synthesized through more than one pathway, and then they may be interconnected via common intermediates, weakening the correlation with the transcript abundance of a particular step. Furthermore, it is known that the synthesis of these metabolites is regulated by feedback inhibition of the amino acid (Less and Galili, 2008).

5.1.4. Glutamine synthetase 1 is the main isoform of the enzyme with a role in microspore embryogenesis

Non-congruent results were also observed between the protein abundance and the transcriptional data of glutamine synthetase, which was analyzed further as an example of such discrepancy discussed in the previous section.

Glutamine synthetase is responsible for the nitrogen assimilation, carried out by two isoforms of the enzyme, present in the chloroplast or in the cytosol. Glutamine synthetase 1, the cytosolic form of the enzyme, was the main isoform present in microspores over the T1-T3 period. It might be working in assimilating nitrogen in the cytosol, thus producing high levels of glutamine in T3 (figure 29). The regulation of gene expression of GS1 has been suggested to occur at the transcriptional and metabolite levels, being the glutamate and glutamine ratio one parameter for this regulation (Ortega et al., 2001; Watanabe et al., 1997). This might explain the non-congruent results observed between the protein abundance and the transcript data of this enzyme.

5.1.5. Fatty acid composition is marginally altered during the first stages of microspore embryogenesis

Fatty acid metabolism starts from the TCA cycle by the production of acetyl CoA. Although researchers have shown an accumulation of unsaturated fatty acids and a decrease of the saturated ones under low temperatures in rice leaves (Cruz et al., 2010), here no significant changes have been observed. Even so, the saturated fatty acids palmitate and lauric acids and their transcripts were slightly induced (without statistical significance) in T2, while the unsaturated acid oleic acid was unaffected. Dicarboxylic acids content, such as suberic and azelaic acids, coming from the fatty acid oxidation (Fujitani et al., 2009) in the peroxisome (Gerhardt, 1992), tended to increase also slightly in T2. This is in agreement with the association of azelaic acid and low temperature stress observed in *Arabidopsis thaliana* (Xu et al., 2011). Additionally, these dicarboxylic acids form sporopollenin, together with medium chain fatty acids, such as lauric, myristic and palmitic acids. Sporopollenin is present in the exine layer of the mature pollen grain (Domínguez et al., 1999). Since the microspore increases in size in T2 stage (Seguí-Simarro and Nuez, 2008), the exine layer and the sporopollenin in it are expected to respond similarly, and therefore, also those metabolites. The sporopollenin content should be measured to confirm this suggestion. Storage of energy, for a later use during the microspore embryogenesis, may be another possible role of this slight accumulation in fatty acids.

5.1.6. Cell reprogramming is achieved in microspore embryogenesis first stages

Molecular and cellular events must occur for a cell to become pluripotent. One of these changes is seen in the metabolism, since the reprogrammed cell state brings new energy requirements. Thus, after the cold stress pretreatment is applied, the metabolome of the microspore has been shown here to change, e.g, in starch, organic acids or amino acids. Such changes might bring new metabolic interactions with the genome, by the action, for example, of epigenetic changes (Kaelin and McKnight,

2013). One example is found in acetyl-CoA, which is part of the TCA cycle, or a building block of amino acids and other compounds. Additionally, it also serves as substrate of acteylation reactions carried out by histone acetyl transferase. S-adenosylmethionine, produced from methionine, contains a methyl donor group used by most methyltransferase enzymes. The metabolic changes reported in this thesis might affect the epigenome of the microspore, bringing a different gene expression, and thus, reprogramming the cell to go through the sporophytic pathway. Further epigenetic studies would clarify this suggestion.

5.2. Plant regeneration is studied in microspore embryogenesis

This thesis revealed that the success in green plant regeneration was molecularly preset even before the process had started. The efficiency of microspore embryogenesis is well known to be affected by the genotype of the plants (Bitsch et al., 1998, Malik et al., 2007, Mitykó et al., 1995). In this study, the genotype was highly affecting the regeneration efficiency, and this was reflected in the metabolome of the plants. Here, amino acid, organic acid and sugars metabolism constitute key pathways for the regeneration rate. Practically, finding a tool to select genotypes with high green plant regeneration rate in early stages would provide benefits for research and breeding programs. It will allow to speed up the process of releasing new varieties and genotypes, reducing the time, costs and labor. Here, metabolic markers in a mapping population of DH lines with different regeneration rates were identified. This allowed the development of a predictive model. Prediction of this rate was possible using few potential markers in the previous stage of the microspore embryogenesis process.

5.2.1. Genotype differences influence the regeneration efficiency through microspore embryogenesis

Previous studies in barley reported a relation between the genotype and the regeneration efficiency or the albino rates (Kharizi et al., 2011). In this thesis this relation has been shown, although the albino rates were very low in all the lines.

Regarding albinism, this is characterized by the loss of the inner membrane of the chloroplasts of the microspores and by the replenishing with lipids and globulins (Kahrizi et al., 2011). This condition also affects the efficiency of the method. However, very low rates were found in this study, proving that good incubation and growing material and methods were used.

Regarding the regeneration efficiency, the phenotype, as well as the genotype, was different between the DH lines. Some phenotypic carachteristics of the embryo, such as the shape and age, are known to be different between lines with different regeneration efficiency (Islam, 2010).

5.2.2. Metabolic profiles in the vacuolated stage determine the green plant regeneration rate

In the metabolic characterization of the DH lines, the reproducibility of the results was supported by the similar profiles found for 'Svilena' in the previous metabolome study shown in section 4.2. This similar profile was also found for most metabolites when all the lines were compared in two groups: high and low GPR rate lines. These two findings validate the previously defined metabolic pathways as essential in the process. However, the main difference resided in the concentrations of the metabolites between the groups of lines. Amino acids and organic acids showed higher concentrations in the high regenerating lines in all the stages. On the other hand, not so clear differences were found in sugars, fatty acids and other compounds. Therefore, high concentrations of metabolites are necessary firstly to resist the cold stress pretreatment, acquiring the totipotency, and later in the cell divisions, when there is a switched cell fate.

Reported roles for the metabolites would be reinforced in the DH lines with high regeneration rate. Since more energy might be produced in the TCA cycle of high GPR rate lines, these lines are able to produce more amino acids than the low GPR rate lines in all stages. In particular, amino acids, involved in protein, nitrogen and carbohydrate metabolism (Pratelli and Pilot, 2014), would have these functions highly activated in those lines. Therefore, their external application showed their ability to increase the

regeneration capacity in wheat embryo culture (Duran et al., 2013). Additionally, an interesting result is shown for the sugar galactose, which was more abundant in the lines with low regeneration rate, in all stages but mainly in the cold stress treatment. Although no explanation is yet found, the cell wall may be affected, probably by inhibiting cell growth (Thorpe et al., 1999).

All this may help the lines with high regeneration rates to tolerate the abrupt drop in temperature and then, to follow the embryogenesis divisions. Therefore, in the low GPR rate lines the reprogramming and embryogenesis steps probably could not be accomplished. Additionally, the source of this metabolic difference remains unclear and needs further characterization. Some studies point to differences in epigenetic modifications to explain the genotype dependence of the success of the microspore embryogenesis (Rodríguez-Sanz et al., 2014a). Different metabolic levels can bring different epigenetic patterns (as discussed in section 5.1.6), thus, epigenetics should be further studied in these samples.

5.2.3. Succesful early prediction of the green plant regeneration rate from metabolic markers

From a practical point of view, metabolic markers can be used to estimate the efficiency of a plant under stress conditions (Feussner and Polle, 2015, Fraire-Velázquez and Balderas-Hernández, 2013). Metabolic markers have been reported in studies under different conditions, such as trehalose in rice under drought stress (Quistián-Martínez et al., 2011), or allantoin in rice under salt stress (Nam et al., 2015). Since a perfect correlation (r=1) was not found for any of the metabolites in this study, the GPR rate could not be explained by only one metabolite. However, a predictive model using a combination of several of them could be built up. With the fordward stepwise regression the metabolites with the highest prediction accuracy were selected. Their concentrations explained high percentage of variance in the predicted GPR rate value. This was revealed by the high adjusted-R^2 value obtained for the variables selected.

Since the model was succesfully built from the results of the T1 stage, the regeneration rate of microspores of wheat DH lines can be determined with a high accuracy before starting the procedure that activates microspore embryogenesis. The subsequent steps of the method and the regeneration could then be omitted and not necessary to know the regeneration efficiency of the line. Therefore, this model allows the selection of genotypes with the best regeneration rate in early stages.

The validation test confirmed the high accuracy of the model. This showed this model to be a potential tool for the GPR rate prediction.

Finally, this model could be used in the improvement of existing breeding methods. However, further implementation of the model must be done with other genotypes.

5.2.4. Protein differences are observed prior to microspore embryogenesis and affect the GPR rate

In this thesis, the proteome of wheat microspores was analyzed by mass spectrometry after trypsin digestion. After the comparison of two cultivars with high and low regeneration rates, proteins involved in biological processes that are beneficial for the success of the plant regeneration arose in the analysis. Major protein changes were found in carbohydrate metabolism, lipid metabolism, transcription, translation, protein metabolism, cytoskeleton and stress-related protein. In all of them, the higher protein levels in T1 in 'Svilena' suggest that i) this genotype might have more resources to overcome the cold stress, that ii) certain levels of proteins were necessary to go through that stage, and that iii) the cell reprogramming was already achieved in the first nuclear division stage. These findings are discussed in the following sections.
.

5.2.4.1. 'Svilena' has initially more resources than 'Berengar' to overcome the cold stress and reprogramming phase

Proteins detected to be significantly more abundant in microspores of 'Svilena' in T1 may be relevant for the microspore embryogenesis success. They established the difference between the lines even before the procedure started. In particular, proteins detected of the carbohydrate metabolism might be providing enough energy in

'Svilena' for the cell to go successfully through the cold stress pretreatment. The three enzymes detected were enolase, phosphoglycerate kinase and pyruvate kinase. All of them presented either a tendency or significant higher levels in T1 in microspores of 'Svilena'. Enolase coverts 2-phosphoglycerate to phosphoenolpyruvate, which would be ready for pyruvate production by pyruvate kinase. That reaction produces ATP, and allows pyruvate to enter the TCA cycle, in which more energy is produced. This agrees with the higher levels of TCA cycle intermediates in 'Svilena' compared to 'Berengar' (results shown in section 4.2.2). Finally, phosphoglycerate kinase catalyzes the conversion of 1,3-biphosphoglycerate and 3-phosphoglycerate producing ATP. The importance of enough energy supply for the microspore competence was shown in a triticale anther culture with low temperature as stress pretreatment (Krzewska et al., 2017), but not in wheat. Therefore, microspores producing more energy would have more success during microspore embryogenesis and the later regeneration. In order to confirm this suggestion, ATP levels should be measured in the samples.

Additionally, the increased levels found in microspores of 'Svilena' in T1 of the proteins with roles in RNA stabilization or with chaperone activity might give to this genotype a better protection against the stress, such as the cold shock protein-1. This protein interacts with nucleic acids and also has chaperone activity (Sasaki and Imai, 2011).

Finally, a stress-related protein was found significantly higher in microspores of 'Svilena' in T1 stage. The ozone-responsive stress-related protein, reacts to an increase in cytosolic calcium specific of ozone (Short et al., 2012), and leads to stress tolerance. This protein might react to the cytosolic calcium generated during the microspore embryogenesis process in 'Svilena'.

The higher abundance of stress related proteins in 'Svilena' microspores in T1 suggests a better protection of this genotype against stress. This coincides with the suggestion formulated in the study of Muñoz-Amatriaín et al. (2009), in which protective genes detected with higher expression were suggested to give more chances to go through microspore embryogenesis with success.

5.2.4.2. Particular protein levels are necessary during the cold stress stage

A different response to cold stress between both genotypes was shown in this study. In T2 stage, protein abundances of most proteins detected in 'Berengar' showed a tendency to increase. In particular, this tendency was found in the proteins detected in carbohydrate metabolism, but also in the ones related to transcription, translation and posttranslation modifications. For example, the small heat shock protein 23.6 exhibited higher abundance in T2 in 'Berengar' microspores. Many stresses can induce the synthesis of these proteins, such as heat shock in rice anthers (Kim et al., 2015).

Interestingly, the abundance of the proteins of 'Berengar' in T2 reached the levels found in T1 in 'Svilena'. This finding suggests that certain protein levels were necessary to overcome the cold stress and achieve the cell reprogramming.

5.2.4.3. Microspores in the T3 stage go through the sporophytic pathway

'Svilena' and 'Berengar' microspores showed similar profiles of proteins in T3 stage. This suggests that the microspores analyzed of both cultivars were already in the same developmental pathway, the sporophytic pathway. In carbohydrate metabolism, the decreased abundance of the identified proteins correlated with the starch synthesis suggested in this thesis in the metabolome analysis of 'Svilena' microspores (discussed in section 5.1.1). Additionally, phospholipase D hydrolyzes phospholipids, which are part of the biological membranes. This protein has been reported to link microtubules and membranes, and to be involved in cell division in *Nicotiana tabacum* (Dhonukshe et al., 2003). UDP-glucose-6-dehydrogenase forms UDP-glucuronic acid, which has a role in plant cell wall formation (Reboul et al., 2011). Therefore, the increased abundances of UDP-glucose-6-dehydrogenase and phospholipase D suggest a role in the mitosis ocurring in T3. Proteins with roles in RNA stabilization, with protein

chaperone activity or involved in translation showed a decrease in the last stage. However, the increased levels in T3 of disulfide isomerase in both genotypes suggest that chaperone activity was present in this stage.

Finally, the increased levels of tubulin found in both genotypes in T3 stage would help in the correct displacements of the nuclei during the first nuclear division. After the central position of the nuclei has been achieved, a symmetric division takes place with an equatorial plane of division (Segui-Simarro and Nuez, 2008).

5.2.4.4. Summary of the proteome analysis and future research

Proteome analyses have been reported during microspore embryogenesis in different species, such as rapeseed (Joosen et al., 2007). However, a proteome comparison during the early stages of the microspore embryogenesis process between genotypes with different regeneration efficiency was not done before in wheat microspores. All the findings shown here indicate that microspores of both cultivars differed at the molecular level, even in T1 stage. Carbohydrate metabolism, transcription, translation and protein metabolism represented the most important differences. Enough protein resources might lead the microspores of 'Svilena' to achieve successfully the reprogramming of the cell. This indicated more availability of proteins for biological processes in the microspores of 'Svilena' that would be necessary to overcome the cold stress and switch the developmental pathway. In T3 stage both genotypes were found with the same protein profiles.

Further analysis is still required, such as measurement of more replicates and genotypes. The proteome of the above analyzed DH lines could be studied together with the metabolome results shown in this thesis. This would allow the determination of essential pathways for the regeneration efficiency. Furthermore, epigenetic modifications might explain these molecular differences, since such modifications can alter the gene expression and then lead to different protein and metabolite abundances. In the reprogramming step, epigenetic signatures already acquired during

the gametophytic development must be changed, achieving totipotency. For example, histone posttranslational modifications could be analyzed, as it has been done in other studies, such as in *B. napus* or barley microspores (Rodriguez-Sanz et al., 2014b; Pandey et al., 2017). Epigenetic modifications were examined in the protein level. In particular, different histone modifications were searched. However, the statistics were not sufficient. Therefore, a targeted study is proposed as a future study. Their inheritance to the next generation (Heard and Martienssen, 2014), which is common in plants, allows the continuity of the success in the microspore embryogenesis, and therefore, further study is of high interest.

6.   Main conclusions

The study has revealed the metabolic and molecular principles of behavior of bread wheat microspores during microspore embryogenesis first stages, using cold stress as inducing pretreatment. In general, energy production, with starch degradation and more active TCA cycle have been suggested to chacarterize the star-like morphology stage, where the de-differentiation occurs. Later, the microspore is already redirected to the sporophytic pathway, characterized by a very active amino acid metabolism, and starch production is also suggested.

Metabolic markers revealed a plausible explanation for the regeneration rate difference between genotypes. This was seen in the previous stage to the application of the low temperature. At that point, more energy produced, and nucleic acid and protein metabolism characterized a genotype with high regeneration efficiency. A possible reason for these different results is proposed to come from different epigenetic marks between genotypes that could be studied further. Finally, the predictive model built can help to improve the efficiency of the breeding method, since it allowed differentiating the genotypes with the best and the lowest regeneration rate before applying the stress pretreatment.

7.   References

Arzani A, Mirodjagh SS. 1999. Response of durum wheat cultivars to immature embryo culture, callus induction and in vitro salt stress. Plant Cell Tissue and Organ Culture, 58: 67-72.

Ay N, Irmler K, Fischer A, Uhlemann R, Reuter G, Humbeck K. 2009. Epigenetic programming via histone methylation at *WRKY53* controls leaf senescence in *Arabidopsis thaliana*. The Plant Journal, 58: 333–346.

Ay N, Janack B and Humbeck K. 2014. Epigenetic control of plant senescence and linked processes. Journal of Experimental Botany, 65: 3875-3887.

Ayed OS, De Buyser J, Picard E, Trifa Y, Amara HS. 2009. Effect of pre-treatment on isolated microspores cultutre ability in durum wheat (*Triticum turgidum* subsp. Durum Desf.). Journal of Plant Breeding and Crop Science, 2: 030-038.

Baenziger PS, DePauw RM. 2009. Wheat Breeding: Procedures and Strategies. In: Wheat Science and Trade. Ames, IA, USA, 273-308.

Bárány I, González-Melendi P, Fadón B, Mitykó J, Risueño M, Testillano PS. 2005. Microspore-derived embryogenesis in pepper (*Capsicum annuum* L.): subcellular rearrangements through development. Biology Cell, 97: 709-22.

Bárány I, Fadón B, Risueño MC, Testillano PS. 2010. Microspore reprogramming to embryogenesis induces changes in cell wall and starch accumulation dynamics associated with proliferation and differentiation events. Plant Signaling and Behavior, 5: 341-345.

Bäumlein H, Miséra S, Luerßen H, Kölle K, Horstmann C, Wobus U, Müller AJ. 1994. The *FUS3* gene of *Arabidopsis thaliana* is a regulator of gene expression during late embryogenesis. The plant Journal, 6: 379-387.

Beligni MV, Fath AB, Lamattina PC, Jones L, Russell L. 2002. Nitric oxide acts as an antioxidant and delays programmed cell death in barley aleurone layers. Plant Physiology, 129: 1642-1650.

Bitsch C, Gröger S, Lelley T. 1998. Effect of parental genotypes on haploid embryo and plantlet formation in wheat × maize crosses. Euphytica, 103: 319–323.

Böttcher C, Centeno D, Freitag J, et al. 2008. Teaching (and learning from) metabolomics: The 2006 PlantMetaNet ETNA Metabolomics Research School. Physiologia Plantarum, 132: 136–149.

Bouché N, Fromm H. 2004. GABA in plants: just a metabolite? Trends in plant science, 9: 110-115.

Boyko A, Blevins T, Yao Y, Golubov A, Bilichak A, Ilnytskyy Y, Hollander J, Meins F, Kovalchukl JR. 2010. Transgenerational adaptation of *Arabidopsis* to stress requires DNA methylation and the function of dicer-like proteins. PLoS ONE, 5: 9514.

Campbell AW, Griffin WB, Burritt DJ, Conner AJ. 2000. Production of wheat doubled haploids via wide crosses in New Zealand wheat, New Zealand Journal of Crop and Horticultural Science, 28: 185-194.

Caredda S, Devaux P, Sangwan RS, Clemént C. 1999. Differential development of plastids during microspore embryogenesis in barley. Protoplasma, 208: 248–256.

Caredda S, Doncoeur C, Devaux P, Sangwan RS, Clément C. 2000. Plastid differentiation during androgenesis in albino and non-albino producing cultivars of barley (*Hordeum vulgare* L.). Sexual Plant Reproduction, 13: 95–104.

Chen Z, Snyder S, Fan Z, Loh W. 1994. Efficient production of doubled haploid plants through chromosome doubling of isolated microspores in *Brassica napus.* Plant Breeding, 113: 217-221.

Cheng Y, Ma R, Jiao Y, Qiao N, Li T. 2013. Impact of genotype, plant growth regulators and activated charcoal on embryogenesis induction in microspore culture of pepper (*Capsicum annuum* L.). South African Journal of Botany, 88: 306–309.

Corral-Martínez P, Parra-Vega V, Seguí-Simarro JM. 2013. Novel features of *Brassica napus* embryogenic microspores revealed by high pressure freezing and freeze substitution: evidence for massive autophagy and excretion-based cytoplasmic cleaning. Journal of Experimental Botany, 64: 3061–3075.

Cruz RPd, Golombieski JI, Bazana MT, Cabreira C, Silveira TF, Silva LPd. 2010. Alterations in fatty acid composition due to cold exposure at the vegetative stage in rice. Brazilian Journal of Plant Physiology, 22: 199-207.

Domínguez E, Mercado AJ, Quesada AM, Heredia A. 1999. Pollen sporopollenin: degradation and structural elucidation. Sexual Plant Reproduction, 12: 171-178.

Dhonukshe P, Laxalt AM, Goedhart J, Gadella TWJ, Munnik T. 2003. Phospholipase D activation correlates with microtubule reorganization in living plant cells. The Plant Cell, 15: 2666-2679.

Dubas E, Wedzony M, Petrovska B, Salaj J, Zur I. 2010. Cell structural reorganization during induction of androgenesis in isolated microspore cultures of Triticale (x*Triticosecale Wittm*.). Acta Biologica Cracovensia Series Botanica, 52: 73-86.

Duran RE, Coskun Y, Demicri T. 2013. Comparison of amino acids for their efficiency on regeneration in wheat embryo culture. Asian Journal of Plant Science and Research, 3: 115-119.

Feussner I, Polle A. 2015. What the transcriptome does not tell—Proteomics and metabolomics are closer to the plants' patho-phenotype. Current Opinion in Plant Biology, 26: 26–31.

El-Tantawy AA, Solís MT, Risueño MC, Testillano PS. 2014. Changes in DNA methylation levels and nuclear distribution patterns after microspore reprogramming to embryogenesis in barley. Cytogenetic and Genome Research, 143: 200-208.

Fernie AR, Carrari F, Sweetlove LJ. 2004. Respiratory metabolism: glycolysis, the TCA cycle and mitochondrial electron transport. Current Opinion in Plant Biology, 7, 254-261.

Fernie AR, Stitt M.2012. On the discordance of metabolomics with proteomics and transcriptomics: coping with increasing complexity in logic, chemistry, and network interactions scientific correspondence. Plant Physiology, 158:1139-1145.

Forster BP, Heberle-Bors E, Kasha KJ, Touraev A. 2007. The resurgence of haploids in higher plants. Trends in Plant Science, 12: 368-375.

Fujitani K, Manami H, Nakazawa M, Oida T, Kawase T. 2009. Preparation of Polycarboxylic Acids by Oxidative Cleavage with Oxygen / Co-Mn-Br System. Journal of Oleo Science, 58: 629-637.

Fraire-Velázquez SL, Balderas-Hernández VE. 2013. Abiotic stress in plants and metabolic responses. In: Vahdati K, Leslie C, editors. Abiotic stress—Plant responses and applications in agriculture. Rijeka: INTECH: 25–46.

Gerhardt B. 1992. Fatty acid degradation in plants. Progress in Lipid Research, 31: 417-446.

Gibon Y, Blaesing OE, Hannemann J, Carillo P, Höhne M, Hendriks JHM, Palacios N, Cross J, Selbig J, Stitt M. 2004. A robot-based platform to measure multiple enzyme activities in arabidopsis using a set of cycling assays: Comparison of changes of enzyme activities and transcript levels during diurnal cycles and in prolonged darkness. Plant Cell, 16: 3304-3325.

Guha S, Maheshwari SC. 1964. In vitro production of embryos from anthers of *Datura*. Nature, 204: 497.

Guzy-Wróbelska J, Szarejko I. 2003. Molecular and agronomic evaluation of wheat doubled haploid lines obtained through maize pollination and anther culture methods. Plant Breeding, 122: 305–313.

Hanin M, Brini F, Ebel C, Toda Y, Takeda S, Masmoudi K. 2011. Plant dehydrins and stress tolerance: Versatile proteins for complex mechanisms. Plant Signaling and Behavior, 6: 1503-1509.

Hause B, van Veenendaal WL, Hause G, van Lammer en AA. 1994. Expression of polarity during early development of microspore-derived and zygotic embryos of *Brassica napus* L. cv Topas. Botanica Acta, 107: 407-415.

Haüsler RE, Ludewig F, Krueger S. 2014. Amino acids – A life between metabolism and signaling. Plant Science, 229: 225-237.

Heard E, Martienssen RA. 2014. Transgenerational Epigenetic Inheritance: myths and mechanisms. Cell, 157: 95-109.

Heidarvand L, Maali Amiri R. 2010. What happens in plant molecular responses to cold stress? Acta Physiologiae Plantarum, 32: 419-431.

Hesse M, Halbritter H, Zetter R, Weber M, Buchner R, Frosch-Radivo A, Ulrich S. 2009. Pollen terminology. An illustrated handbook. New York: SpringerWein, 264.

Hoekstra S, van Zijderveld MH, Louwerse JD, Heidekamp F, van der Mark F. 1992. Anther and microspore culture of *Hordeum vulgare* L. cv. Igri. Plant Science, 86: 89-96.

Hosp J, Tashpulatov A, Roessner U, Barsova E, Katholnigg H, Steinborn R, Melikant B, Lukyanov S, Heberle-Bors E, Touraev A. 2007. Transcriptional and metabolic profiles of stress-induced, embryogenic tobacco microspores. Plant Molecular Biology, 63: 137-149.

Islam SM. 2010. Effect of embryoids age, size and shape for improvement of regeneration efficiency from microspore-derived embryos in wheat (*Triticum aestivum* L.). Plant Omics Journal, 3: 149-153.

Jacquard C, Nolin F, Hécart C. et al. 2009. Microspore embryogenesis and programmed cell death in barley: effects of copper on albinism in recalcitrant cultivars. Plant Cell Reports, 28: 1329.

Jiang J, Zhang Z, Cao J. 2012. Pollen wall development: The associated enzymes and metabolic pathways. Plant biology: 1-15.

Joosen R, Cordewener J, Supena EDJ, et al. 2007. Combined transcriptome and proteome analysis identifies pathways and markers associated with the establishment of rapeseed microspore-derived embryo development. Plant Physiology, 144: 155–172.

Kaelin WG, McKnight SL. 2013. Influence of Metabolism on Epigenetics and Disease. Cell, 153: 56-69.

Kahrizi D,Mahmoodi S, Bakshi Khaniki G, Mirzaei M. 2011. Effect of genotype on androgenesis in barley (*Hordeum vulgare* L.). Biharean Biologist, 5: 132-134.

Kandror O, DeLeon A, Goldberg AL. 2002. Trehalose synthesis is induced upon exposure of *Escherichia coli* to cold and is essential for viability at low temperatures. Proceedings of the National Academy of Sciences, 99: 9727-9732.

Kaplan F, Kopka J, Haskell DW, Zhao W, Schiller KC, Gatzke N,Sung DY, Guy CL. 2004. Exploring the temperature-stress metabolome of Arabidopsis. Plant Physiology, 136: 4159-4168

Kasarda DD. 2013. Can an increase in celiac disease be attributed to an increase in the gluten content of wheat as a consequence of wheat breeding? Journal of Agricultural and Food Chemistry, 61: 1155-1159.

Khalequzzaman M, Haq N, Hoque E, Aditya TL. 2005. Regeneration efficiency and genotypic effect of some indica type Bangaldeshi rice (*Oryza sativa L*.) landraces. Plant Tissue Culture and Biotechnology, 15: 33-42.

Kim M, Kim H, Lee W, Lee Y, Kwon S-W, Lee J. 2015. Quantitative shotgun proteomics analysis of rice anther proteins after exposure to high temperature. International Journal of Genomics, 238704.

Köhler C, Wolff P, Spillane C. 2012. Epigenetic mechanisms underlying genomic imprinting in plants. Annual Review of Plant Biology, 63: 331-352.

Korzun V, Röder MS, Ganal MW, Worland AJ, Law CN. 1998. Genetic analysis of the dwarfing gene (*Rht8*) in wheat. Part I. Molecular mapping of *Rht8* on the short arm of chromosome 2D of bread wheat (*Triticum aestivum* L.). Theoretical and Applied Genetics, 96: 1104-1109.

Krishna P, Sacco M, Cherutti JF, Hill S. 1995. Cold-induced accumulation of hsp90 transcripts in *Brassica napus*. Plant Physiology, 107: 915-923.

Krzewska M, Gołębiowska-Pikania G, Dubas E, Gawin M, Żur I. 2017. Identification of proteins related to microspore embryogenesis responsiveness in anther cultures of winter triticale (x*Triticosecale* Wittm.). Euphytica, 213: 192.

Lantos C, Páricsi S, Zofajova A, Weyen J, Pauk J. 2006. Isolated microspore culture of wheat (*Triticum aestivum* L.) with Hungarian cultivars. Acta Biologica Szegediensis, 50:31-35.

Lantos C, Weyen J, Orsini JM, et al. 2013. Efficient application of in vitro anther culture for different European winter wheat (*Triticum aestivum* L.) breeding programmes. Plant Breeding, 132: 149-154.

Less H, Galili G. 2008.Principal transcriptional programs regulating plant amino acid metabolism in response to abiotic stresses. Plant Physiology, 147: 316-330.

Lev-Yadun S, Gopher A, Abbo S. 2000. The cradle of agriculture. Science, 288: 1602-1603.

Lichter R. 1982. Induction of haploid plants from isolated pollen of *Brassica napus*. Z Pflanzenphysiology, 105: 427–434.

Lippmann R, Kaspar S, Rutten T, Melzer M, Kumlehn J, Matros A, Mock H-P. 2009. Protein and metabolite analysis reveals permanent induction of stress defense and cell regeneration processes in a tobacco cell suspension culture. International Journal of Molecular Sciences, 10: 3012-3032.

Lippmann R, Friedel S, Mock H-P, Kumlehn J. 2015. The low molecular weight fraction of compounds released from immature wheat pistils supports barley pollen embryogenesis. Frontiers in Plant Science, 6: 498.

Liu W, Zheng MY, Konzak CF. 2002. Improving green plant production via isolated microspore culture in bread wheat (*Triticum aestivum* L.). Plant Cell Reports, 20: 821-824.

Liu D, Zhang H, Zhang L, Yuan Z, Hao M, Zheng Y. 2014. Distant hybridization: A tool for interspecific manipulation of chromosomes. In: A. Pratap and J. Kumar (eds.), Alien gene transfer in crop plants, Volume 1: Innovations, Methods and Risk Assessmen, 25-42.

López-Bucio J, Nieto-Jacobo MF, Ramírez-Rodríguez V, Herrera-Estrella L. 2000. Organic acid metabolism in plants: from adaptive physiology to transgenic varieties for cultivation in extreme soils. Plant Science, 160: 1-13.

Magnard JL, Vergne P, Dumas C. 1996. Complexity and genetic variability of heat-shock protein expression in isolated maize microspores. Plant Physiology, 111: 1085-1096.

Makowska K, Oleszczuk S. 2014. Albinism in barley androgenesis. Plant Cell Reports, 33: 385-392.

Malik MR, Wang F, Dirpaul JM, Zhou N, Polowick PL, Ferrie AMR , Krochko JE. 2007. Transcript profiling and identification of molecular markers for early microspore embryogenesis in *Brassica napus*. Plant Physiology, 144: 134-154.

Maluszynski M, Kasha KL, Forster BP, Szarejko I. 2003. Doubled haploid production in crop plants. A Manual. Kluwer Academic Publisher.

Maraschin SF, Lamers GEM, de Pater BS, Spaink HP, Wang M. 2003. 14-3-3 isoforms and pattern formation during barley microspore embryogenesis. Journal of Experimental Botany, 54: 1033-1043.

Maraschin SF, de Priester W, Spaink HP, Wang M. 2005a. Androgenic switch: an example of plant embryogenesis from the male gametophyte perspective. Journal of Experimental Botany, 56: 1711-1726.

Maraschin SF, Vennik M, Lamers GEM, Spaink HP, Wang M. 2005b. Time-lapse tracking of barley androgenesis reveals position-determined cell death within pro-embryos. Planta, 220: 531-40.

Maraschin SF, Caspers M, Potokina E, Wülfert F, Graner A, Spaink HP, Wang M. 2006. cDNA array analysis of stress-induced gene expression in barley androgenesis. Physiologia Plantarum 127: 535-550.

Mathias R and Röbbelen G. 1991. Effective diploidization of microspore-derived haploids of rape (*Brassica napus* L.) by invitro colchicine treatment. Plant Breeding, 106: 82-84.

Mitykó J, Andrásfalvy A, Csilléry G, Fári M. 1995. Anther-culture response in different genotypes and F_1 hybrids of pepper (*Capsicum annuum* L.). Plant Breeding, 114: 78–80.

Miura K, Furumoto T. 2013. Cold signaling and cold response in plants. International Journal of Molecular Sciences, 14: 5312-5337.

Molina MD, Aponte EM, Cortina H, Moreno G. 2002. The effect of genotype and explant age on somatic embryogenesis of coffee. Plant Cell Tissue and Organ Culture, 71: 117-123.

Möllers C, Iqbal M, Röbbelen G. 1994. Efficient production of doubled haploid *Brassica napus* plants by colchicine treatment of microspores. Euphytica, 75: 95-104.

Muñoz-Amatriaín M, Svensson JT, Castillo AM, Close TJ, Vallés MP. 2009. Microspore embryogenesis: assignment of genes to embryo formation and green vs. albino plant production. Functional and Integrative Genomics, 9: 311-323.

Nam HM, Bang E, Kwon YT, Kim Y, Kim HE, Cho K, et al. 2015. Metabolite profiling of diverse rice germplasm and identification of conserved metabolic markers of rice roots in response to long-term mild salinity stress. International Journal of Molecular Sciences, 16: 21959–21974.

Nejadsadeghi L, Maali-Amiri R, Zeinali H, Ramezanpour S, Sadeghzade B. 2014. Comparative analysis of physio-biochemical responses to cold stress in tetraploid and hexaploid wheat. Cell Biochemistry and Biophysics, 70: 399-408.

Nevo E, Korol AB, Beiles A, Fahima T. 2002. Domestication of wheats. In Evolution of Wild Emmer and Wheat Improvement, eds. Nevo E, Korol AB, Beiles A, Fahima T . Springer Berlin Heidelberg, 3-10.

Niemirowicz-Szczytt, K. 1997. Excessive homozygosity in doubled haploids e advantages and disadvantages for plant breeding and fundamental research. Acta Physiologiae Plantarum, 19: 155-167.

Niroula RK, Bimb HP. 2009. Overview of wheat X maize system of crosses for dihaploid induction in wheat. World Applied Sciences Journal, 7: 1037-1045.

Ortega JL, Temple SJ, Sengupta-Gopalan C. 2001. Constitutive overexpression of cytosolic glutamine synthetase (GS_1) gene in transgenic alfalfa demonstrates that GS_1 may be regulated at the level of RNA stability and protein turnover. Plant Physiology, 126: 109-121.

Pandey P, Houben A, Kumlehn J, Melzer M, Rutten T. 2013. Chromatin alterations during pollen development in *Hordeum vulgare*. Cytogenetic Genome Research, 141: 50-57.

Pandey P, Daghma D S, Houben A, Kumlehn J, Melzer M, Rutten T. 2017. Dynamics of post-translationally modified histones during barley pollen embryogenesis in the presence or absence of the epi-drug trichostatin A. Plant Reproduction, 30: 95-105

Parker GD, Chalmers KJ, Rathjen AJ, Langridge P. 1998. Mapping loci associated with flour colour in wheat (*Triticum aestivum* L*.)*. Theoretical and Applied Genetics, 97: 238-245.

Petersen G, Seberg O, Yde M, Berthelsen K. 2006. Phylogenetic relationships of *Triticum* and *Aegilops* and evidence for the origin of the A, B, and D genomes of common wheat *(Triticum aestivum)*. Molecular and Phylogenetic Evolution, 39: 70–82**.**

Pikaard CS, Scheid OM. 2014.Epigenetic regulation in plants. Cold Spring Harbor Perspectives in Biology, 6.

Poersch-Bortolon LB, Mansur Scagliusi SM, Yamazaki-Lau E, Bodanese-Zanettini MH. 2016. Androgenic response of Brazilian wheat genotypes to different pretreatments of spikes and to a gelling agent. Pesquisa Agropecuária Brasileira, 51: 1839-1847.

Pratelli R, Pilot G. 2014. Regulation of amino acid metabolic enzymes and transporters in plants. Journal of Experimental Botany, 65: 5535-5556.

Quarrie SA, Gulli M, Calestani C, Steed A, Marmiroli N. 1994. Location of a gene regulating drought-induced abscisic acid production on the long arm of chromosome 5A of wheat. Theoretical and Applied Genetics, 89: 794-800.

Quilichini TD, Grienenberger E, Douglas CJ. 2014. The biosynthesis, composition and assembly of the outer pollen wall: A tough case to crack. Phytochemistry, 113: 170-182.

Quistián-Martínez D, Estrada-Luna AA, Altamirano-Hernández J, Peña-Cabriales JJ, Oca-Luna RM, Cabrera-Ponce JL. 2011. Use of trehalose metabolism as a biochemical marker in rice breeding. Molecular Breeding, 30: 469–477.

Ramakrishna A, Ravishankar GA. 2011. Influence of abiotic stress signals on secondary metabolites in plants. Plant Signaling and Behavior, 6: 1720-1731.

Reboul R, Geserick C, Pabst M, Frey B, Wittmann D, Lütz-Meindl U, Léonard R, Tenhaken R. 2011. Down-regulation of UDP-glucuronic acid biosynthesis leads to swollen plant cell walls and severe developmental defects associated with changes in pectic polysaccharides. The Journal of Biological Chemistry. 286: 39982-39992.

Renaut J, Lutts S, Hoffmann L, Hausman JF. 2004. Responses of poplar to chilling temperatures: Proteomic and physiological aspects. Plant biology, 6: 81-90.

Rodríguez-Serrano M, Bárány I, Prem D, Coronado M-J, Risueño MC, Testillano PS. 2011. NO, ROS, and cell death associated with caspase-like activity increase in stress-induced microspore embryogenesis of barley. Journal of Experimental Botany, 63: 1-18.

Rodríguez-Sanz H, Manzanera J-A, Solís M-T, Gómez-Garay A, Pintos B, Risueño MC, Testillano PS. 2014a. Early markers are present in both embryogenesis pathways from microspores and immature zygotic embryos in cork oak, *Quercus suber* L. BMC Plant Biology, 14, 224.

Rodríguez-Sanz H, Moreno-Romero J, Solís MT, Köhler C, Risueño MC, Testillano PS. 2014b. Changes in histone methylation and acetylation during microspore reprogramming to embryogenesis occur concomitantly with nHKMT and BnHAT expression and are associated with cell totipotency, proliferation, and differentiation in *Brassica napus*. Cytogenetic Genome Research, 143: 209-218.

Rohn H, Junker A, Hartmann A, Grafahrend-Belau E, Treutler H, Klapperstück M, Czauderna T, Klukas C, Schreiber F. 2012: VANTED v2: a framework for systems biology applications. BMC Systems Biology, 6: 139.

Rubtsova M, Gnad H, Melzer M, Weyen J, Gils M. 2013. The auxins centrophenoxine and 2,4-D differ in their effects on non-directly induced chromosome doubling in anther culture of wheat (*T. aestivum* L.). Plant Biotechnology Reports, 7: 247-255.

Sánchez-Díaz RA, Castillo AM, Vallés MP. 2013. Microspore embryogenesis in wheat: new marker genes for early, middle and late stages of embryo development. Plant Reproduction, 26: 287-96.

Sasaki K, Imai R. 2011. Pleiotropic Roles of Cold Shock Domain Proteins in Plants. Frontiers in plant science, 2: 116.

Schlegel R, Belchev I, Kostov K, Atanassova M. 2000. Inheritance of high anther culture response in hexaploid wheat, *Triticum aestivum* L. var. Svilena. Bulgarian Journal of Agricultural Science, 6: 261-270.

Schreiber F, Colmsee C, Czauderna T, Grafahrend-Belau E, Hartmann A, Junker A, Junker BH, Klapperstück M, Scholz U, Weise S. 2012. MetaCrop 2.0: managing

and exploring information about crop plant metabolism. Nucleic Acids Research, 40: D1173–D1177.

Seguí-Simarro JM, Nuez F. 2008. How microspores transform into haploid embryos: changes associated with embryogenesis induction and microspore-derived embryogenesis. Physiologia Plantarum, 134: 1-12.

Seifert F, Bössow S, Kumlehn J, Gnad H, Scholten S. 2016. Analysis of wheat microspore embryogenesis induction by transcriptome and small RNA sequencing using the highly responsive cultivar "Svilena". BMC Plant Biology, 16: 1-16.

Shariatpanahi M, Belogradova K, Hessamvaziri L, Heberle-Bors E, Touraev A. 2006. Efficient embryogenesis and regeneration in freshly isolated and cultured wheat (*Triticum aestivum* L.) microspores without stress pretreatment. Plant Cell Reports, 25: 1294-1299.

Shewry PR. 2009. Wheat. Journal of Experimental Botany, 60: 1537–1553.

Short EF, North KA, Roberts MR, Hetherington AM, Shirras AD, McAinsh MR. 2012. A stress-specific calcium signature regulating an ozone-responsive gene expression network in Arabidopsis. The Plant Journal, 71: 948-961.

Silva TD. 2012. Microspore embryogenesis. In: Sato KI, ed. Embryogenesis. Rijeka: InTech, 573-596.

Solís MT, Rodríguez-Serrano M, Meijón M, Cañal MJ, Cifuentes A, Risueño MC, Testillano PS. 2012. DNA methylation dynamics and *MET1a-like* gene expression changes during stress-induced pollen reprogramming to embryogenesis. Journal of Experimental Botany, 63: 6431–6444.

Somleva MN, Schmidt EDL, de Vries SC. 2000. Embryogenic cells in *Dactylis glomerata* L. (Poaceae) explants identified by cell tracking and by SERK expression. Plant Cell Reports, 19: 718-726.

Soriano M, Li H, Boutilier K. 2013. Microspore embryogenesis: establishment of embryo identity and pattern in culture. Plant Reproduction, 26: 181–196.

Stelpflug SC, Eichten SR, Hermanson PJ, Springer NM, Kaeppler SM. 2014. Consistent and heritable alterations of DNA methylation are induced by tissue culture in maize. Genetics, 198: 209–218.

Strand Å, Hurry V, Henkes S, Huner N, Gustafsson P, Gardeström P, Stitt M. 1999. Acclimation of arabidopsis leaves developing at low temperatures. Increasing cytoplasmic volume accompanies increased activities of enzymes in the Calvin cycle and in the sucrose-biosynthesis pathway. Plant Physiology, 119: 1387-1398.

Suarez MF, Filonova LH, Smertenko A, Savenkov EI, Clapham DH, von Arnold S, Zhivotovsky B, Bozhkov PV. 2004. Metacaspase-dependent programmed cell death is essential for plant embryogenesis. Current Biology, 14: 339-340.

Sugie A, Naydenov N, Mizuno N, Nakamura C, Takumi S. 2006. Overexpression of wheat alternative oxidase gene *Waox1a* alters respiration capacity and response to reactive oxygen species under low temperature in transgenic *Arabidopsis*. Genes and Genetic Systems, 81: 349-354.

Takahata Y, Komatsu H, Kaizuma N. 1996. Microspore culture of radish (*Raphanus sativus* L.): influence of genotype and culture conditions on embryogenesis. Plant Cell Reports, 16: 163–166.

Talbert LE, Bruckner PL, Smith LY, Sears R, Martin TJ. 1996. Development of PCR markers linked to resistance to wheat streak mosaic virus in wheat. Theoretical and Applied Genetics, 93: 463-467.

Tang Z, Zhang L, Xu C, Yuan S, Zhang F, Zheng Y, Zhao C. 2012. Uncovering small RNA-mediated responses to cold stress in a wheat thermosensitive genic male-sterile line by deep sequencing. Plant Physiology, 159: 721-738.

Telmer CA, Newcomb W, Simmonds DH. 1995. Cellular changes during heat shock induction and embryo development of cultured microspores of *Brassica napus* cv. Topas. Protoplasma, 185: 106-112.

Tina OC, Prisecaru M, Brezeanu C, Brezeanu M. 2013. Effect of carbohydrate type over the microspore embryogenesis at *Brassica Oleracea* L. Romanian Biotechnological Letters, 18: 8877-8684.

Thomé OW. 1886. Flora von Deutschland, Österreich und der Schweiz: in Wort und Bild. Band I. Köhler E (ed.). Gera-Untermhaus, PL 50.

Thorpe MR, MacRae EA, Minchin PEH, Edwards CM. 1999. Galactose stimulation of carbon import into roots is confined to the Poaceae. Journal of Experimental Botany, 50: 1613-1618.

Touraev A, Vicente O, Heberle-Bors E. 1997. Initiation of micropsore embryogenesis by stress. Trends in Plant Science, 2: 297 – 302.

Wang A, Xia Q, Xie W, Datla R, Selvaraj G. 2003. The classical Ubisch bodies carry a sporophytically produced structural protein (RAFTIN) that is essential for pollen development. Proceedings of the National Academy of Sciences of the United States of America, 100: 14487-14492.

Watanabe S, Takagi N, Hayashi H, Chino M, Watanabe A. 1997. Internal Gln/Glu ratio as a potential regulatory parameter for the expression of a cytosolic glutamine synthetase gene of radish in cultured cells. Plant Cell Physiology, 38: 1000–1006.

Winter H, Huber SC. 2000. Regulation of sucrose metabolism in higher plants: Localization and regulation of activity of key enzymes. Critical Reviews in Biochemistry and Molecular Biology, 35: 253-289.

Winter G, Todd CD, Trovato M, Forlani G, Funck D. 2015. Physiological implications of arginine metabolism in plants. Frontiers in Plant Science, 6: 534.

Xu ZY, Zhang X, Schläppi M, Xu ZQ. 2011. Cold-inducible expression of AZI1 and its function in improvement of freezing tolerance of *Arabidopsis thaliana* and *Saccharomyces cerevisiae*. Journal of Plant Physiology, 168: 1576-1587.

Yaish MWF, Doxey AC, McConkey BJ, Moffatt BA, Griffith M. 2006. Cold-active winter rye glucanases with ice-binding capacity. Plant Physiology, 141: 1459-1472.

Yaish MW, Colasanti J, Rothstein SJ. 2011. The role of epigenetic processes in controlling flowering time in plants exposed to stress. Journal of Experimental Botany, 62: 3727-3735.

Yaffe MB, Rittinger K, Volinia S, Caron PR, Aitken A, Leffers H, Gamblin SJ, Smerdon AJ, Cantley LC. 1997. The structural basis for 14-3-3: Phosphopeptide binding specificity. Cell, 91: 961-971.

Zabalza A, van Dongen JT, Froehlich A, et al. 2009. Regulation of respiration and fermentation to control the plant internal oxygen concentration. Plant Physiology, 149: 1087-1098.

Zheng M, Weng Y, Liu W, Konzak C. 2002. The effect of ovary-conditioned medium on microspore embryogenesis in common wheat (*Triticum aestivum* L.). Plant Cell Reports*, 20: 802–807.

Zheng MY. 2003. Microspore culture in wheat (*Triticum aestivum*) — doubled haploid production via induced embryogenesis. Review of Plant Biotechnology and Applied Genetics, 73: 213-230.

Zheng MY, Liu W, Weng Y, Polle E, Konzak CF. 2003. Production of doubled haploids in wheat (*Triticum aestivum* L.) through microspore embryogenesis triggered by inducer chemicals. In *Doubled Haploid Production in Crop Plants*, eds Maluszynski M, Kasha K J, Forster B P, Szarejko I, editors. (Dordrecht: Springer), 83–94.

Żur I, Dubas E, Golemiec E, Szechyńska-Hebda M, Gołebiowska G, Wedzony M. 2009. Stress-related variation in antioxidative enzymes activity and cell metabolism efficiency associated with embryogenesis induction in isolated microspore culture of triticale (x *Triticosecale Wittm*.). Plant Cell Reports, 28: 1279-1287.

Żur I, Dubas E, Krzewska M, Waligórski P, Dziurka M, Janowiak F. 2015. Hormonal requirements for effective induction of microspore embryogenesis in triticale (× *Triticosecale* Wittm.) anther cultures. Plant Cell Reports, 34:47-62.

8. Abbreviations

AcN: Acetonitrile

ADP-glc: Adenosine diphosphate glucuronic acid

Ala: Alanine

Arg: Arginine

Asn: Asparragine

Asp: Aspartic acid

ATP: Adenosine triphosphate

BAM: Barely any meristem

BBM: Baby boom

Ber: Berengar

$CHCl_3$: Chloroform

CoA: Coenzyme A

Cys: Cystein

DH: Doubled haploid

DTT: Dithioerythritol

EDTA: Ethylenediaminetetraacetic acid

EGTA: Ethylene-bis(oxyethylenenitrilo)tetraacetic acid

ESI: Electrospray ionization

FUS3: Fusca3

G1P: Glucose-1-Phosphate

G6P: Glucose-6-Phosphate

GABA: gamma-aminobutyric acid

GC: Gas chromatography

Gln: Glutamine

Glu: Glutamic acid

Gly: Glycine

GPR: Green plant regeneration

GS: Glutamine synthetase

GS-GOGAT: Glutamine synthetase-glutamine oxoglutarate aminotransferase

GST: Glutathione-S-Transferase

HEPES-KOH: 4-(2-hydroxyethyl)-1-piperazineethanesulfonic acid- potassium hydroxyde

His: Histidine

HSP: heat shock proteins

Ile: Isoleucine

LEC: Leafy cotyledon

Leu: Leucine

LPT: Lipid transfer protein

Lys: Lysine

MAH: methoxyamine hydrochloride

MeOH: Methanol

Met: Methionine

miRNA: microRNA

MSTFA: N-methyl-[N-trimethylsilyl]trifluoroacteamide

Na_2CO_3: Sodium carbonate

nanoLC: nano liquid chromatography

Nor: Norvaline

PCD: Programmed cell death

PDVF: Polyvinylidene difluoride

Phe: Phenylalanine

PR: Pathogenesis related protein

Pro: Proline

PVP: Poly(vinylpyrrolidinone)

Q TOF: Quadrupole time of flight

SBNG: Systems biology graphical notation

SDS: sodium dodecyl sulfate

SDS-PAGE: sodium dodecyl sulfate polyacrylamide gel electrophoresis

Ser: Serine

SERK: Somatic embryogenesis receptor-like kinase

siRNA: small interfering RNA

SU-BIO: Saaten Union Biotech GmbH

Svi: Svilena

T6P: Trehalose-6-Phosphate

TBST: Tris buffered saline buffer with Tween20

TCA: Tricarboxylic acid

TE: Tris EDTA buffer

Thr: Threonine

Tri-me: Trimethylation

Trp: Tryptophan

Tyr: Tyrosine

UDP-glc: Uridine diphosphate glucuronic acid

UDP-glu: Uridine diphosphate glucose

UDP-xyl: Uridine diphosphate xylose

UPLC: Ultra performance liquid chromatography

Val: Valine

VANTED: Visualization and analysis of networks containing experimental data

WCOR410: Wheat cold-regulated protein

WCS19: Wheat cold-regulated protein

9.   Curriculum vitae

Name: Teresa Pérez-Piñar López

Date of birth: 04.11.1986**; Place of birth**: Madrid**; Nationality:** Spanish

Address: Leibniz Institute of Plant Genetics and Crop Plant Research, Department of Physiology and Cell Biology, Applied Biochemistry group, Corrensstraße 3, 06466 Gatersleben, Germany

Telephone: +49 394825740; **Email**: pinar@ipk-gatersleben.de

Academic details

Nov.2013 - Jan.2019: PhD in Biology. In Leibniz-Institut für Pflanzengenetik und Kulturpflanzenforschung (IPK Gatersleben), department of Physiology and Celular Biology, in Applied Biochemistry group. Title: *"Study of the metabolism during microspore embryogenesis in wheat DH lines using – omics approaches"*.

Sept.2004 - Sept.2010: Bachelor´s degree in Biology, in Universidad Autónoma de Madrid, Spain.

Final degree project (2010): *"Implication of the epigenetic regulation in the expression of the provirus HIV in non-progressor patients (LTNPs) and elite controllers (EC)".* In Hospital Carlos III of Madrid.

Sept.2002 - Jun.2004: Bachillerato, in Valdeluz School, Madrid.

Professional experience

Nov. 2013- present   PhD associated to the project: *"SpeedWheat: Omicsbasierte Effizienzsteigerung der Erzeugung von DH-Linien in der Weizenzüchtung" (Improvement of the efficiency of the production of wheat DH lines based in –omics).* Leibniz-Institut für Pflanzengenetik und Kulturpflanzenforschung (IPK, Gatersleben).

Oct. 2010- Oct. 2012: Research assistant. In Fundación de Investigaciones Biomédicas of Hospital Carlos III of Madrid, associated to the project: *"Identification of B and T epitopes of Anisakis simplex allergens: applications to the diagnostic of Anisakis simplex allergy".*

Peer-reviewed publications

Perez-Pinar T, Meister A, Bössow S, Gnad H, Mock HP. Metabolic changes during androgenic induction in a segregating population of bread wheat and prediction of green plant regeneration**.** Under preparation

Perez-Pinar T, Hartmann A, Bössow S, Gnad H, Mock HP. Metabolic changes during wheat microspore embryogenesis induction using the highly responsive cultivar Svilena. BMC Plant Biology. 2018. Submitted.

Cho MK, Park MK, Kang SA, Caballero ML, **Perez-Pinar T**, Rodriguez-Perez R, Ock MS, Cha HJ, Hong YC, Yu HS. Allergenicity of two Anisakis simplex allergens evaluated in vivo using an experimental mouse model. Exp Parasitol. 2014 Nov;146:71-7.

García-Mayoral MF, Treviño MA, **Pérez-Piñar T**, Caballero ML, Knaute T, Umpierrez A, Bruix M, Rodríguez-Pérez R. Relationships between IgE/IgG4 epitopes, structure and function in Anisakis simplex Ani s 5, a member of the SXP/RAL-2 protein family. PLoS Negl Trop Dis. 2014 Mar 6;8(3):e2735.

Rodriguez-Perez R, Monsalve R, Galán A, **Pérez-Piñar T**, Umpierrez A, Lluch-Bernal M, Polo F, Caballero ML. Cross-reactivity between Anisakis spp. and wasp venom allergens. Int Arch Allergy Immunol. 2014;163(3):179-84.

Caballero ML, Umpierrez A, **Pérez-Piñar T**, Moneo I, de Burgos C, Asturias JA, Rodríguez-Pérez R. Anisakis simplex Recombinant Allergens Increase Diagnosis Specificity Preserving High Sensitivity. Int Arch Allergy Immunol. 2012;158(3):232-40.

Palacios JA, **Pérez-Piñar T**, Toro C, Sanz B, Moreno V, Valencia E, Gómez-Hernando C, Rodés B. LTNP/EC patients who control viraemia have a higher percentage of methylation in their HIV-1 proviral promoter than aviremic patients receiving HAART. J Virol. 2012 Dec;86(23):13081-4.

Pádua E, Rodés B, **Pérez-Piñar T**, Silva AF, Jiménez V, Ferreira F, Toro C. Molecular characterization of human T cell leukaemia virus type 1 subtypes in a group of infected individuals diagnosed in Portugal and Spain. AIDS Res Hum Retroviruses. 2011 Mar;27(3):317-22.

Presentations in international conferences

Perez-Pinar T, Bössow S, Gnad H, Mock HP. Metabolic characterization of wheat DH lines with different regeneration rates during microspore embryogenesis. 12th Plant Science Student Conference. Gatersleben, Germany. July 2016 (Poster).

Gnad H, Scholten S, Seifert F, **Pinar T**, Mock H-P, Weyen J. Improvement of anther culture for doubled haploid line production in wheat (Triticum aestivum) using omics-based techniques. Conference of the European association for Research on Plant Breeding (EUCARPIA). Wernigrode, Germany. July 2015 (Poster).

Jozefowicz A, Arens N, Matros A, Peukert M, Hartmann A, **Perez-Pinar T**, Kaspar S, Mock H-P. Nutrient deficiency responses of potato (Solanum tuberosum L.) revealed by combined proteomics and metabolomics approaches. Conference of the American Society for Mass Spectrometry. Baltimore, EEUU. June 2014 (Poster).

Pérez-Piñar T, Caballero M, Knaute T, Umpierrez A, Rodriguez-Perez R. Mapping of the IgE sequential epitopes of Ani s 1, the major *Anisakis simplex* allergen, with a peptide microarray-based immunoassay. Conference of the European Academy of Allergy and Clinical Immunology. Geneva, Switzerland. June 2012 (Poster).

Rodriguez-Perez R, **Pérez-Piñar T**, Umpierrez A, Caballero M. Relationship between wasp venom allergy and Anisakis simplex specific IgE. Conference of the European Academy of Allergy and Clinical Immunology. Geneva, Switzerland. June 2012 (Poster).

García-Mayoral MF, Treviño M, **Perez-Piñar T**, Caballero ML, Knaute T, Umpierrez A, Bruix M, Rodriguez-Perez R. Solution structure and Identification of IgE sequential epitopes of Ani s 5, an Anisakis allergen. Conference of the European Academy of Allergy and Clinical Immunology. Milan, Italy. June 2013 (Poster).

García-Mayoral MF, Treviño M, **Perez-Piñar T**, Rodriguez-Perez R, Bruix M.   Structural studies reveal clues about the possible functions of Ani s 5, an Anisakis simplex allergen. Congress of Sociedad Biofísica de España. Valencia, Spain. June 2013 (Poster).

Gatersleben, January 2019

10. **Affirmation**

I hereby declare that the submitted work has been completed by me, the undersigned, and that I have not used any other than permitted reference sources or materials or engaged any plagiarism. All the references and the other sources used in the presented work have been appropriately acknowledged in the work. I further declare that the work has not been previously submitted for the purpose of academic examination, either in its original or similar form, anywhere else.

Hiermit erkläre ich, dass ich diese Arbeit selbständig verfasst und keine anderen als die angegebenen Quellen und Hilfsmittel verwendet habe. Die den benutzten Hilfsmitteln wörtlich oder inhaltlich entnommenen Stellen habe ich unter Quellenangaben kenntlich gemacht. Die vorliegende Arbeit wurde in gleicher oder ähnlicher Form noch keiner anderen Institution oder Prüfungsbehörde vorgelegt.

_____ _____

Datum / Date   Unterschrift des Antragstellers /

                                Signature of the applicant

11. Acknowledgements

I would firstly like to thank my supervisor Dr. Hans-Peter Mock for his help, advice and encouragement for the completion of the thesis. Dr. Mock contributed with his supervision, knowledge, experience and enthusiasm about science, providing a supportive and challenging enviroment to develop as a researcher. I would also like to thank Prof. Dr. Humbeck and Prof. Dr. Żur for the evaluation of this thesis.

Thanks also to the colaborators of the SpeedWheat project, Dr. Heike Gnad, Sandra Bossow, Dr. Stefan Scholten and Dr. Felix Seifert, which contributed to the development of the project from which this thesis arises. All of them provided essential data and samples for the development of the study.

The financial support given by the Federal Ministry of Education and Research (BMBF) and the IPK Gatersleben is acknowledged here, since it allowed this study to be done.

My deepest thanks to Dr. Anja Hartmann and Dr. Armin Meister, for their kindly collaboration in the study. Dr. Hartmann helped with the VANTED software, providing her knowledge and support. Dr. Meister supported and supervised nicely the statistical analysis.

I am grateful to my colleagues from the Applied Biochemistry group, for their scientific and personal support, for their advice, suggestions and nice discussions. Thank you Andrea, Anna, Anne, Annegret, Annika, Antonis, Dominic, Elena, Johanna, Johannes, Manuela, Nadja, Petra, Stefanie, Wang, and everyone else.

I also want to thank my colleagues from the Physiology and Cell Biology department, for their nice scientific discussions in my department seminars. Thanks to people in administration and in the whole IPK. I am specially grateful to Dr. Britt Leps, for all the nice help and predisposition that made it possible to arrive and live in Germany.

Last but not least I would like to thank my family and friends, specially my husband, for their continuing support and understanding in doing this thesis.